UNIVERSIDADE DE BRASÍLIA
INSTITUTO DE CIÊNCIAS BIOLÓGICAS
PROGRAMA DE PÓS-GRADUAÇÃO EM ECOLOGIA

RAIANE GONÇALVES BEÚ

VULNERABILIDADE À SECA DE FLORESTAS NA BORDA SUL DA AMAZÔNIA

VULNERABILITY TO DROUGHT OF FORESTS ON THE SOUTHERN EDGE OF THE AMAZON

BRASÍLIA – DF
FEVEREIRO DE 2025

UNIVERSIDADE DE BRASÍLIA
INSTITUTO DE CIÊNCIAS BIOLÓGICAS
PROGRAMA DE PÓS-GRADUAÇÃO EM ECOLOGIA

RAIANE GONÇALVES BEÚ

VULNERABILIDADE À SECA DE FLORESTAS NA BORDA SUL DA AMAZÔNIA

VULNERABILITY TO DROUGHT OF FORESTS ON THE SOUTHERN EDGE OF THE AMAZON

Projeto de Tese apresentado ao Programa de Pós-Graduação em Ecologia da Universidade de Brasília como parte das exigências para a obtenção do título de Doutora em Ecologia.

Thesis Project presented to the Postgraduate Program in Ecology at the University of Brasília as part of the requirements for obtaining the title of Doctor in Ecology.

Orientador: AUGUSTO CESAR FRANCO

Coorientador: DAVID GALBRAITH

BRASÍLIA – DF
FEVEREIRO DE 2025

AGRADECIMENTOS

Sou grata a Deus, que, através da natureza, sempre me mostra sua grandiosidade, me ensina com sua força e resiliência e me inspira a continuar caminhando.

Ao meu orientador, Prof. Augusto Cesar Franco, pela dedicação, incentivo e ensinamentos ao longo do doutorado que, contribuíram para meu crescimento intelectual e profissional.

Ao meu coorientador, Prof. David Galbraith, por todo apoio e valiosas contribuições em todas as etapas do projeto. Aos professores Beatriz Marimon, Ben Hur Marimon e Manuel Gloor, pelo suporte logístico e pelas discussões enriquecedoras.

Aos amigos Carla Heloisa, José Wemerson, Martin Acosta e Calil Torres, cuja parceria e dedicação foram essenciais nas expedições de campo.

Ao Luis Paulo, Solange, Dona Eva, Paiaco, Aline e Mariane, pelo acolhimento e suporte durante a estadia da equipe de campo em Ribeirão Cascalheira (MT) e Gaúcha do Norte (MT).

Aos amigos, Julia Tavares, Edmar Almeida, Luciano Pereira, Emma Docherty, Halina Jancoski e Nayane Prestes, pela disponibilidade em esclarecer dúvidas, pelo apoio na metodologia e sugestões importantíssimas. A colaboração e generosidade de vocês tornaram essa jornada mais leve.

Aos meus pais, Ezi Gonçalves (in memoriam) e Nelson Beú (in memoriam), que não acompanharam essa jornada fisicamente, mas que foram e sempre serão minha maior fonte de inspiração.

Ao meu companheiro, Lucas Dos Santos, pelo incentivo, paciência e cuidado ao longo dessa caminhada!

Aos meus familiares pelo apoio constante e carinho: Elda, Verinha, Eni, Edson, Gerson, Zélia (in memoriam), Beatriz, Victor, Danilo, Fatima, Ana, Mariana, Arthur.

Aos colegas e amigos do laboratório de Ecofisiologia (UnB) e do LABEV (UNEMAT), pelo incentivo e por tornarem os dias de trabalho árduo mais agradáveis: Tayara Colins, Profa. Cristiane, Nathaly, Eduardo, Karen, Prof. Thomas, Julia, Marcele, Lucas, Luana, Flavinha, Larissa Chacon, Thamilles, Nayane Prestes, Jairo, Regiane, Daniel, Ediméia, Maelly, Priscila, Eder, Denilson, Paulo, Bruno.

Aos amigos, antigos e novos, pelo incentivo constante e acolhimento: Marina Scalon, Deliane Penha, Karoline Chaves, Mayda, Luane Botelho, Priscila Petrazini, José Cruz, Renata Freitag, Toninha, Karla Silva e Dani.

Aos membros da banca de doutorado, pela atenção, disponibilidade e sugestões valiosas: Profa. Dra. Grazielle Sales, Profa. Dra. Mercedes Bustamante, Dr. Mauro Brum e Profa. Dra. Cassia Beatriz.

Às instituições Universidade de Brasília, Universidade do Estado de Mato Grosso e Universidade de Leeds-UK, ao Programa de Pós-Graduação em Ecologia (UnB) pelo suporte científico e financeiro para execução do projeto de pesquisa. À CAPES, pela concessão da bolsa de doutorado.

Ao longo desta jornada, aprendi que ciência se faz, obrigatoriamente, de forma colaborativa. A cada pessoa que, de alguma maneira, contribuiu para essa trajetória, meu mais sincero agradecimento.

Com esperança de que você lute
para salvar os náufragos no mar da sua escola.

Cristovam Buarque

Aos meus país, Ezi Gonçalves e Nelson Beú,
dedico esta conquista, fruto do amor,
força e valores que me ensinaram.

SUMÁRIO

LISTA DE FIGURAS

Capítulo 1

Capítulo 2

LISTA DE TABELAS

Capítulo 1

Capítulo 2

RESUMO

A borda sul da Amazônia, uma região de transição entre os biomas Amazônia e Cerrado no estado do Mato Grosso, enfrenta condições climáticas extremas devido ao aquecimento climático, que tem provocado um aumento da duração e intensidade da estação seca e temperaturas crescentes. Estas condições aumentam o estresse hídrico para as árvores aumentando o risco de falha hidráulica, quando o transporte de água pelo xilema é interrompido, ocasionando a mortalidade de árvores que ocorrem em florestas desta região. Este estudo teve como objetivo avançar na compreensão da vulnerabilidade à seca das florestas na borda sul da Amazônia, ampliando a amostragem de florestas nessa região e considerando o efeito da fertilidade do solo nas estratégias hidráulicas de espécies arbóreas. A tese está estruturada em dois capítulos, que tem como foco principal, atributos hidráulicos críticos que afetam a vulnerabilidade à seca, ou seja, o potencial hídrico que provoca uma perda de 50% de (Ψ_{50}) e 88% (Ψ_{88}) da condutividade hidráulica do xilema, potencial hídrico foliar medido ao longo do dia no período de seca (Ψ_{leaf}), margem de segurança hidráulica (HSM_{50}), diferença entre Ψ_{50} e o menor valor de Ψ_{leaf} medido na estação seca (Ψ_{dry}) para cada indivíduo e densidade da madeira (WD_{branch}) em ramos da copa de espécies arbóreas representativas destas florestas. No primeiro capítulo, testamos se árvores que ocorrem em solos com maior disponibilidade de nutrientes têm margens de segurança hidráulica mais estreitas do que aquelas que ocorrem em solos menos férteis. Para tanto, comparamos métricas hidráulicas, concentração de macro e micronutrientes nas folhas e atributos anatômicos de ramos coletados de árvores em duas florestas adjacentes que ocorrem sob condições de fertilidade de solo contrastantes, uma caracterizada como Terra Preta da Amazônia, rica em nutrientes (ADE), e outra caracterizada como latossolo vermelho-amarelo, pobre em nutrientes (NDE). Não foram identificadas diferenças na anatomia do lenho entre os dois tipos de floresta, contudo, as árvores em solos ADE apresentaram concentrações mais elevadas de P, Ca e Mg nas folhas. Além disso, árvores em solos ADE exibiram menores valores de HSM_{50} e Ψ_{leaf} mais negativos, indicando uma estratégia de menor segurança hidráulica, especialmente para espécies que ocorrem em ambos os tipos de solos. No entanto, espécies exclusivas de ADE mantiveram maior HSM_{50}, o que confere um risco menor de ocorrer falha hidráulica, além de indicar estratégias funcionais distintas entre espécies que foram encontradas nos dois tipos de floresta e espécies que não coocorrem, ou seja, estão presentes em apenas um dos tipos de floresta. No segundo capítulo, medimos Ψ_{dry}, Ψ_{50} e HSM_{50} de árvores de quatro florestas na borda sul da Amazônia para testar a hipótese de que as condições climáticas predominantes nesta região estão forçando as árvores a operar perto ou além de seu limite hidráulico. Também compilamos dados sobre Ψ_{dry}, Ψ_{50} e HSM_{50} de outras 10 florestas distribuídas pela Amazônia para analisar as relações entre essas métricas e o déficit hídrico acumulado máximo (MCWD). Observamos maior resistência hidráulica nas florestas do sul da Amazônia expresso por valores de Ψ_{50} mais negativos, mas com HSM_{50} variando de positivo a negativo indicando diferenças na sensibilidade a seca entre florestas da borda sul da Amazônia. Ao integrar os nossos dados das quatro florestas da borda sul da Amazônia, com os obtidos em 10 florestas distribuídas ao longo da região amazônica, encontramos relação positiva do Ψ_{50} e Ψ_{dry} com MCWD, em nível de comunidade, com estas métricas hidráulicas ponderados pela área basal das espécies que foram medidas. Contudo, ao examinar as relações entre as métricas hidráulicas em nível do conjunto de espécies, utilizando os valores médios obtidos para cada espécie em cada floresta, observamos coordenação entre Ψ_{50} e Ψ_{dry} apenas para região de MCWD intermediário, mas não nos extremos seco e úmido, sugerindo pressões seletivas divergentes entre as regiões. Neste estudo, demonstramos a influência da fertilidade do solo nas estratégias hidráulicas de árvores da borda sul da Amazônia,

mostrando através de um experimento natural, o eixo de variação de HSM_{50} em relação a disponibilidade de nutrientes do solo. Os resultados obtidos também fornecem evidências de que embora as condições climáticas prevalecentes na borda sul da Amazônia tenham contribuído para selecionar espécies arbóreas com alta resistência hidráulica, elas não são igualmente seguras em termos de HSM_{50}. Contudo, em nível do bioma Amazônico, em um gradiente amplo de variação de MCWD, não foi possível detectar uma relação significativa entre HSM e MCWD e só encontramos evidências de coordenação hidráulica para as espécies arbóreas que ocorreram na região de MCWD intermediário.

Palavras chave: Terra preta da Amazônia, falha hidráulica, margem de segurança hidráulica, hidráulica de plantas, relações planta-água, embolia do xilema

ABSTRACT

The southern edge of the Amazon, a transition region between the Amazon and Cerrado biomes in the state of Mato Grosso, faces extreme climatic conditions due to climate warming, which has caused an increase in the duration and intensity of the dry season, as well as rising temperatures. These conditions increase water stress for trees, increasing the risk of hydraulic failure, when the transport of water through the xylem is interrupted, causing the mortality of trees that occur in the forests of this region. This study aimed to advance the understanding of drought vulnerability in the forests at the southern edge of the Amazon, expanding the number of forests sampled in this region and considering the effect of soil fertility on the hydraulic strategies of tree species found in these forests. The thesis is structured in two chapters, which focus mainly on key hydraulic attributes that affect vulnerability to drought, that is, water potential that causes a loss of 50% (Ψ_{50}) and 88% (Ψ_{88}) of the xylem hydraulic conductivity, leaf water potential measured throughout the day in the dry season (Ψ_{leaf}), hydraulic safety margin (HSM_{50}), defined as the difference between Ψ_{50} and the lowest value of Ψleaf measured in the dry season (Ψ_{dry}) for each individual and wood density (WD_{branch}) in canopy branches of tree species representative of these forests. In the first chapter, we tested whether trees occurring in soils with higher nutrient availability have lower HSM_{50} than those occurring in less fertile soils. To test this hypothesis, we compared hydraulic metrics, leaf concentrations of macro and micronutrients, and anatomical traits of branches collected from trees in two adjacent forests found under contrasting soil fertility conditions, one characterized as nutrient-rich Amazonian Dark Earth (ADE), and the other characterized as nutrient-poor Yellow-Red Oxisol (NDE). No differences in wood anatomy were identified between trees of the two forest types; however, trees in ADE soils had higher leaf concentrations of P, Ca, and Mg. In addition, trees in ADE soils exhibited lower HSM_{50} values and more negative Ψ_{leaf}, suggesting a strategy of low hydraulic safety, especially for species that occur in both soil types. However, species exclusive to ADE maintained higher HSM_{50}, which suggests a lower risk of hydraulic failure, in addition to indicating distinct functional strategies between species that were found in both forest types and species that do not co-occur, meaning they are present in only one of the forest types. In the second chapter, we measured Ψ_{dry}, Ψ_{50}, HSM_{50} of trees from four forests on the southern edge of the Amazon to test the hypothesis that the prevailing climatic conditions in this region are forcing trees to operate close to or beyond their hydraulic limit. We also compiled data on Ψ_{dry}, Ψ_{50}, HSM_{50} from ten other forests distributed across the Amazon to analyze the relationships between these hydraulic metrics and the maximum accumulated water deficit (MCWD). We observed greater hydraulic resistance in the forests of the southern Amazon expressed by more negative Ψ_{50} values, but with HSM_{50} ranging from positive to negative, indicating variation in sensitivity to drought in forests on the southern edge of the Amazon. When integrating our data for four forests, with those from the other 10 forests distributed across the Amazon region, we found a negative relationship between Ψ_{50} and Ψ_{dry} with MCWD, at the community level, with these hydraulic metrics weighted by the basal area of the species measured. When examining the relationships between hydraulic metrics at the species level, using the mean values obtained for each species in each forest, we observed coordination between Ψ_{50} and Ψ_{dry} only for the intermediate

MCWD region, but not in the dry and wet extremes, suggesting divergent selective pressures between regions. In this study, we demonstrate the influence of soil fertility on the hydraulic strategies of trees in the Southern edge of the Amazon, showing through a natural experiment the variation of HSM_{50} in relation to soil nutrient availability. The results also provide evidence that, although the prevailing climatic conditions at the Southern edge of the Amazon have contributed to selection of tree species with high hydraulic resistance, species are not equally safe in terms of HSM_{50}. Furthermore, at the Amazonian biome level, in a broad gradient of MCWD variation, it was not possible to detect a significant relationship between HSM_{50} and MCWD. We found evidence of hydraulic coordination only for the pool of species measured in the forests located in the intermediate MCWD region.

Key words: Amazonian dark earths, hydraulic failure, hydraulic safety margins, plant hydraulics, plant–water relations, xylem embolism

INTRODUÇÃO GERAL

Ao longo da evolução biológica em ecossistemas terrestres, a disponibilidade de água tem sido um fator determinante na seleção de atributos que afetam o desempenho fisiológico das plantas, moldando sua diversificação e distribuição ecológica. O transporte de água nas plantas ocorre sob gradientes negativos de pressão, impulsionado pelo déficit de pressão de vapor na interface folha-atmosfera e que determina a transpiração e transporte de água (Dixon, 1914). Esse mecanismo, descrito pela teoria da coesão-tensão, estabelece um gradiente de pressão que se estende das raízes às folhas, permitindo o movimento ascendente da água pelo xilema, o tecido vascular especializado no transporte de água e nutrientes (Dixon, 1914, Tyree & Sperry, 1989, Tyree & Zimmermann, 2002). Contudo, o sistema de transporte de água das plantas é vulnerável às condições de seca severa. Durante eventos de extremos climáticos, seca e calor, a atmosfera aumenta seu déficit de pressão de vapor (VPD) e diminui a umidade do solo, esses dois fatores juntos ou separados tensionam a coluna de água do xilema (Venturas et al., 2017). Nessas situações, a tensão excessiva na coluna de água pode provocar o embolismo, um processo no qual bolhas de ar se formam dentro do xilema e se expandem, resultando no bloqueio do fluxo de água e leva a falha do sistema de suprimento de água (Dixon & Joly et al., 1895; Tyree & Zimmermann, 2002). Esse processo representa um grande risco para a sobrevivência das plantas, pois compromete processos essenciais para sua manutenção e funcionamento, como o fornecimento de água para os tecidos da parte aérea, especialmente para as folhas, limitando a abertura dos estômatos, a fotossíntese e desencadeando o dessecamento da planta (Adams et al., 2017).

A resistência à embolia, frequentemente quantificada como o potencial hídrico do xilema no qual 50% da condutividade hidráulica é perdida (Ψ_{50}), é um determinante fundamental da vulnerabilidade à seca (Meinzer et al., 2009). Geralmente espécies com Ψ_{50} mais negativo são mais resistentes à embolia e, portanto, mais tolerantes à seca. Medidas de Ψ_{50} juntamente com os valores de potencial hídrico mais negativo (Ψ_{min}) experimentado pela planta em condições de campo, geralmente medido no auge na seca (Ψ_{dry}) permitem a estimativa da margem de segurança hidráulica (HSM), que é a diferença entre Ψ_{dry} e Ψ_{50} (Delzon et al., 2014; Meinzer et al., 2009; Bhaskar et al., 2006). Valores de HSM maiores que zero indicam maior tolerância à seca, pois a planta está operando dentro de um intervalo de pressão que não compromete e não causam interrupção do funcionamento do transporte de água pelo xilema. A HSM tem sido considerada como uma das principais preditoras de mortalidade induzida pela seca (Anderegg et al., 2016;

Powers et al., 2020). Um estudo recente na Amazônia mostrou que a HSM é também um forte indicador das trajetórias de acumulação e perda de biomassa em escala de ecossistema ao longo do tempo (Tavares et al., 2023).

Alguns estudos sugeriram que as florestas ao redor do mundo são igualmente vulneráveis à seca, apresentando uma HSM estreita (HSM < 1) (Choat et al., 2012; Peters et al., 2021). No entanto, os valores de HSM publicados para algumas regiões da Amazônia apontam que essa generalização não se sustenta (Tavares et al., 2023; Barros et al., 2019). As florestas tropicais são conhecidas por sua alta biodiversidade, ocorrem em ambientes altamente heterogêneos, onde, além da precipitação e temperatura, fatores como topografia, solo e disponibilidade de nutrientes também desempenham papéis centrais na determinação da heterogeneidade da vegetação (ter Steege et al., 2000; Schietti et al., 2014; Oliveira et al., 2019). Recentemente, um estudo de revisão sugeriu um eixo de variação da HSM em função da disponibilidade de nutrientes do solo, que pode modular a estratégia de crescimento das plantas (Oliveira et al., 2021). Nesse contexto, habitats ricos em nutrientes selecionariam espécies de árvores com estratégias mais aquisitivas, promovendo crescimento rápido, mas com baixa margem de segurança hidráulica, o que aumenta risco de mortalidade sob condições de seca (Grime, 2006; Reich et al. 2014; Guillemot et al., 2022). Em contraste, estratégias de tolerância ao estresse que favorecem uma alta HSM seriam cruciais para árvores de habitats pobres em nutrientes, pois estas não teriam recursos suficientes para recuperar tecidos perdidos, resultando em um menor risco de mortalidade induzida pela seca (Markesteijn et al., 2010; Reich et al., 2014; Mori et al., 2019).

A elevada diversidade de espécies em florestas tropicais torna desafiadora a compreensão dos processos que determinam a vulnerabilidade à seca dessas florestas, exigindo um esforço de amostragem ampliado que capture a diversidade de cenários ambientais e biológicos para fornecer uma visão mais abrangente sobre sua resiliência às mudanças climáticas. A borda sul da Amazônia é uma região naturalmente dinâmica por tratar de uma transição entre dois biomas, Amazônia e Cerrado (Marimon et al., 2014). Além disso é uma região que já vem experimentando condições climáticas extremas, com aumento da intensidade dos períodos de seca e temperaturas (Fu et al., 2013; Jiménez-Muñoz, et al., 2013). Alguns estudos realizados nessa região demonstraram uma perda generalizada de densidade de árvores e alterações na composição florísticas de comunidade vegetais (Prestes et al., 2024; Esquivel-Muelbert et al., 2017;2020), com florestas operando com HSM além do limite de segurança (Tavares et al., 2023) e

enfrentando temperaturas que já podem estar afetando a fotossíntese dessas árvores (Tiwari et al., 2020).

Desse modo, o presente estudo teve como objetivo avançar na compreensão da vulnerabilidade à seca das florestas da borda sul da Amazônia. No Capítulo 1, utilizamos uma abordagem integrando a hidráulica das plantas e a disponibilidade de nutrientes no solo, para avaliar se árvores que ocorrem em solos com maior disponibilidade de nutrientes têm margens de segurança hidráulica mais estreitas do que aquelas que ocorrem em solos menos férteis. No Capítulo 2, amostramos quatro florestas localizadas na borda sul da Amazônia para avaliar se o padrão de HSM extremamente negativo observado no único local previamente estudado na região é representativo de outras florestas da região. Além disso, incorporamos dados disponíveis na literatura para outras regiões da Amzônia, ampliando a análise e permitindo uma visão mais abrangente dos padrões regionais.

REFERÊNCIAS BIBLIOGRÁFICAS

Adams, H.D., Zeppel, M.J., Anderegg, W.R., Hartmann, H., Landhäusser, S.M., Tissue, D.T., Hudson, P.J., Franz, T.E., Allen, C.D., Anderegg, L.D., Barron-Gafford, G.A., Beerling, D.J., Breshears, D.D., Brodribb, T.J., Bugmann, H., Cobb, R.C., Collins, A.D., Dickman, L.T., Duan, H., Ewers, B.E., … McDowell, N.G. (2017). A multi-species synthesis of physiological mechanisms in drought-induced tree mortality. *Nature ecology & evolution*, **1**, 1285-1291.

Anderegg W.R., Klein, T., Bartlett, M., Sack, L., Pellegrini, A.F., Choat, B., & Jansen, S. (2016). Meta-analysis reveals that hydraulic traits explain cross-species patterns of drought-induced tree mortality across the globe. *Proceedings of the National Academy of Sciences, USA* **113**: 5024–5029

Bhaskar, R., & Ackerly, D.D. (2006). Ecological relevance of minimum seasonal water potentials. *Physiologia Plantarum*, **127**, 353–359.

Choat, B., Jansen, S., Brodribb, T.J., Cochard, H., Delzon, S., Bhaskar, R., Bucci, S.J., Feild, T.S., Gleason, S.M., Hacke, U.G. & Jacobsen, A.L., (2012). Global convergence in the vulnerability of forests to drought. *Nature*, **491**, 752-755.

Delzon, S., & Cochard, H. (2014) Recent advances in tree hydraulics highlight the ecological significance of the hydraulic safety margin. *New phytologist*, **203**, 355–358.

Dixon, H. H. (1914). *Transpiration and the ascent of sap in plants*. Macmillan and Company, limited.

Esquivel-Muelbert, A., Baker, T.R., Dexter, K.G., Lewis, S.L., Ter Steege, H., Lopez-Gonzalez, G., Mendoza, A.M., Brienen, R., Feldpausch, T.R., Pitman, N., Alonso, A., Heijden, V.D.G., Peña-Claros, M., Ahuite, M., Alexiaides, M., Dávila, E.Á., Murakami,

A.A., Arroyo, L., Aulestia, M., Balslev, H., ... & Phillips, O. L. (2017). Seasonal drought limits tree species across the Neotropics. *Ecography*, **40**, 618-629.

Esquivel-Muelbert, A., Phillips, O.L., Brienen, R.J., Fauset, S., Sullivan, M.J., Baker, T. R., Chao, K.J., Feldpausch, T.R., Gloor, E., Higuchi, N., Houwing-Duistermaat, J., Lloyd, J., Liu, H., Malhi, Y., Marimons, B. S., Mamimon-Junior, B., Monteagudo-Mendoza, A., Poorter, L., Silveira, M., ... & Galbraith, D. (2020). Tree mode of death and mortality risk factors across Amazon forests. *Nature communications*, **11**, 5515.

Fu, R., Yin, L., Li, W., Arias, P.A., Dickinson, R. E., Huang, L., Chakraborty, S., Fernandes, K., Liebmann, B., Fisher, R., & Myneni, R. B. (2013). Increased dry-season length over southern Amazonia in recent decades and its implication for future climate projection. Proceedings of the National Academy of Sciences, 110, 18110-18115.

Grime, J.P., 2006. Plant Strategies, Vegetation Processes, and Ecosystem Properties. Wiley, 2nd Edition, 464 pp. ISBN: 978-0-470-85040-4

Guillemot, J., Martin-StPaul, N.K., Bulascoschi, L., Poorter, L., Morin, X., Pinho, B.X., le Maire, G., Bittencourt, P. R. L., Oliveira, R. S., Bongers, F., Brouwer, R., Pereira, L., Gonzalez Melo, G.A., Boonman, C.C.F., Brown, K.A., Cerabolini, B.E.L., Niinemets, Ü., Onoda, Y., Schneider, J. V., … Brancalion, P. H. S. (2022). Small and slow is safe: On the drought tolerance of tropical tree species. *Global Change Biology*, **28**, 2622-2638.

Jiménez-Muñoz J.C., Mattar, C., Barichivich, J., Santamaría-Artigas, A., Takahashi, K., Malhi, Y., Sobrino, J.A., Schrier, G.V.D., (2016). Record-breaking warming and extreme drought in the Amazon rainforest during the course of El Niño 2015–2016. *Scientific Reports* **6**: 33130.

Marimon, B.S., Marimon-Junior, B.H., Feldpausch, T.R., Oliveira-Santos, C., Mews, H.A., Lopez-Gonzalez, G., Lloyd, J., Franczak, D.D., de Oliveira, E.A., Maracahipes, L. & Miguel, A. (2014). Disequilibrium and hyperdynamic tree turnover at the forest–cerrado transition zone in southern Amazonia. *Plant Ecology & Diversity*, **7**, 281-292.

Markesteijn, L., Poorter, L., Bongers, F., Paz, H. and Sack, L. (2011). Hydraulics and life history of tropical dry forest tree species: coordination of species' drought and shade tolerance. *New phytologist*, 191, 480-495.

Meinzer, F.C., Johnson, D.M., Lachenbruch, B., McCulloh, K.A., & Woodruff, D.R. (2009). Xylem hydraulic safety margins in woody plants: coordination of stomatal control of xylem tension with hydraulic capacitance. *Functional Ecology*, **23**, 922–930.

Mori, G.B., Schietti, J., Poorter, L., Piedade, M.T.F., (2019). Trait divergence and habitat specialization in tropical floodplain forests trees. *PLoS One* **14**: 0212232.

Oliveira, R.S., Costa, F.R.C., van Baalen, E., de Jonge, A., Bittencourt, P.R., Almanza, Y., Barros, F.d.V., Cordoba, E.C., Fagundes, M.V., Garcia, S., Guimaraes, Z., Hertel, M., Schietti, J., Rodrigues-Souza, J. & Poorter, L. (2019), Embolism resistance drives the distribution of Amazonian rainforest trees pecies along hydrotopographic gradients. *New Phytologist*, **221**,1457–1465.

Oliveira, R. S., Eller, C. B., Barros, F.V., Hirota, M., Brum, M., & Bittencourt P. (2021). Linking plant hydraulics and the fast–slow continuum to understand resilience to drought in tropical ecosystems. *New Phytologist*, **230**, 904-923.

Powers, J.S., Vargas, G.G., Brodribb, T.J., Schwartz, N.B., Pérez-Aviles, D., Smith-Martin, C.M., Becknell, J.M., Aureli, F., Blanco, R., Calderón-Morales, E., Calvo-Alvarado, J.C., Calvo-Obando, A.J., Chavarría, M.M., Carvajal-Vanegas, D., Jiménez-Rodríguez, C.D., Chacon, E.m., Schaffner, C.M., Werden, L.K., Xu, X., & Medvigy, D. (2020). A catastrophic tropical drought kills hydraulically vulnerable tree species. *Global Change Biology*, **26**, 3122–3133.

Prestes, N. C., Marimon, B. S., Morandi, P. S., Reis, S. M., Junior, B. H. M., Cruz, W. J., Oliveira, E. A., Mariano, L.H., Elias, F., Santos, D.M., Esquiviel-Muelbert, A., & Phillips, O. L. (2024). Impact of the extreme 2015-16 El Niño climate event on forest and savanna tree species of the Amazonia-Cerrado transition. *Flora, 319*, 152597.

Reich PB. (2014). The world-wide 'fast–slow' plant economics spectrum: a traitsmanifesto. Journal of Ecology, **102**, 275–301.

Rowland, L. Costa, A.C.L., Galbraith, D.R., Oliveira, R.S., Binks, O.J., Oliveira, A.A.R., Pullen, A.M., Doughty, C. E., Metcalfe, D. B., Vasconcelos, S. S., Ferreira, L. V., Malhi, Grace, J.Y., Mencuccini, M., & Meir, P. (2015). Death from drought in tropical forests is triggered by hydraulics not carbon starvation. *Nature*, **528**, 119-122.

Sanchez-Martinez, P., Martínez-Vilalta, J., Dexter, K.G., Segovia, R.A., & Mencuccini, M. (2020). Adaptation and coordinated evolution of plant hydraulic traits. *Ecology Letters*, **23**, 1599-1610.

Schietti, J., Emilio, T., Rennó, C. D., Drucker, D. P., Costa, F. R., Nogueira, A., Baccaro, F.B., Figueiredo, F., Castilho, C.V., Kinupp, V., Guillaumet, JL., Garcia, A.R.M., Lima, A.P., & Magnusson, W. E. 2014. Vertical distance from drainage drives floristic composition changes in an Amazonian rainforest. *Plant Ecology & Diversity*, **7**, 241-253.

Tavares, J.V., Oliveira, R.S., Mencuccini, M., Signori-Müller, C., Pereira, L., Diniz, F.C., Gilpin, M., Zevallos, M.J.M., Yupayccana, C.A.S., Acosta, M., Mullisaca, F.M.P., Barros, F.V., Bittencourt, P., Jancoski, H., Scalon, M.C., Maridixonmon, B.S., Menor, I.M., Marimon-Junior, B.H., Fancourt, M., & Galbraith, D.R. (2023) Basin-wide variation in tree hydraulic safety margins predicts the carbon balance of Amazon forests. *Nature*, v. **617**, 11-117.

Ter Steege, H., Sabatier, D., Castellanos, H., Van Andel, T.I.N.D E., Duivenvoorden, J., Oliveira, A. A., Ek, R., Lilwah, R., Maas, P., & Mori, S. (2000). An analysis of the floristic composition and diversity of Amazonian forests including those of the Guiana Shield. *Journal of tropical ecology*, 16, 801-828.

Tiwari, R., Gloor, E., Cruz, W.J.A., Marimon, B.S., Marimon-Junior, B.H., Reis, S.M., Aráujo, I.S., Krause, H.G., Slot, M., Winter, K., Ashley, D., Beú, R.G., Borges, C.S., Cunha, M., Fauset, S., Ferreira, L.D.S., Gonçalves, M.D.A., Lopes, T., Marques, E.Q., ... & Galbraith, D. (2021). Photosynthetic quantum efficiency in south-eastern Amazonian trees may be already affected by climate change. *Plant, Cell & Environment*, **44**, 2428-2439.

Tyree, M.T., & Zimmermann, M. H. (2002). Xylem Structure and the Ascent of Sap. Heidelberg.

Tyree, M.T., Sperry, J.S. (1989). Vulnerability of xylem to cavitation and embolism. *Annu. Rev. Plant Phys. Mol. Bio* **40**, 19-38.

CAPÍTULO 1

Soil fertility as a filter for hydraulic strategies in trees from southern Amazonian tropical forests.

to be submitted to Plant, Cell & Environment

ABSTRACT

Amazonian forests occur in a mosaic of soils. Although it has been hypothesized that trees growing on more fertile soils have lower hydraulic safety margins (HSM) than those on lower fertility soils, studies addressing this hypothesis are lacking. We used a natural fertilization experiment in southern Amazonia to compare key xylem hydraulic and anatomical traits of trees in a nutrient-poor oxisol (NDE) and in a neighboring nutrient-rich forest plot of Amazonian dark earths (ADE), both within the same forest fragment. ADE trees were taller with leaves richer in Ca, Mg and P. The ADE tree community had lower HSM and more negative leaf water potentials (Ψ_{leaf}). Species occurring on both ADE and NDE plots (*i.e.* co-occurring species) were closer to hydraulic failure in the ADE plot. ADE-exclusive species maintained a higher HSM being less prone to hydraulic failure. ADE and NDE tree communities and co-occurring species did not differ in branch wood density, wood anatomy and Ψ at 50% (Ψ_{50}) and 88% (Ψ_{88}) embolism formation**.** However, co-occurring, NDE- and ADE-exclusive species segregated in multivariate trait space, revealing distinct functional typologies. Our results highlight the role of soil fertility in shaping tree vulnerability to drought and functional composition in southern Amazonian.

Key words: Amazonian dark earths, xylem hydraulic traits, hydraulic failure, hydraulic safety margins, plant hydraulics, plant–water relations, xylem embolism

INTRODUCTION

Amazonian forests play a fundamental role in maintaining biodiversity, capturing carbon, sustaining hydrological cycles and regulating biogeochemical cycles on a global scale (Bonan et al., 2009; Philips et al., 2009). To better understand the dynamics of these ecosystems, investigating factors that affect the functioning of trees has become a crucial area of interest, mainly due to the complexity of conditions under which forests are formed (Brodribb et al., 2020; Mcdowell et al., 2020). Among these factors, the hydraulic relationships of plants gain prominence, mainly because hydraulic failure is an important trigger for drought-induced tree mortality worldwide (Allen et al., 2010, 2015; Rowland et al., 2015; Anderegg et al., 2016; Moore et al., 2016; Adams et al., 2017). This becomes even more relevant given the current climatic context of changes in the dynamics of rainfall, which has resulted in more frequent and intense droughts (Duffy et al., 2015, Jiménez-Muñoz et al., 2018, Smith et al., 2023).

Hydraulic failure occurs when the transport of water is interrupted due to embolism formation induced by high xylem tensions caused by low soil moisture or high atmospheric evaporative demand (Dixon & Joly et al., 1895; Jones & Sutherland 1991; Tyree & Zimmermann 2022). Several parameters allow us to evaluate the vulnerability of plants to embolism, including the hydraulic safety margin (HSM). HSM is the difference between Ψ_{50}, xylem water potential associated with 50% embolism formation and Ψ_{min}, which is the minimum water potential recorded *in situ* at the peak of the dry season (Bhaskar et al., 2006; Delzon et al., 2014). Thus, HSM indicates how far the plant is operating from hydraulic failure (Meinzer et al., 2009; Anderegg et al., 2016). HSM has been shown to be an effective measure for predicting drought-induced tree mortality (Powers et al., 2020; Tavares et al., 2023).

However, studies on tree vulnerability to drought are often more focused on exploring the interactions with climatic variables such as precipitation and vapour pressure deficit, while less attention has been paid to relationships with the availability of nutrients in the soil (Oliveira et al., 2021; Gessler et al., 2016). A hydraulic economy has recently been proposed, where hydraulic attributes are linked to plant growth strategy and which in turn can be modulated by soil nutrient availability (Oliveira et al., 2021; Rowland et al., 2023). In this context, nutrient-rich habitats would select for tree species with fast (more acquisitive) strategies resulting in rapid growth and low HSM, leading to a high risk of mortality when exposed to drought (Grime, 2006; Reich et al. 2014; Guillemot et al., 2022). In contrast, slow (more conservative) strategies favoring a high

HSM would be crucial for trees from nutrient-poor habitats, as they do not have sufficient resources to recover lost tissues, resulting in a lower risk of drought-induced mortality (Markesteijn et al., 2010; Reich et al., 2014; Mori et al., 2019). Which would require adjustments in the hydraulic architecture to increase hydraulic transport efficiency at the expense however of hydraulic safety, decreasing HSM (Hacke and Sperry 2001, Sperry 2015).

Amazonian forests exist in a highly heterogeneous mosaic of soil fertility (Quesada et al., 2012). They occur in habitats ranging from highly weathered Oxisols and Argisols, characterized by high acidity and low nutrient concentrations, to Anthrosols such as the Amazonian Dark Earths (ADE), characterized by highly fertile with high concentrations of pyrogenic charcoal particles (Oliveira et al., 2022). The most widespread hypothesis that explains the greater fertility of the ADE is that pre-Columbian human occupation in these forests led to an increase in soil fertility due to their way of life (Heckenberger et al., 2008; Oliveira et al., 2020). However, a more recent hypothesis argues that fertility originates from exogenous mineral sources and that pre-Columbian people exploited these naturally fertile areas but were not responsible for their genesis (Silva et al., 2021).

The southern Amazonian ADE forests can achieve greater above-ground biomass than the surrounding forests (Oliveira et al., 2022). In a study of above- and net primary productivity (NPP) of ten Amazonian forests, the highest values of NPP were measured in an ADE forest (Aragão et al., 2009). They have access to a higher availability of soil nutrients such as calcium (Ca), magnesium (Mg), potassium (K) and phosphorus (P) (Silva et al., 2021; Bauters et al., 2022; Oliveira et al., 2022). Ca is an essential element for cellular structure, metabolism and signaling in plants (White et al., 2003). Mg and K contribute critically to the photosynthesis process and long-distance transport of photoassimilates (Trankner et al., 2018). To date, Ca, Mg, and K have received less attention in studies investigating plant responses to nutrient availability (Sardans & Peñuelas 2015; Gaviria et al., 2017; Bauters et al., 2022) compared to nitrogen (N) and phosphorus (P), which also play a key role in plant growth (Quesada et al., 2009; Gessler et al., 2016; Wright et al., 2019).

Because ADE forests occur side-by-side with forests on nutrient-poor soils and thus share the same climate space (Quesada et al., 2012), ADE and non-ADE (NDE) forests provide a natural experiment to study the influence of soil fertility on tree hydraulic strategies that have been little explored to date. In this study, we explicitly test

the hypothesis that trees occurring in more fertile soils have lower hydraulic safety margins than those occurring in less fertile soils (e.g. Oliveira et al. 2021) and examine how different nutrients affect tree hydraulic strategies. We expect that trees from ADE sites would have higher access to soil nutrients, a more acquisitive strategy and be more prone to drought-induced hydraulic failure. On the other hand, NDE trees would have a more conservative hydraulic strategy with greater daily regulation of leaf water potential the day, avoiding negative HSM and therefore being less prone to the risk of embolism. We also expect that species occurring on both ADE and NDE areas are able to adjust their hydraulic architecture to the prevailing edaphic conditions. To address these hypotheses, we performed a comparative study of xylem hydraulic traits, and leaf nutrients in 15 co-occurring (i.e., occurring in both ADE and NDE areas) and non-co-occurring (occurring only in ADE or NDE areas) tree species in an ADE and a contiguous NDE forest in southern Amazonia.

MATERIALS AND METHODS

Study Area

The study was conducted in two Seasonal Evergreen Forest plots located on the southern edge of the Amazonia (Fig.1), in the municipality of Gaúcha do Norte, in the state of Mato Grosso (13º14'S; 53º04'W). The climate is Aw, according to Köppen's classification (Kottek et al., 2006), with a dry period typically from April to September and a rainy period from October to March (Silva et al., 2008). These two forest plots are close to each other, located within the same forest fragment that covers approximately 116 ha, being approximately 800 meters apart. The transition between these two forest types is gradual and is associated with changes in soil chemical composition.

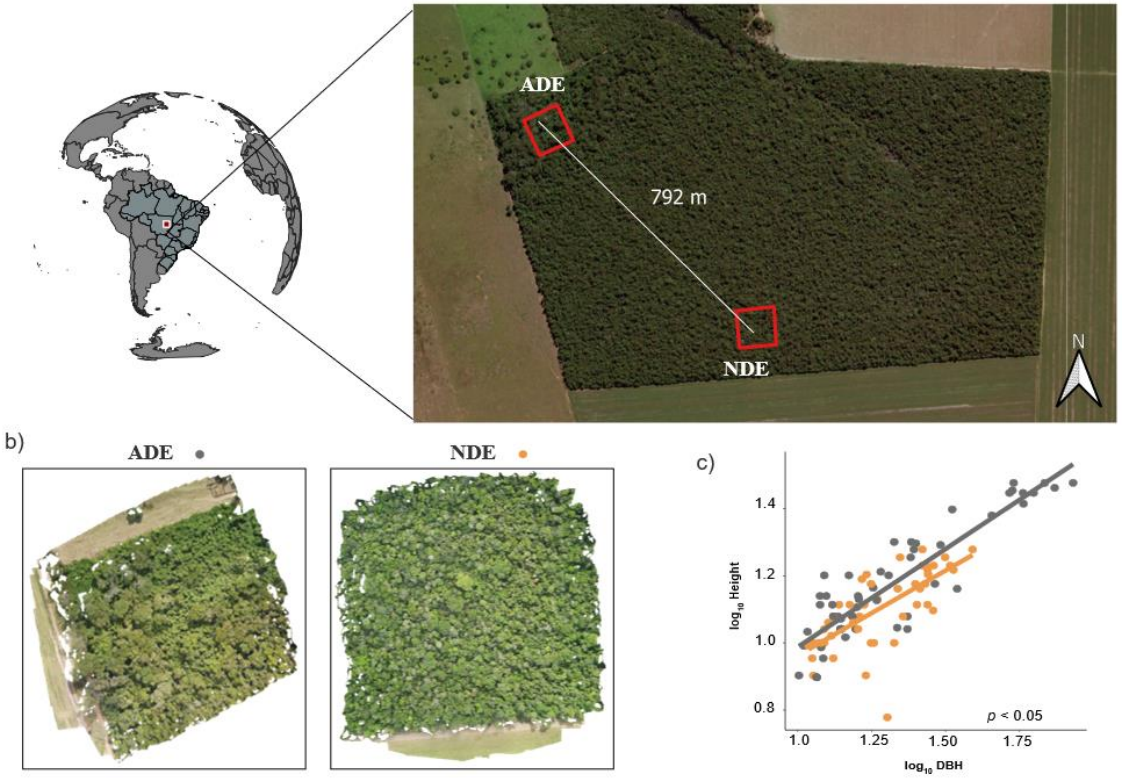

Fig. 1 (a) Location of the study sites in the southern Amazonia, ADE = Amazonian Dark Earths; NDE = non-ADE; (b) mosaic made with drone images of the forest canopy; and (c) the relationship between tree height (Height; m) and stem diameter (DBH; cm) of ADE (grey circles and line) and NDE (orange circles and line) trees that were sampled in this study. Relationships were obtained with $\log_{10}$ transformed values. Equation for ADE: $\log_{10}$ Height = 0.61 + 0.45 $\log_{10}$ DBH, R^2_m = 0.49, R^2_c=0.67 and for NDE: $\log_{10}$ Height = 0.37 + 0.59 $\log_{10}$ DBH, R^2_m = 0.21, R^2_c = 0.41.

One of the forests grows on a soil characterized as Amazonian Dark Earth (ADE) by Oliveira et al. (2020). ADE soil stands out for its higher fertility, exhibiting higher values of nutrients such as calcium (Ca) and phosphorus (P) (Table 1). The second forest plot, hereafter referred to as NDE occurs on the region's characteristic Yellow-Red Oxisol soil. This is a highly weathered soil low in nutrients (Table 1). In both forests, the soil is acidic, with a higher level of acidity in the NDE soil. The areas do not differ in terms of soil texture, with similar amounts of clay, sand and silt (Table 1).

The ADE trees reached larger sizes than the NDE trees (Fig. 1; Fig.S1). Some species occur in both forests (*i.e.* are co-occurring) while others are restricted to one plot or the other (Table 2).

Table 1 Chemical and physical properties (mean ± SD; n=5) of the superficial soil layer (0-10 cm) of the two evergreen seasonal forest plots studied in the southern Brazilian Amazonia: ADE = Amazonian Dark Earths; NDE = non - ADE. Data were extracted from Oliveira et al., (2020). *P*-values are based on T-tests for normally distributed data or Wilcoxon tests for non-normally distributed data.

Nutrients/soil texture	NDE	ADE	P- value
Calcium (cmolc/dm³)	0.02 ± 0.01	0.17 ± 0.27	0.0007
Phosphorus (mg/dm³)	1.35 ± 0.09	3.79 ± 1.1	0.0001
Potassium (cmolc/dm³)	0.04 ± 0.01	0.04 ± 0.01	0.5164
Magnesium (cmolc/dm³)	0.1 ± 0.1	0.1 ± 0.08	0.9394
pH_H_2O	3.9 ± 0.08	4.49 ± 0.19	0.0001
Organic matter (g/dm³)	24.1 ± 7.17	15.13 ± 3.18	0.0033
CTC (cmolc/dm³)	9.62 ± 2.12	7.46 ± 1.22	0.0143
Sand (g/kg)	812.89 ± 25	827.8 ± 33.68	0.3373
Clay (g/kg)	143.33 ± 20.9	125.2 ± 24.24	0.1446
Silt (g/kg)	43.78 ± 24.13	47 ± 27.57	0.8637

Species selection

In each of these forests, permanent 1-hectare plots were established as part of the long-term monitoring projects PELD (Cerrado-Amazônia Transition: ecological and socio-environmental bases for conservation) and RAINFOR (Amazon network of forest inventories, http://www.forestplots.net). All trees with a diameter at breast height ≥ 10 cm were and continue to be inventoried, identified, and tagged. For species selection, we used inventory data collected in 2018 by the CNPq/PELD III project (#441244/2016-5) led by the Plant Ecology laboratory of UNEMAT, Nova Xavantina campus, Mato Grosso, Brazil. The ADE trees reached larger sizes than the NDE trees (Fig. 1; Fig.S1). Some species occur in both forests (*i.e.* are co-occurring) while others are restricted to one plot or the other (Table 2).

The criteria for species selection were based on the Importance Value Index (IVI) which is the arithmetic sum of the relative values of abundance, basal area and frequency or that the species occurred in both plots (Table 2). We selected 15 species; 13 of them occurred in the ADE, 10 occurred in the NDE and eight were found in both ADE and NDE plots. Therefore, five species only occur in ADE, and two only occur in NDE.

Table 2 Selected species with their respective botanical families in parentheses for the two forest plots studied in the southern Brazilian Amazon. IVI = importance value index; ADE = Amazonian Dark Earths; NDE = non – ADE.

Species	IVI (%)	
	ADE	NDE
Amaioua guianensis Aubl. (Rubiaceae)	12.42	4.65
Chaetocarpus echinocarpus (Baill.) Ducke (Peraceae)	2.33	6.11
Copaifera langsdorffii Desf. (Fabaceae)	7.72	-
Dacryodes microcarpa Cuatrec. (Burseraceae)	-	12.86
Hymenaea courbaril L. (Fabaceae)	12.85	-
Matayba arborescens (Aubl.) Radlk. (Sapindaceae)	1.07	7.80
Micropholis venulosa (Mart. & Eichler) Pierre (Sapotaceae)	3.17	-
Mouriri apiranga Spruce ex Triana (Melastomataceae)	0.48	-
Myrciaria floribunda (H.Wesr ex Willd.) O. Berg (Myrtaceae)	13.58	0.70
Ocotea velloziana (Meisn.) Mez (Lauraceae)	3.36	8.65
Protium pilosissimum Engl. (Burseraceae)	1.29	6.55
Sacoglottis guianensis Benth. (Humiriaceae)	0.96	5.03
Vochysia vismiifolia Spruce ex Warm. (Vochysiaceae)	-	4.69
Xylopia amazonica R.E.Fr (Annonaceae)	3.36	4.88
Xylopia benthamii R.E.Fr (Annonaceae)	4.57	-

All measurements (*i.e.*, xylem hydraulic traits, leaf water potential and leaf nutrients) were from sun-exposed top-canopy branches (or branches at the maximum height reachable by the climber).

Leaf nutrient analysis

For nutrient analyses, we collected leaf samples in May 2022 from the same branches used for hydraulic vulnerability to embolism measurements. In the field, the collected material was dried to remove moisture and ensure the preservation of the material. Upon returning to the laboratory, we dried the samples again in an oven at 70ºC for 72 hours, and then sent them for analysis of nitrogen (N), phosphorus (P), potassium (K), calcium (Ca), and magnesium (Mg) at the Viçosa Soil Analysis Laboratory, Minas Gerais, Brazil. The Kjeldahl method was used for N (digestion with sulfuric acid in the presence of selenium, copper and sodium) followed by distillation in a Nitrogen Distiller MA 036 – MARCONI using sodium hydroxide and hydrochloric acid. Nitroperchloric digestion was applied for P, followed by determination in a spectrophotometer (CELM Mod. E 225 D) at a wavelength of 725 nm. For K, Ca and Mg, nitroperchloric digestion

was also used, followed by determination by flame emission photometry (Micronal Mod. B 462) for K and by atomic absorption spectrophotometry (Varian Mod. Spect. A 20) for Ca and Mg.

Embolism vulnerability measurements using the pneumatic method

Field Procedures

We determined hydraulic vulnerability in May 2022, at the end of the rainy season/beginning of the dry season when the soil was fully hydrated. The predawn leaf water potential ranged from -0.1 to -1.0 MPa. Branches were collected in the field between 4 AM and sunrise, a time when the plants generally have a balanced water status with the soil. In the field, we collected two branches measuring up to 1 meter for 3 individuals of each species, placing them inside a moist black plastic bag and transporting them to the laboratory for measurements. We did not measure hydraulic vulnerability for *Matayba arborescens* because it was producing flowers during the period in which the measurements were carried out.

Laboratory procedures

The vulnerability curves were estimated by the relationship between the amount of air extracted from the dehydrating branches and the xylem water potential using the manual pneumatic method (Pereira et al., 2016; Bittencourt et al., 2018) which considers the volume of air discharged from the branches as a proxy for embolism formation. As commonly used when applying the manual pneumatic method, we considered an interval of 2.5 minutes to account for air discharge (Bittencourt et al., 2018, Tavares et al., 2023). Between each measurement, the branches were exposed to the environment for 30 minutes to 1 hour to dehydrate, after which they were placed inside a black plastic bag to equilibrate leaf water potential (Ψ_{leaf}) with stem water potential (Ψ_{stem}). Ψ_{leaf} was measured using a 1505D-EXP pressure chamber (PMS Instruments Co., Albany, USA; Scholander 1965). We repeated the pneumatic air discharge and Ψ_{leaf} measurements until the branch was completely dehydrated.

We calculated Ψ_{50} and Ψ_{88} (xylem water potential associated with 50 and 88% embolism formation) by fitting the data to a Weibull function:

(Eqn 1)

$$PAD = \frac{100}{1 + exp\left(\frac{S}{25}(\Psi_x - \Psi_{50})\right)}$$

where PAD is the percent air discharged at Ψ_x, expressed as a percentage difference between the amount of air discharged when the branch was completely dehydrated and the amount of air discharged when the branch was fully hydrated. S is the slope of the curve, Ψ_x is the xylem water potential (MPa) and Ψ_{50} is the Ψ_x corresponding to a PAD of 50%.

Field measurements of leaf water potential (Ψ_{leaf})

We measured Ψ_{leaf} in ADE in the second half of September and NDE at the end of September and the beginning of October, at the peak of the dry period of 2021. Measurements were conducted using a 1505D-EXP pressure chamber (PMS Instruments Co., Albany, USA). Sampling was performed at different times throughout the day, starting at predawn (4:00 am to 6:00 am), and then at 9:00 am to 10:30 am, midday (12:00 pm to 2:00 pm) and 4:00 pm to 5:30 pm. In both forest plots, we selected five individuals of each species, collecting one branch per individual where we selected three mature leaves per individual with a healthy appearance and exposed to sunlight. The branches were collected, identified, and placed inside a tightly sealed black plastic bag, and quickly transported to the point of measurement in the field. This entire process took less than 10 minutes.

Hydraulic safety margin (HSM)

HSM_{50} was calculated as the difference between Ψ_{dry} and Ψ_{50}, where Ψ_{dry} corresponds to the most negative Ψ_{leaf} values measured in the field during the dry period. We used Ψ_{50}, which is more commonly used and shows greater agreement in relation to the Ψ_{50} estimated with the pneumatic method and other methods (Adams et al., 2017; Paligi et al., 2023).

Wood density and branch anatomy

Anatomical traits and wood density (WD_{branch}) were determined on the same branches that were collected for the vulnerability curves (n = 3 individuals). In the laboratory, we cut fragments of up to 2.5 centimeters length, removed the bark, and immersed the samples in water for at least 12 hours. The fresh volume at saturation was calculated using the mass displacement method, then the samples were dried at 60ºC for 72 hours, and the wood density calculated as the dry mass per volume at saturation ($g.cm^{-3}$) (Osazuwa-Peters & Zanne, 2010).

Samples from the same branches were also taken for anatomical analysis. Each sample was soaked in a water/glycerin solution (4:1 ratio), and histological sections were

prepared using a sliding microtome. Sections were clarified with sodium hypochlorite (20%), dehydrated in an alcoholic series (30-50%) and stained with alcoholic Safranin (1%) (Johansen, 1940). Tissues were visualized under a digital camera connected to an optical microscope (Bioval Microscope, software 2.0). The images were photographed and processed at a magnification of 25x. The characterization of the anatomical elements was done according to the International Association of Wood Anatomists (IAWA) standards (Wheeler et al., 1989). Measurements were performed semi automatically using the ImageJ program (version 1.53a for Windows), to determine vessel area (VA, μm²) and vessel diameter (VD; μm). The potential hydraulic conductivity was calculated for each sample according to the Hagen–Poiseuille equation (Schuldt et al., 2016):

(Eqn 2)

$$K_p = ((\pi \times \sum VD^4/128\eta) \times \rho)/A_{xylem}$$

Where K_p is the potential hydraulic conductivity (in kg m^{-1} MPa^{-1} s^{-1}), η is the viscosity of water at 20ºC (1.002 × 10^{-3} Pa s), ρ is the density of water at 20ºC (998.2 kg m^{-3}), A_{xylem} is the analysed xylem area (mm^2) and D is the hydraulically weighted vessel diameter (μm).

Data analysis

The analyses were conducted considering the following three groups: the community (all species from each plot), the co-occurring species (species occurring in both ADE and NDE plots) and the non-co-occurring species (species that occur only in one of the forests).

We used paired T-tests or Wilcoxon tests to evaluate whether species occurring in both plots differed in leaf nutrient status and hydraulic attributes after testing for normality and homoscedasticity using the Shapiro-Wilk and Levene tests (Levene 1960; Shapiro-Wilk 1965). We constructed linear mixed models with forest type (NDE and ADE) as a fixed effect and species as a random effect to assess whether ADE trees are more prone to hydraulic failure relative to NDE, with hydraulic metrics (Ψ_{dry}, Ψ_{50}, Ψ_{88} and HSM_{50}) as response variables and to assess whether ADE trees differ from NDE trees in hydraulic architecture, with branch wood density (WD_{branch}), vessel area, VD, Kp, stem diameter and tree height as response variables.

We verified the relationships between Ψ_{dry} and Ψ_{50} and leaf nutrients (Ca, Mg and P) that differed between the two forests also using linear mixed models, with

hydraulic metrics as response variables, nutrients as a fixed effect and species as a random effect. Finally, a principal component analysis (PCA) identified the main axes of variation in the total dataset of functional traits analyzed and how the co-occurring and non-co-occurring species groups were distributed.

We also calculated the community weighted mean (CWM) for each hydraulic trait (Ψ_{dry}, Ψ_{50}, Ψ_{88} and HSM_{50}), weighted by the IVI (CWM_{ivi}), (Garnier et al., 2004). To test for differences in CWM_{ivi} between ADE and NDE forests we used the Monte Carlo simulation method with the difference in the weighted means as the test statistic, randomizing the location and repeating 10000 times.

For all analyses, a significance level of 0.05 was used. We performed all analyses using R software version 4.3.1 (R Core Team 2023). For linear mixed models, we used the lmerTest function (Kuznetsova et al., 2017) in the lme4 package (Crawley, 2013; Pinheiro et al., 2024). We followed Zuur et al. (2009) and Thomas et al. (2017) to assess the significance of model terms and validate model assumptions. We assessed model performance using marginal (R^2_m) and conditional (R^2_c) pseudo-R^2 calculated using the "r.squaredGLMM" function from the "MuMIn" package (Barton, 2024).

RESULTS

Leaf nutrients

At the community level, ADE trees exhibited significantly higher values of leaf Ca, P and Mg ($P < 0.001$; Fig. 2), while leaf N did not differ ($P = 0.13$) between forests. The same pattern of higher leaf Ca, P, Mg for the ADE tree community was maintained in pairwise mean comparisons of species occurring in both plots ($P < 0.001$) and for the comparison of community means for the non-co-occurring species ($P < 0.001$). The results of leaf Ca and P correspond to the same nutrients showing higher amounts in the ADE soil (Table 1). Ca in the ADE forest stands out with considerably higher values both for the soil (ADE = 0.17 and NDE = 0.02 cmolc/dm³) and for the leaves (ADE = 0.74 and NDE = 0.32 dag/kg). As for K, we found no significant differences between the co-occurring paired species ($P = 0.15$) and the non-co-occurring species ($P = 0.17$), but when combining the two groups and comparing at the community level, a significant difference was observed ($P = 0.009$), with an average of 0.06 dag/kg in the NDE and 0.08 dag/kg in the ADE.

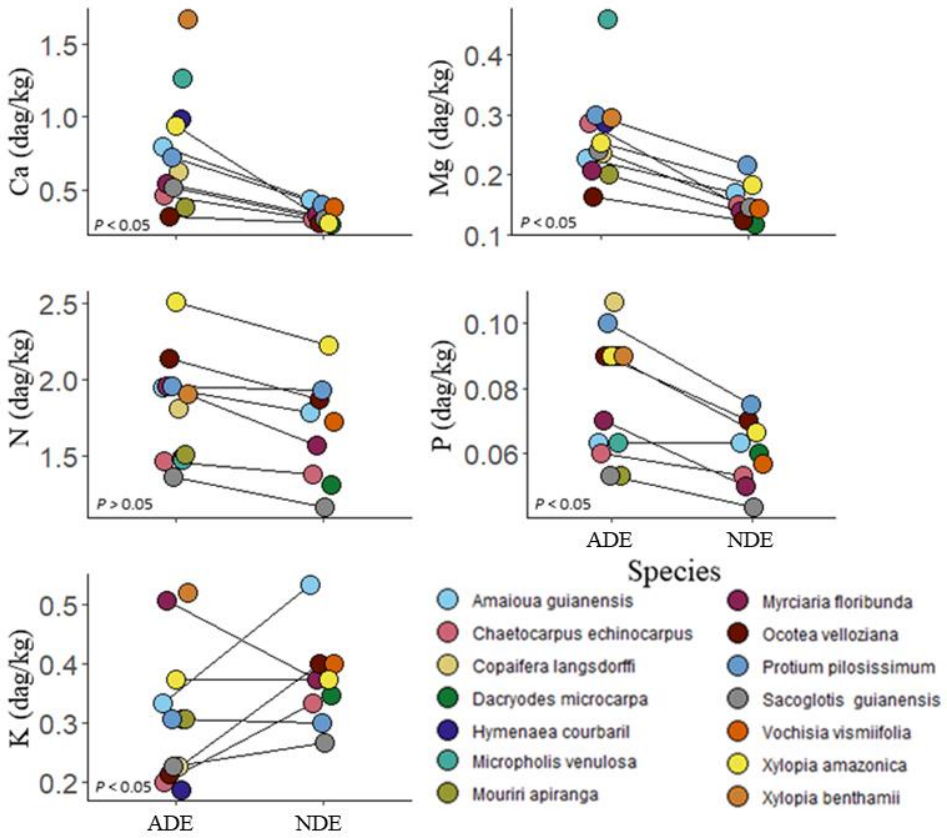

Fig. 2 Leaf nutrients in tree species occurring in two contrasting evergreen seasonal forests in southern Amazonia. (a) Ca = calcium; (b) Mg = magnesium; (c) N = nitrogen; (d) P = phosphorus; (e) K= potassium. ADE = Amazonian Dark Earths; NDE = non-ADE. Co-occurring tree species are connected by lines.

Hydraulic vulnerability

We did not detect any differences in Ψ_{50} and Ψ_{88} between the two forest communities studied ($P > 0.05$; Fig. 3a, b). The same pattern holds for pairwise mean comparisons of co-occurring species ($P > 0.05$, Table S1). However, for the non-co-occurring species, Ψ_{50} was significantly more negative in the ADE ($P < 0.05$) while Ψ_{88} showed no differences between the two communities (Table S1).

Ψ_{dry} was more negative and the HSM_{50} closer to zero for the trees in the ADE, both for the community ($P < 0.05$; Fig. 3c, d) and for the species present on both forests ($P < 0.05$; Table S1). In the case of species that did not occur in both forests, Ψ_{dry} was significantly more negative in the ADE ($P < 0.001$). However, this did not result in significant differences in HSM_{50} ($P = 0.376$) between these species, due to the more negative Ψ_{50} of species occurring only in the ADE compared to those occurring only in the NDE.

Alternative analyses using community weighted means of hydraulic traits led to the same overall results as when using unweighted values, *i.e.*, community-level differences in $\Psi_{predawn}$, Ψ_{dry}, and HSM_{50} were observed but not in Ψ_{88} (Table S2). This analysis detected a decrease in Ψ_{50} which was more negative in the ADE. However, Ψ_{dry} was more negative than Ψ_{50} in the ADE, resulting in a negative HSM_{50} in the ADE but not in the NDE (Table S2).

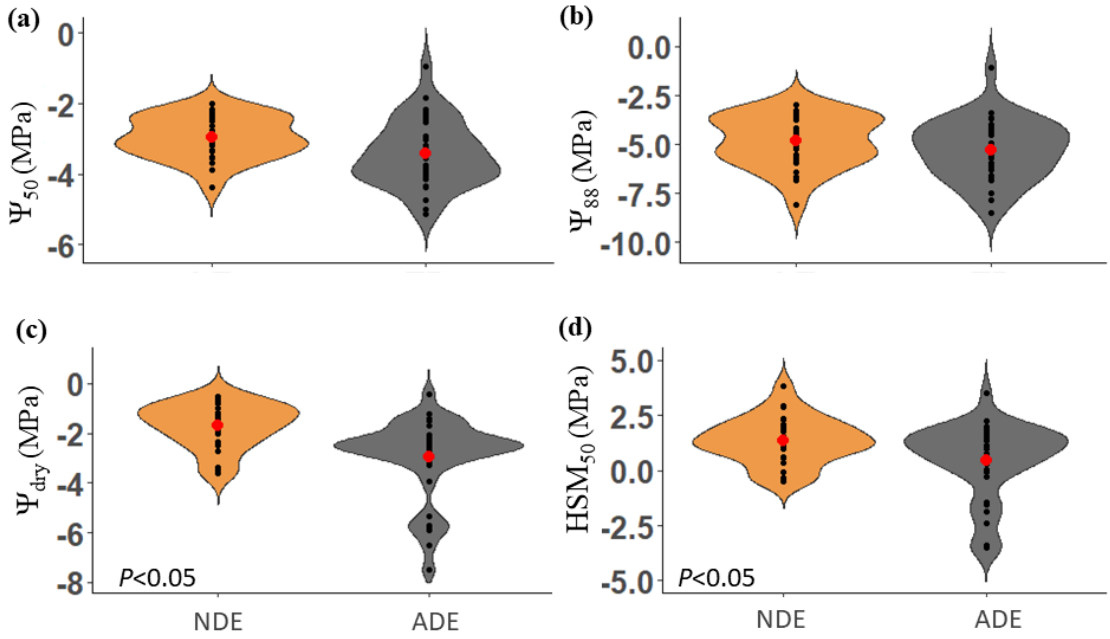

Fig. 3 Xylem water potential associated with (a) 50% (Ψ_{50}) and (b) 88% (Ψ_{88}) embolism formation (c) the most negative leaf water potential measured in the field during the dry period (Ψ_{dry}), (d) hydraulic safety margin (HSM_{50}) for the two forest communities in southern Amazonia. The colors represent the forest communities, Amazonian Dark Earths (ADE) = gray; non - ADE (NDE) = orange. Red dots = community average values.

Diurnal course of leaf water potential (Ψ_{leaf})

At the community level, leaf water potentials were significantly more negative in ADE at all times of the day measured, including predawn ($P < 0.001$; Fig. 4; Table S1). This same pattern holds for the co-occurring species ($P < 0.05$, for all tests), with the exception of *S. guianensis*, which maintained the same range of leaf water potential in both forest communities ($P > 0.05$; Fig. 5).

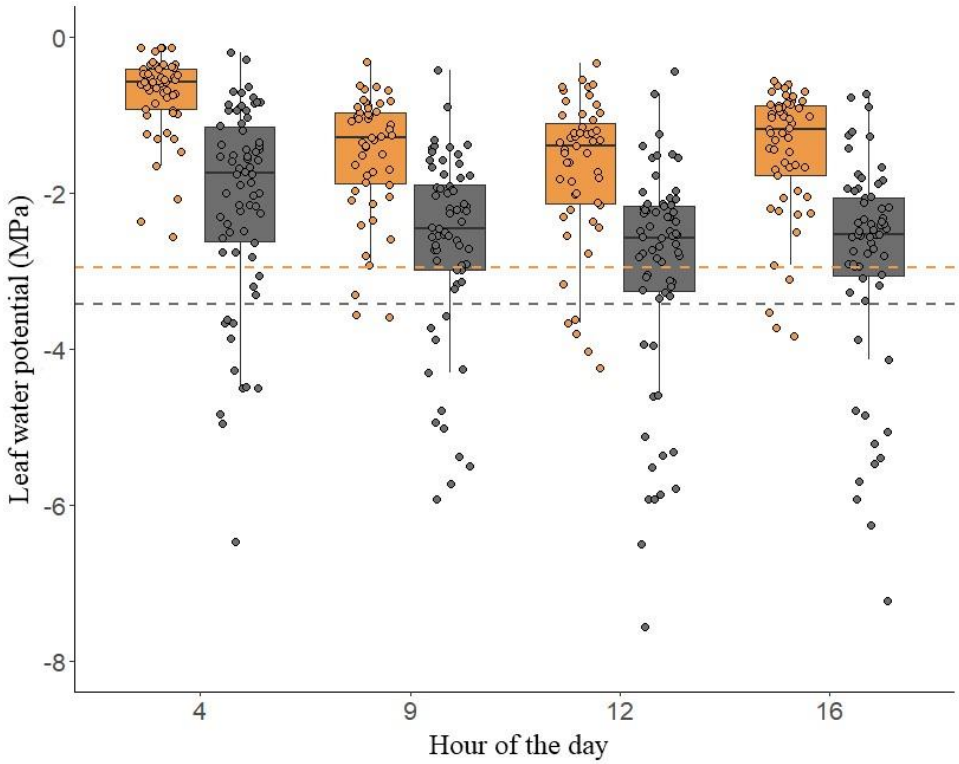

Fig. 4 Leaf water potential measured at the peak of the dry season over a day in the two forest communities. Dashed lines indicate the average Ψ_{50} of each community. Both for the lines and for the box plots, the colors represent the forest communities, Amazonian Dark Earths (ADE) = gray; non - ADE (NDE) = orange. The boxplots show the 25th percentile, median, and 75th percentile. The vertical bars represent the interquartile range, and data points beyond these bars are considered outliers (n = 65 individuals for ADE and 50 individuals for NDE).

Of the species that occurred in both forest types, *A. guianensis* stood out for operating throughout the day with Ψ_{leaf} beyond Ψ_{50} (Fig. 5), resulting in a negative HSM_{50} in both forests i.e HSM_{50} = -3.09 MPa in the ADE and HSM_{50} = -0.2 MPa in the NDE. *M. floribunda* showed negative HSM_{50} values in the ADE while maintaining a positive safety margin in the NDE (ADE = -2.26; NDE = 0.43 MPa). NDE- and ADE-exclusive species maintained positive values of HSM_{50} throughout the day.

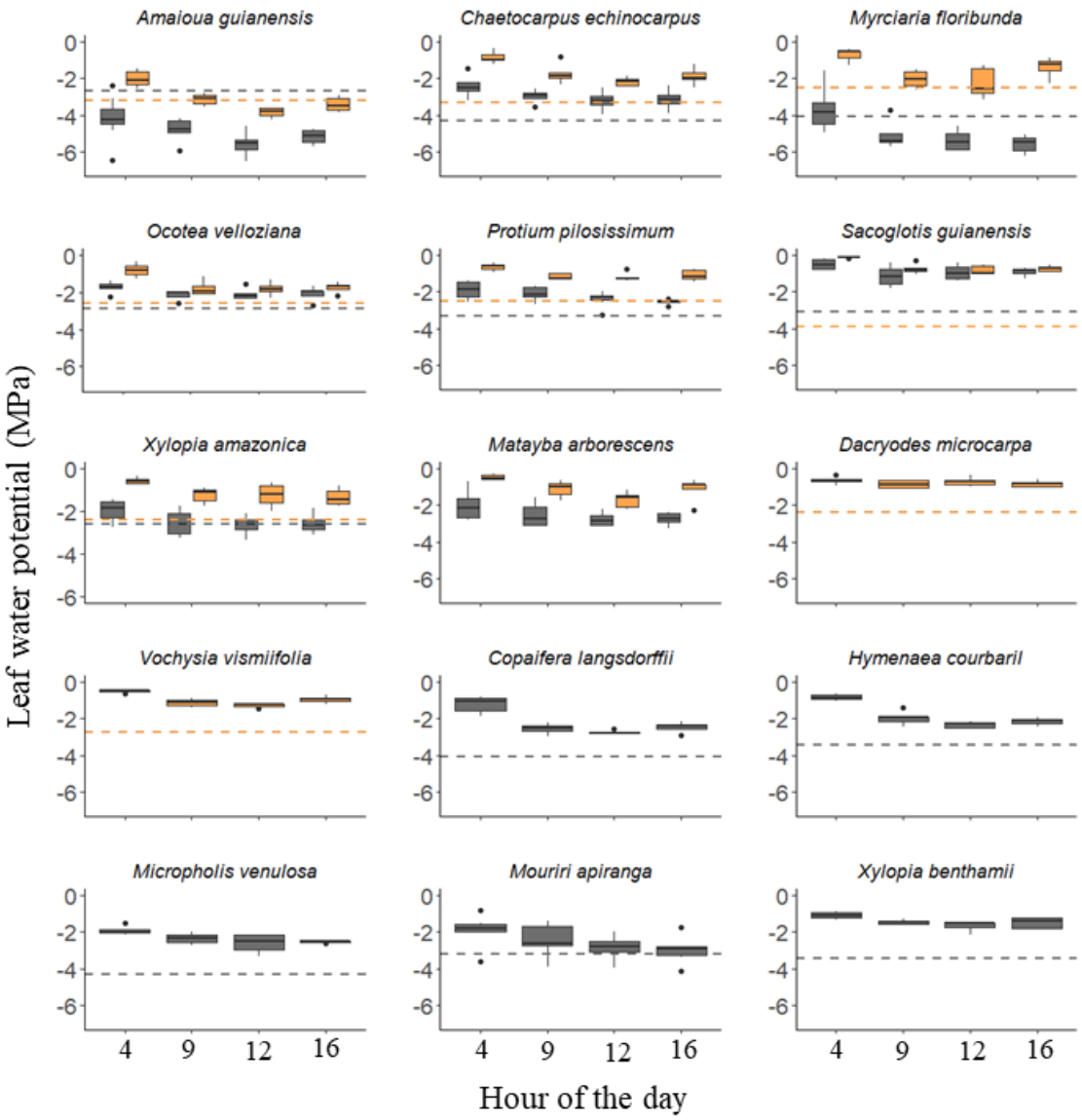

Fig. 5 Leaf water potential for co-occurring and non-co-occurring species measured at the peak of the dry season over a day at four different times in the two forest communities in southern Amazonia. Dashed lines indicate the average Ψ_{50} for the species at each community. Both for the lines and for the box plots, the colors represent the forest communities, Amazonian Dark Earths (ADE) = gray; non - ADE (NDE) = orange.

Branch wood density and anatomy

Forest-level comparisons did not detect any differences in wood density or anatomical parameters between the two forest communities ($P > 0.05$; Fig. 6), between co-occurring species, and between non-co-occurring species ($P > 0.05$; Table S1).

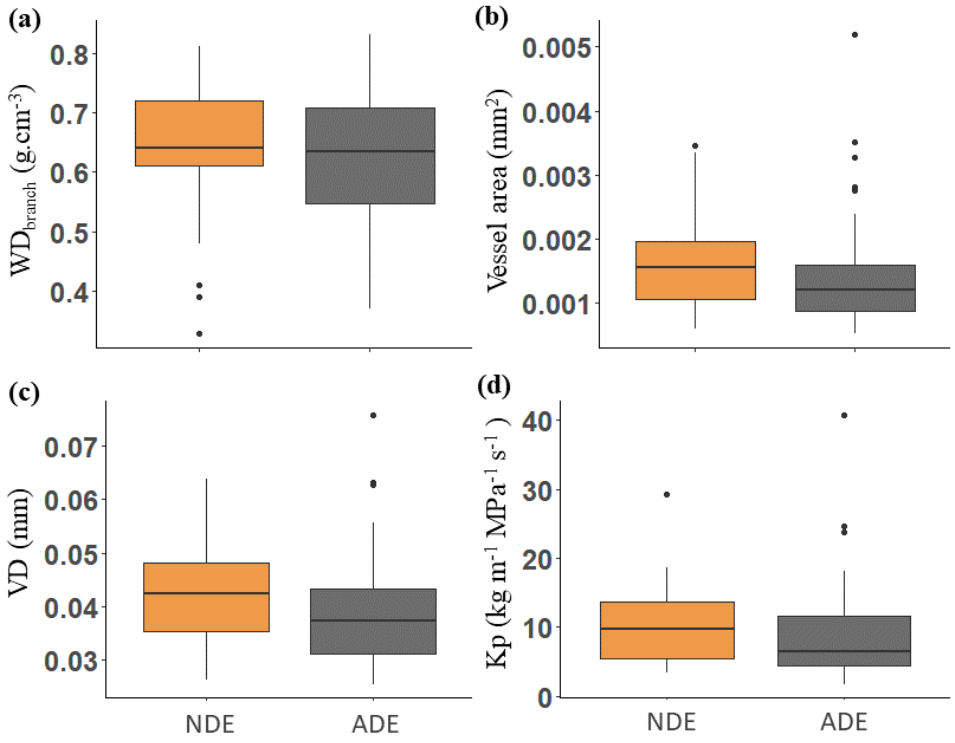

Fig. 6 Box plot values of (a) branch wood density (WD_{branch}), (b) vessel area, (c) = vessel diameter (VD), (d) potential hydraulic conductivity (Kp; kg m^{-1} MPa^{-1} s^{-1}), of the two forest communities in southern Amazonia. Amazonian Dark Earths (ADE) = orange; Not-ADE (NDE) = gray. In all cases, $P > 0.05$.

Hydraulic trait relationships with leaf nutrients and tree size

Leaf Ca and Ψ_{dry} and leaf Mg and Ψ_{dry} were negatively related for co-occurring ($P < 0.05$; Fig. 7a and 7b) and non-co-occurring species ($P < 0.05$; Fig. 8a and 8b), while P was negatively related with Ψ_{dry} for the co-occurring species, but showed no relation with Ψ_{dry} for the non-co-occurring species (Fig. 7c and 8c; Table S3). In contrast, only NDE- and ADE-exclusive species showed a significant relationship between leaf Ca and Ψ_{50} (Fig. 7d and 8d; Table S4) and between leaf Mg and Ψ_{50} (Fig. 7e and 8e; Table S4). No trend was detected between leaf P and Ψ_{50} (Fig. 7f and 8f; Table S4). All significant relationships had similar trends, where hydraulic metrics became more negative as the concentration of Ca, Mg or P in leaves increased.

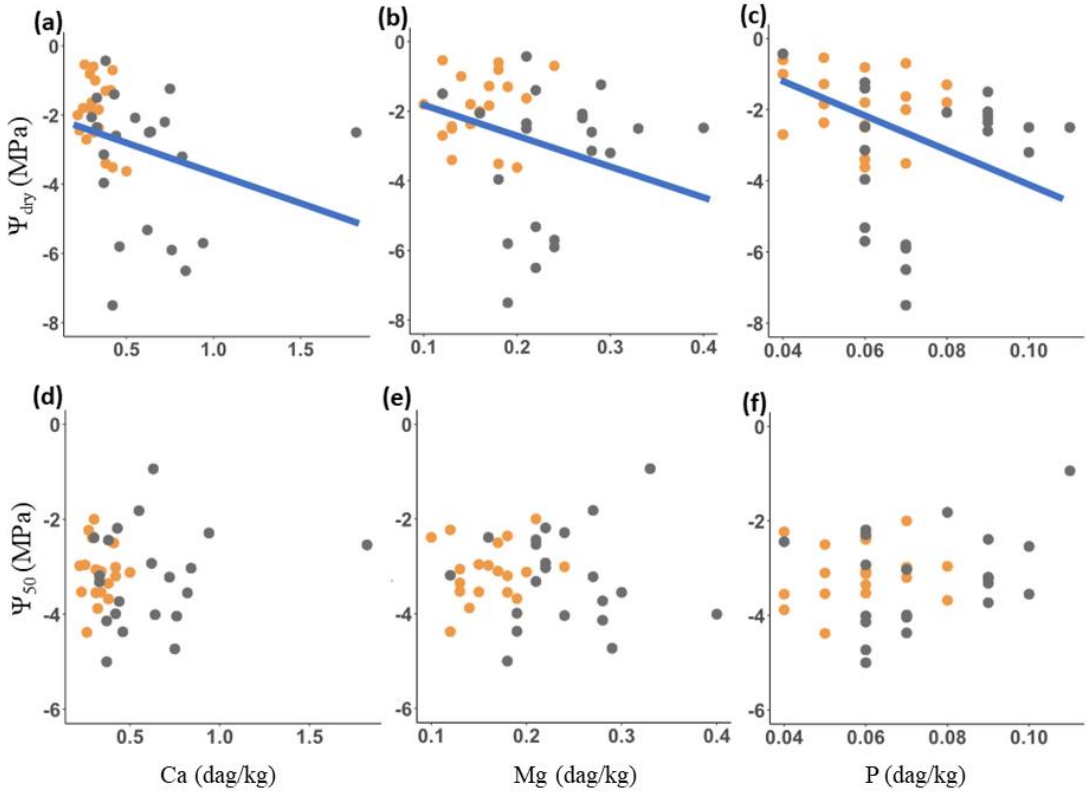

Fig.7 Relationship between (a) leaf calcium (Ca) and minimum leaf water potential (Ψ_{dry}), (b) leaf magnesium (Mg) and Ψ_{dry}, (c) leaf phosphorus (P) and $\Psi_{dry,}$ (d) leaf Ca and branch xylem water potential at which 50% of embolism occurs (Ψ_{50}), (e) leaf Mg and $\Psi_{50,}$ (f) leaf P and Ψ_{50} for co-occurring species in the two forest communities in southern Amazonia. Amazonian Dark Earths (ADE) = ADE gray; non – (NDE) = orange. Lines were drawn for the relationships that were significant ($P < 0.05$).

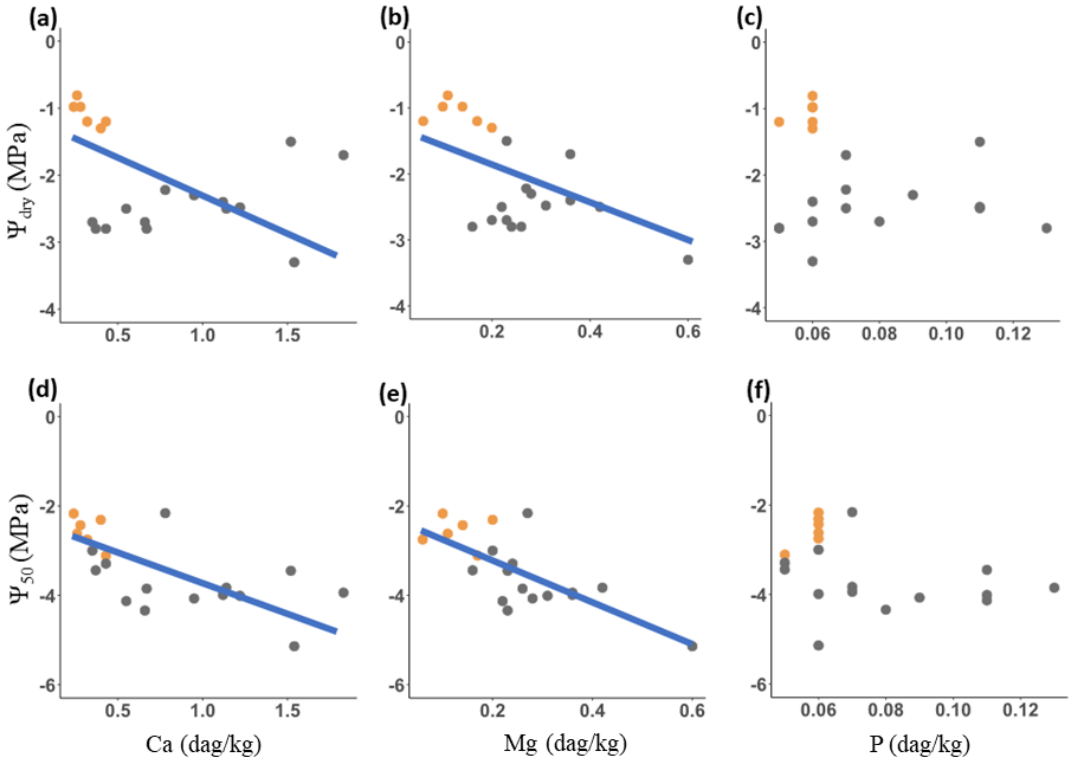

Fig. 8 Relationship between (a) leaf calcium (Ca) and minimum leaf water potential (Ψ_{dry}), (b) leaf magnesium (Mg) and Ψ_{dry}, leaf phosphorus (P) and Ψ_{dry}, (d) leaf Ca and branch xylem water potential at which 50% of embolism occurs (Ψ_{50}), (e) leaf Mg and $\Psi_{50,}$ (f) leaf P and $\Psi_{50,}$ for non-co-occurring species in the two forest communities in southern Amazonia. Amazonian Dark Earths (ADE) = ADE gray; non – (NDE) = orange. Lines were drawn for the relationships that were significant ($P < 0.05$).

$\Psi_{predawn}$, and tree diameter at breast height did not correlate with Ψ_{50} and Ψ_{min} (Table S5). We also did not find a significant relationship between tree height and Ψ_{50} and Ψ_{min} (results not shown).

DISCUSSION

This study investigated the impact of soil fertility on tree vulnerability to drought in two forests with contrasting soils: nutrient-rich Amazonian Dark Earths (ADE) and nutrient-poor non-ADE (NDE), both forests located within the same forest fragment and sharing the same climatic envelope in the southern edge of the Amazonia. We found community-level differences in Ψ_{dry} and HSM_{50} between the two forest types but not in xylem resistance to embolism, wood density (WD_{branch}), vessel area, mean vessel diameter (VD) and potential hydraulic conductivity (Kp). These differences in Ψ_{dry} and HSM_{50} show that soil fertility influences hydraulic strategies. Leaf calcium and

magnesium concentrations were negatively related to Ψ_{dry} for all species groupings evaluated (the full dataset, species occurring in both ADE and NDE forests and ADE- and NDE-exclusive species). These nutrients were also negatively related to Ψ_{50} for ADE- and NDE-exclusive species, but not for ADE- and NDE-co-occurring species. In contrast, leaf P only related to Ψ_{dry} for the group of co-occurring species whereas no trend was detected between leaf P and Ψ_{50}.

Plant hydraulic responses to increased nutrient availability

Our results support our hypothesis that the more acquisitive strategy of ADE trees would increase the risk of drought-induced hydraulic failure while NDE trees would have a more conservative strategy with greater regulation of leaf water potential throughout the day, avoiding negative HSM and therefore being less prone to the risk of embolism. This risk of hydraulic failure in the NDE forest was even more evident when we weighted the hydraulic traits (Ψ_{dry}, Ψ_{50}, Ψ_{88} and HSM_{50}) by the importance value index of each species, which was the measure chosen to represent how dominant a species is in the ADE and NDE forests. This has important implications for the use of plant hydraulics in ecological models, as variation in the HSM can help predict the carbon balance and tree mortality in Amazonian forests (Tavares et al., 2023). Incorporating soil fertility as an axis of HSM variation can result in more realistic models of the dynamics and functioning of tropical forests.

We find that the underlying driver of reduced HSM in the ADE site was not reduced xylem vulnerability to embolism (Ψ_{50}) but lower leaf water potential (Ψ_{leaf}), reflected not only in lower Ψ_{dry} but also lower $\Psi_{predawn}$ in the ADE (Fig. 4, Tables S1 and S2). Overall, $\Psi_{predawn}$ reflects the water potential of the soil within the root zone, representing the moment when the plant readjusts its water balance to that of the soil due to the nocturnal reduction in transpiration, allowing for the plant's water reservoirs to be recharged (Tardieu and Simonneau, 1998). Given the geographic proximity of the two forests, and the lack of difference in soil texture (Table 1; Oliveira et al., 2020) and topography between them, it is unlikely that this difference in $\Psi_{predawn}$ and HSM_{50} between ADE and NDE trees arises due to differences in soil structure or depth, that have previously been found to influence xylem vulnerability to embolism in Amazon forests (Garcia et al., 2023). Rather, a possible explanation for this difference may be related to a greater reduction of water reserves in the ADE soil due to a higher tree water use.

Relative to the NDE trees, the greater growth of ADE trees may result in higher transpiration rates, thus increasing the demand for soil water (Reich et al., 2014, Lugli et al., 2021; Bartholomew et al., 2022). While the larger tree size in the ADE (Fig 1c) might be expected to translate into deeper rooting depth (Brum et al., 2018) and thus greater capacity to take up water from depth, our data reveals that this effect, if it exists in the ADE, is insufficient to compensate for the extra plant water stress experienced.

Our results do not support our second prediction that species occurring on both ADE and NDE areas are able to adjust their hydraulic architecture to the prevailing edaphic conditions, as we found no differences between sites in co-occurring species resistance to embolism (Ψ_{50} and Ψ_{88}) or in wood density, vessel area, vessel diameter, and in potential hydraulic conductivity. Being part of the same forest fragment, the ADE and NDE plots are close to each other and connected, in this case it is expected that they share the same pollinators and seed dispersers, promoting genetic exchange between co-occurring species (Maherali et al., 2004; Rowland., et al 2023). This possibly reduces plasticity in hydraulic attributes in relation to soil fertility for co-occurring species. For non-co-occurring species, the fact that Ψ_{50} differs significantly could possibly be justified by the fact that they are phylogenetically distinct species (Cochard et al., 2008; Anderegg et al., 2015).

The absence of differences in the anatomical parameters between NDE and ADE trees suggests that they did not play a significant role in explaining the differences in safety margins observed between co-occurring species, nor in explaining the greater hydraulic safety among non-co-occurring species. In fact, vessel diameter is not a direct trait for embolism resistance in many cases and intervessel pit characteristics instead are supposed to be mechanistically related to embolism vulnerability in angiosperms (Jansen et al., 2009; Lens et al., 2022).

Calcium and magnesium are more strongly related to tree hydraulic status than phosphorus

Overall, we found leaf nutrient concentrations to be better predictors of Ψ_{dry} than of embolism resistance (Ψ_{50}). For ADE-and NDE-co-occurring species, we found that leaf Ca, Mg and P were significantly related to Ψ_{dry} while leaf Ca and Mg but not P were related to Ψ_{dry} for non-co-occurring species. While previous studies have found soil P to be correlated with Ψ_{50} in Amazon forests (Oliveira et al., 2019, Garcia et al., 2023) and with a cavitation vulnerability index calculated as the ratio between vessel diameter and

vessel density for Cerrado species. (Silva et al., 2021), we did not find a correlation between leaf P and Ψ_{50} for any of the groups studied although we did find that leaf Ca and Mg were significantly negatively related to Ψ_{50} in non-co-occurring species.

Our findings that trees in soils with higher availability of Ca face greater drought risk (lower HSM) are consistent with results of fertilization experiments at the ecosystem level. Green et al. (2012) reported that Ca addition altered local hydrology by temporarily increasing evapotranspiration (in this case defined as the difference between precipitation and runoff) and primary productivity in mountain forests in the northern United States. For tropical forests, 8 months after the addition of nutrients, trees from secondary vegetation in the Amazon increased net photosynthesis rates and presented more negative Ψ_{midday} values and lower soil moisture upon fertilization by both Ca and P, but not when fertilized only with P (Silva et al., 2008).

Hydraulic traits as a filter for community assembly in southern Amazon forests

The availability of resources such as soil nutrients is a predominant driver of tree community assembly in tropical forests (Peguero et al., 2023). Our results point to a clear niche separation between ADE-exclusive and NDE-exclusive species (Fig. 9) such that these two groups of species do not overlap in the multivariate trait space. The species exclusive to the NDE forest are grouped based on hydraulic traits, whereas those found only in the ADE forest are clustered according to leaf nutrients, tree height, and stem diameter. As expected, this pattern of separation was not as strong for the co-occurring species and they are clustered between the ADE-and NDE-exclusive species in the multivariate space. Although these results need further confirmation, this pattern suggests that ADE species may require environments with higher soil resource availability and have likely undergone selection for traits that enhance resource acquisition and growth, as they exhibit greater height and larger stem diameters. In fact, soil fertility was the most relevant factor for the occurrence of *Hymenaea parvifolia* in lowlands of Bolivia (Toledo et al., 2012), which corroborated our findings with a species of the same genus (*Hymenaea courbaril*) that occurred exclusively in ADE. It is important to note that among the non-co-occurring species are the species with the greatest biomass contribution to each forest where they occur, and possibly due to being in their optimal environment, they were able to maintain a higher HSM which suggests they would be less vulnerable to hydraulic failure during prolonged periods of drought. Co-occurring

species appear to be generalists and were more prone to hydraulic failure in an environment with higher nutrient availability.

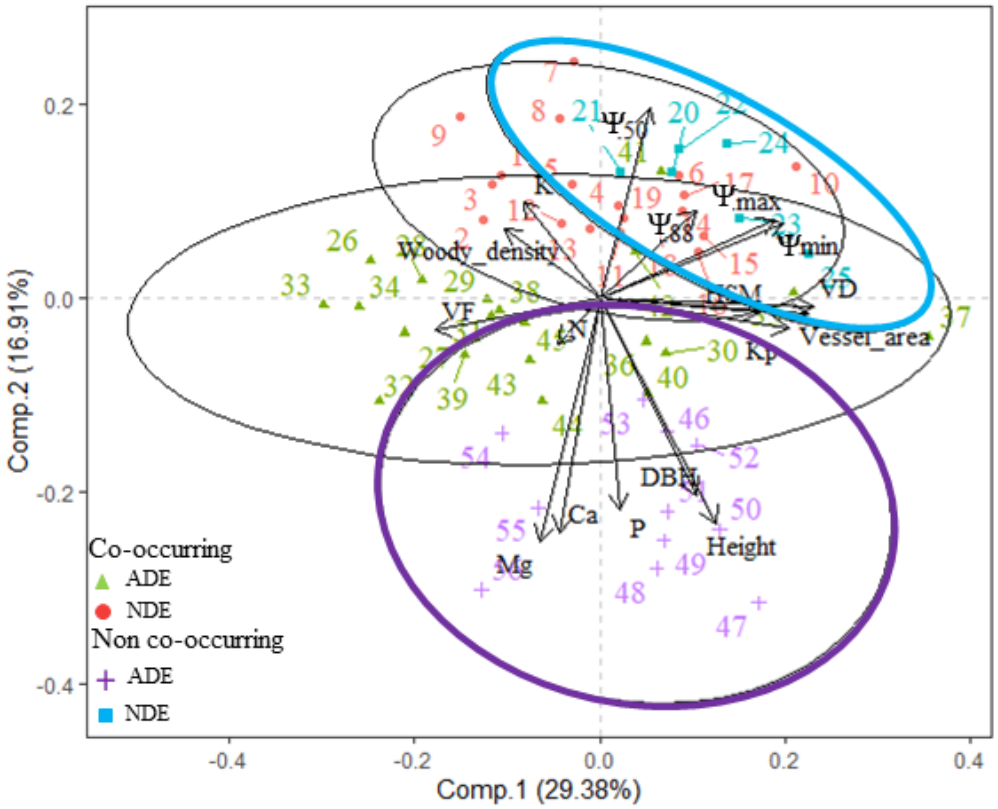

Fig. 9 Plots of the first two principal components (comp. 1 and comp. 2) in an analysis of variation of hydraulic and leaf nutrient traits for all species studied. Individuals plotted by groups, variability of individuals from each group, and their distributions along the trait axes were represented by dispersion ellipses. The larger the area of the ellipse, the greater the variation for the group. The ellipses highlighted in blue, and purple refer to the set of non-cooccurring species from Amazonian Dark Earths (ADE) and non – ADE (NDE), while the grey ellipses corresponded to the species occurring on both ADE and NDE plots (co-occurring species).

CONCLUSION

This study reveals significant differences in the hydraulic safety margin (HSM_{50}) between two forests with contrasting soils - the Amazonian Dark Earths (ADE) and the non-ADE forest (NDE), within the same climatic envelope. ADE, with its greater resource availability in soil and leaves, exhibited a narrower HSM_{50} compared to NDE. Furthermore, the distinction between co-occurring and non-co-occurring species revealed distinct adaptive strategies in response to soil resource availability. Our study highlights the importance of considering the axis of hydraulic characteristics linked to growth

modulated by nutrient availability in the soil. More studies that advance the understanding of plant responses involving this axis will allow for better informed models of the ecological strategies of vegetation, contributing to better representative predictions of the responses of tropical forests to the current trend of climate warming.

ACKNOWLEDGEMENTS

The authors acknowledge the Coordenação de Aperfeiçoamento de Pessoal de Nível Superior (CAPES, Brazil) under Financing Code 001 and for the scholarships (Process Number 88882.329278/2019-01 to JRVA, 88887.808009/2023-00 to JRVA); the National Council for Scientific and Technological Development (CNPq, Brazil) grant number 312336/2023-3 awarded to ACF and fellowships (RGB, CHLO, JWS). Fieldwork was supported by the NERC-funded ARBOLES (NE/S011811/1) project, Royal Society Newton Advanced International Fellowship (NAF\R1\180405) and by the University of Brasília through a PROEX resource. We also acknowledge financing by the State of São Paulo Research Foundation - FAPESP (Young Researcher Grant - JP 2018/01847-0 awarded to PG; and grant 2018/24514-7 to JRVA). We also thank Luciano Pereira for revising the manuscript.

AUTHOR CONTRIBUTIONS

RGB, DG, BM, BJM and ACF conceived the research. RGB, DG, ACF carried out the analysis and interpretation of the results and drafted the manuscript. RGB, CHLO, JWS, CT, MA collected data on leaf water potential, vulnerability curves and wood density. JA, MT, PG carried out the processing and anatomical analysis of the wood samples. JT, EG, EAO, PG, MT contributed to the analysis and interpretation of the results and commented on previous versions of the manuscript. All authors approved the final version of the manuscript.

SUPPORTING INFORMATION

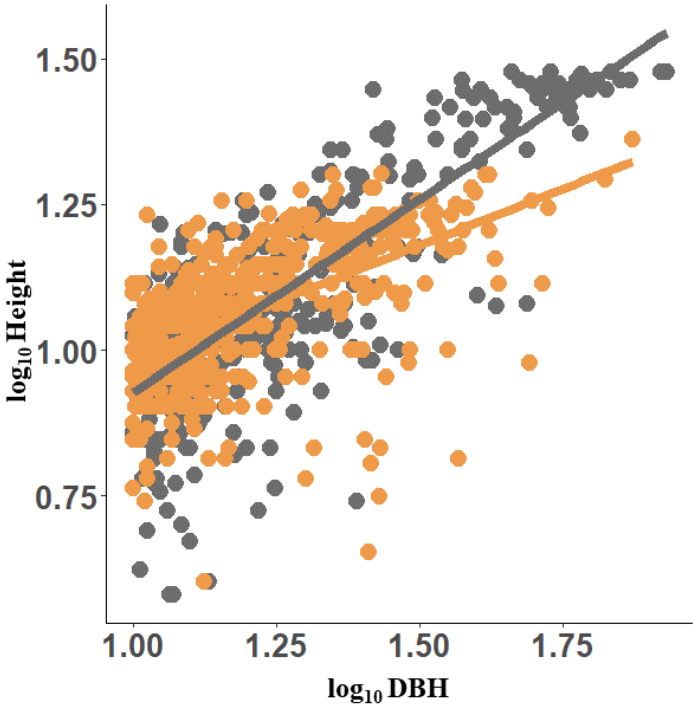

Fig S1 The relationship between tree height (Height; m) and stem diameter (DBH; cm) for all species of the ADE (gray circles and gray line) and NDE (orange circles and orange line) forest plots. Relationships were obtained with $\log_{10}$ transformed values. Straight line equation for ADE: $\log_{10}$ Height = 0.26 + 0.66 $\log_{10}$ DBH, R^2_m = 0.78, R^2_c=0.84 and for NDE: $\log_{10}$ Height = 0.61 + 0.39 $\log_{10}$ DBH, R^2_m = 0.49, R^2_c = 0.73.

Table S1 Mean values and the *P*-values of the mixed linear model with forest type (NDE and ADE) as a fixed effect and species as a random effect for the comparison of hydraulic attributes and wood anatomical properties of branches for co-occurring and non-co-occurring tree species of the two forest communities in southern Amazonia. ADE = Amazonian Dark Earth and NDE = non-ADE. Values in bold represent significant differences at the 95% confidence level ($P < 0.05$).

	Co-occurring			Non-co-occurring		
	ADE	NDE	*P*-value	ADE	NDE	*P*-value
Ψ_{50} (MPa)	-3.23	-3.06	0.49	-3.7	-2.56	**0.02**
Ψ_{88} (MPa)	-5.30	-5.13	0.70	-5.2	-3.76	0.1
Ψ_{dry} (MPa)	-3.35	-1.86	**0.0006**	-2.4	-1.07	**0.0001**
$\Psi_{predawn}$ (MPa)	-2.46	-0.73	**0.00**	-1.36	-0.63	**0.002**
HSM_{50} (MPa)	-0.12	1.25	**0.02**	1.28	1.69	0.37
WD_{branch} (g cm^{-3})	0.63	0.65	0.73	0.61	0.57	0.6
Vessel area (mm^2)	0.001	0.001	0.71	0.001	0.002	0.25
VD (mm)	0.03	0.04	0.57	0.04	0.04	0.24
Kp	9.41	9.85	0.80	9.70	11.13	0.6

Table S2 Summary of hydraulic traits and statistical results for unweighted and weighted averages for the two forest communities in southern Amazonia (ADE - Amazonian Dark Earths; NDE - non-ADE). The CWM_{ivi} is the result of a Monte Carlo method probability distribution with the test statistic being difference in the CWM_{ivi} trait between the two forest types. Values in bold represent significant differences at the 95% confidence level ($P < 0.05$)

	ADE				**NDE**				**Statistics**		
Traits	mean	sd	CWM_{ivi}	95%	Mean	Sd	CWM_{ivi}	95%	*P*	T	P_{CWMivi}
Ψ_{50}	-3.40	0.66	-3.5	-3.05	-2.95	0.53	-2.89	3.2	0.077	-1.76	**0.001**
Ψ_{88}	-5.30	1.34	-5.48	-3.86	-4.82	1.14	-4.63	-4.8	0.447	-0.81	0.11
Ψ_{dry}	-3.0	1.59	-3.83	-3.1	-1.60	0.93	-1.40	-0.63	**0.016**	-3.3	**0.001**
$\Psi_{predawn}$	-2.70	1.33	-2.55	-1.93	-0.73	0.53	-0.77	-0.01	**0.000**	-7.19	**0.002**
HSM_{50}	0.49	1.61	-0.32	1.86	1.34	1.03	1.48	0.14	**0.032**	-2.77	**0.003**

Table S3: Results of the linear mixed models that test the relationships between leaf calcium (Ca), magnesium (Mg) and phosphorus (P) and Ψ_{dry}, the minimum leaf water potential measured in the dry season for co-occurring and non-co-occurring species in the Amazonian Dark Earths (ADE) and non – ADE (NDE) forests of southern Amazonia. Ψ_{dry} as response variable, Ca, Mg and P as fixed effect and species as random effect (1|species). R^2_m and R^2_c are, respectively, marginal and conditional pseudo-R^2.

Model	Co-occurring			Non co-occurring		
Ψ_{dry} ~ Ca + (1|Species)	Parameters	Value	Standard Error	Parameters	Value	Standard Error
	Intercept	-1.8	0.61	Intercept	-1.1	0.38
	Ca	-1.7	0.69	Ca	-1.2	0.22
	Species			Species		
	P value = 0.01			*P* value = 0.00		
	R^2_m = 0.07			R^2_m = 0.28		
	R^2_c = 0.58			R^2_c = 0.98		

Model	Co-occurring			Non co-occurring		
Ψ_{dry} ~ Mg + (1|Species)	Parameters	Value	Standard Error	Parameters	Value	Standard Error
	Intercept	-1.2	0.85	Intercept	-1.3	0.27
	Mg	-7.3	3.22	Mg	-2.8	0.54
	Species			Species		
	P value = 0.02			*P* value = 3.297e-05		
	R^2_m = 0.06			R^2_m = 0.22		
	R^2_c = 0.62			R^2_c = 0.96		

Model	Co-occurring			Non co-occurring		
Ψ_{dry} ~ P + (1| Species)	Parameters	Value	Standard Error	Parameters	Value	Standard Error
	Intercept	0.98	1.20	Intercept	1.98	0.41
	P	52.80	14.72	P	-0.73	3.96
	Species			Species		
	P value = 0.001			*P* value = 0.83		
	R^2_m=0.18			R^2_m= 0.00		
	R^2_c=0.77			R^2_c= 0.91		

Table S4: Results of the linear mixed models that test the relationships between leaf calcium (Ca), magnesium (Mg) and phosphorus (P) and Ψ_{50}, branch xylem water potential at which 50% of embolism occurs for co-occurring and non-co-occurring species in the Amazonian Dark Earth (ADE) and non – ADE (NDE) forests of southern Amazonia. Ψ_{min} as response variable, Ca, Mg and P as fixed effects and species as random effect (1|species). R^2_m and R^2_c are, respectively, marginal and conditional pseudo-R^2.

Model	Co-occurring			Non co-occurring		
Ψ_{50} ~ Ca + (1| Species)	Parameters	Value	Standard Error	Parameters	Value	Standard Error
	Intercept	-3.19	0.28	Intercept	-2.33	0.4
	Ca	0.007	0.46	Ca	-1.38	0.42
	Species			Species		
	P value = 0.83			*P* value = 0.00		
	R^2_m = 0.00			R^2_m = 0.47		
	R^2_c = 0.14			R^2_c = 0.79		

Model	Co-occurring			Non co-occurring		
Ψ_{50} ~ Mg + (1| Species)	Parameters	Value	Standard Error	Parameters	Value	Standard Error
	Intercept	-3.11	0.46	Intercept	-2.24	0.33
	Mg	-0.23	2.1	Mg	-4.71	1.18
	Species			Species		
	P value = 0.92			*P* value = 0.00		
	R^2_m = 0.00			R^2_m = 0.50		
	R^2_c = 0.15			R^2_c = 0.60		

Model	Co-occurring			Non co-occurring		
Ψ_{50} ~ P + (1| Species)	Parameters	Value	Standard Error	Parameters	Value	Standard Error
	Intercept	-3.64	0.58	Intercept	-2.81	0.65
	P	7.04	8.25	P	-8.08	8.13
	Species			Species		
	P value = 0.32			*P* value = 0.28		
	R^2_m =0.02			R^2_m = 0.05		
	R^2_c = 0.09			R^2_c= 0.49		

Table S5: Results of the linear mixed models that test the relationships between tree diameter at breast height (DBH) and Ψ_{50}, branch xylem water potential at which 50% of embolism occurs and Ψ_{dry}, which is the minimum water potential recorded in situ at the peak of the dry season and $\Psi_{predawn}$, for co-occurring and non-co-occurring species in the Amazonian Dark Earth (ADE) and non – ADE (NDE) forests of southern Amazonia. Hydraulics traits as response variable, DBH as fixed effect and species as random effect (1|species). R^2_m and R^2_c are, respectively, marginal and conditional pseudo-R^2.

Model	Co-occurring			Non co-occurring		
Ψ_{50} ~ DBH + (1| Species)	Parameter	Value	Standard Error	Parameters	Value	Standard Error
	Intercept	-2.89	0.51	Intercept	-3.48	0.56
	DBH	-0.02	0.02	DBH	0.00	0.01
	Species			Species		
	P value = 0.509			*P* value = 0.961		
	R^2_m = 0.002			R^2_m = 0.00		
	R^2_c = 0.31			R^2_c = 0.57		

Model	Co-occurring			Non co-occurring		
Ψ_{dry} ~ DBH + (1| Species)	Parameter	Value	Standard Error	Parameters	Value	Standard Error
	Intercept	-2.12	0.58	Intercept	-2.34	0.38
	DBH	-0.04	0.02	DBH	0.01	0.00
	Species			Species		
	P value = 0.145			*P* value = 0.194		
	R^2_m = 0.01			R^2_m = 0.001		
	R^2_c = 0.72			R^2_c =0.946		

Model	Co-occurring			Non co-occurring		
$\Psi_{predawn}$ ~ DBH + (1| Species)	Parameter	Value	Standard Error	Parameters	Value	Standard Error
	Intercept	-0.95	0.54	Intercept	-1.19	0.30
	DBH	-0.04	0.02	DBH	0.00	0.01
	Species			Species		
	P value = 0.11			*P* value = 0.63		
	R^2_m =0.02			R^2_m = 0.00		
	R^2_c = 0.65			R^2_c= 0.79		

REFERENCES

Adams HD, Zeppel MJ, Anderegg WR, Hartmann H, Landhäusser SM, Tissue DT, Hudson PJ, Franz TE, Allen CD, Anderegg LD., et al 2017. A multi-species synthesis of physiological mechanisms in drought-induced tree mortality. *Nature ecology & evolution* **1**: 1285-1291.

Allen CD, Macalady AK, Chenchouni H, Bachelet D, McDowell N, Vennetier M, Kitzberger T, Rigling A, Breshears DD, Hogg TEH, et al. 2010. A global overview of drought and heat-induced tree mortality reveals emerging climate change risks for forests. *Forest Ecology and Management* **259**: 660-684.

Allen CD, Breshears DD, McDowell NG. 2015. On underestimation of global vulnerability to tree mortality and forest die-off from hotter drought in the Anthropocene. *Ecosphere* **6:** 1–55.

Anderegg WRL. 2015. Spatial and temporal variation in plant hydraulic traits and their relevance for climate change impacts on vegetation. *New Phytologist* **205**: 1008-1014.

Anderegg WR, Klein T, Bartlett M, Sack L,Pellegrini AF, Choat B, Jansen S. 2016. Meta-analysis reveals that hydraulic traits explain cross-species patterns of drought-induced tree mortality across the globe. *Proceedings of the National Academy of Sciences, USA* **113**: 5024–5029

Aragão LEOC, Malhi Y, Metcalfe DB, Silva-Espejo JE, Jiménez E, Navarrete D, Almeida S, Costa ACL, Salinas N, Phillips OL et al. 2009. Above-and below-ground net primary productivity across ten Amazonian forests on contrasting soils. *Biogeosciences* **6: 2759–2778.**

Bartholomew DC, Banin LF, Bittencourt PR, Suis MA F, Mercado LM, Nilus R, Burslem DFRP, Rowland, L. 2022. Differential nutrient limitation and tree height control leaf physiology, supporting niche partitioning in tropical dipterocarp forests. *Functional Ecology* **36:** 2084-2103.**Barton K. 2024.**

MuMIn: multi-model inference. [WWW document] https://cran.rproject.org/web/packages/MuMIn/index.html. [accessed 1 August 2024].

Bauters M, Janssens IA, Wasner D, Doetterl S, Vermeir P, Griepentrog M, Drake TW, Six J, Barthel M, Baumgartner S. 2022. Increasing calcium scarcity along Afrotropical forest succession. *Nature Ecology & Evolution* 6: p. 1122-1131.

Bhaskar R, Ackerly DD. 2006. Ecological relevance of minimum seasonal water potentials. *Physiologia Plantarum* **127:** 353–359.

Bittencourt PRL, Pereira L, Oliveira RS. 2018. Pneumatic Method to Measure Plant Xylem Embolism. *Bio-protocol* **8**: 20.

Bonan GB. 2008. Forests and climate change: forcings, feedbacks, and the climate benefits of forests. *Science* **320**: 1444–1449.

Brodribb TJ, Powers J, Cochard H, Choat B. 2020. Hanging by a thread? Forests and drought. *Science* **368**: 261-266.

Brum M, Vadeboncoeur MA, Ivanov V, Asbjornsen H, Saleska S, Alves LF, Penha D, Dias JD, Aragão LEOC, Barros F et al. 2018. Hydrological niche segregation defines forest structure and drought tolerance strategies in a seasonal Amazon forest. *Journal of Ecology*. **107**: 318-333.

Cochard H, Barigah ST, Kleinhentz M, Eshel, A. 2008. Is xylem cavitation resistance a relevant criterion for screening drought resistance among Prunus species? *Journal of Plant Physiology* **165**: 976-982.

Crawley MJ. 2013. **The R book. Wiley Publishing.**

Delzon S, Cochard H. 2014. Recent advances in tree hydraulics highlight the ecological significance of the hydraulic safety margin. *New Phytologist* **203:** 355-358.

Dixon HH, & Joly J. 1895. On the ascent of sap. Philosophical Transactions of the Royal Society of London. B.,186, 563–576.

ForestPlots.net et al. 2021. Taking the pulse of Earth's tropical forests using networks of highly. *Biologival Conservation* **260**:108849.

Duffy PB, Brando P, Asner GP, Field CB. 2015. Projections of future meteorological drought and wet periods in the Amazon. *Proceedings of the National Academy of Sciences* **112**: 13172-13177.

Garcia MN, Domingues TF, Oliveira RS, Costa FRC. 2023. The biogeography of embolism resistance across resource gradients in the Amazon. *Global Ecology and Biogeography* **32:** 2199-2211.

Garnier E, Cortez J, Billès G, Navas ML, Roumet C, Debussche M, Laurent G, Blanchard, A, Aubry D, Bellmann A, Neill C. 2004. Plant functional markers capture ecosystem properties during secondary succession. *Ecology*, **85**: 2630-2637.

Grime JP. 2006. Plant Strategies, Vegetation Processes, and Ecosystem Properties. Wiley, 2nd Edition, 464 pp. ISBN: 978-0-470-85040-4

Guillemot, J. Martin-StPaul NK, Bulascoschi L, Poorter L, Morin X, Pinho BX, Maire G, Bittencourt P, Oliveira RS, Bongers F, et al. 2022. Small and slow is safe: On the drought tolerance of tropical tree species. *Global Change Biology* **28**: 2622-2638.

Green MB, Bailey AS, Bailey SW, Battles JJ, Campbell JL, Driscoll CT, Fahey TJ, Lepine LC, Likens GE, Ollinger SV, Schaberg, PG. 2013. Decreased water flowing from a forest amended with calcium silicate. *Proceedings of the National Academy of Sciences* **110:** 5999-6003.

Heckenberger M J, Russell JC, Fausto C, Toney JR, Schmidt MJ, Pereira E, Franchetto B, Kuikuro A. 2008. Pre-Columbian urbanism, anthropogenic landscapes, and the future of the Amazon. *Science* **321**: 1214-1217.

Huang G, Hayes PE, Ryan MH, Pang J, Lambers H. 2017. Peppermint trees shift their phosphorus-acquisition strategy along a strong gradient of plant-available phosphorus by increasing their transpiration at very low phosphorus availability. *Oecologia* **185**: 387-400.

Iriarte J, Elliott S, Maezumi SY, Alves D, Gonda R, Robinson M, Souza JG, Watling J, Handley J, et al. 2020. The origins of Amazonian landscapes: Plant cultivation,

domestication and the spread of food production in tropical South America. *Quaternary Science Reviews* **248**: 106582.

Jansen S, Choat B, Pletsers A. 2009. Morphological variation of intervessel pit membranes and implications to xylem function in angiosperms. *American Journal of Botany*, ***96:*** 409-419.

Jiménez-Muñoz JC, Mattar C, Barichivich J, Santamaría-Artigas A, Takahashi K, Malhi Y, Sobrino JA, Schrier GVD. 2016. Record-breaking warming and extreme drought in the Amazon rainforest during the course of El Niño 2015–2016. *Scientific Reports* **6**: 33130.

Johnson DA. **1940**. Plant Microtechniques. McGraw-Hill Book Co. Inc.

Jones, H. G., & Sutherland, R. A. 1991. Stomatal control of xylem embolism. *Plant, Cell & Environment*, 14: 607-612.

Kuznetsova A, Brockhoff PB, Christensen, RHB. 2017**. lmerTest Package: Tests in linear mixed effects models. *Journal of Statistical Software*** 82**: 1–26.**

Lens F, Gleason SM, Bortolami G, Brodersen C, Delzon S, Jansen S. 2022. Functional xylem characteristics associated with drought-induced embolism in angiosperms. *New Phytologist* **236**: 2019-2036.

Levene H. 1960. Robust tests for the equality of variance In: Olkin, I., Contributions to Probability and Statistics: Essays in Honor of Harold Hotelling.

Lloyd J, Domingues TF, Schrodt F, Ishida FY, Feldpausch TR, Saiz G, Quesada CA, Schwarz M, Torello-Raventos M, Gilpin M et al. 2015. Edaphic, structural and physiological contrasts across Amazon basin forest-savanna ecotones suggest a role for potassium as a key modulator of tropical woody vegetation structure and function. *Biogeosciences* **12**: 6529–6571.

Lugli LF, Rosa JS, Andersen KM, Di Ponzio R., Almeida RV, Pires M, Cordeiro AL, Cunha HF, Martins NP, Assis RL. 2021. Rapid responses of root traits and productivity to phosphorus and cation additions in a tropical lowland forest in Amazonia. *New Phytologist* 230: 116-128.

Maherali H, Pockman WT, Jackson RB. 2004. Adaptive variation in the vulnerability of woody plants to xylem cavitation. *Ecology* **85:** 2184-2199.

Markesteijn L, Poorter L, Paz H, Sack L, Bongers F. 2011. Ecological differentiation in xylem cavitation resistance is associated with stem and leaf structural traits. *Plant, Cell and Environment* **34**: 137–148.

McBratney AB, Santos MM, Minasny B. 2003. On digital soil mapping. *Geoderma*, **117**: 3-52.

Mcdowell NG, Allen CD, Anderson-Teixeira K, Aukema BH, Bond-Lamberty B, Chini L, Clark JS, Dietze M, Grossiord C, Hanbury-Brown A, et al. 2020. Pervasive shifts in forest dynamics in a changing world. *Science* **368**: 9463.

Meinzer FC, Johnson DM, Lachenbruch B, McCulloh KA, Woodruff DR. 2009. Xylem hydraulic safety margins in woody plants: coordination of stomatal control of xylem tension with hydraulic capacitance. *Functional Ecology* **23:** 922–930

Moore GW, Edgar CB., Vogel JG, Washington-Allen RA, March RG, Zehnder R. 2016. Tree mortality from an exceptional drought spanning mesic to semiarid ecoregions. *Ecological Applications* **26**: 602-611.

Mori GB, Schietti, J, Poorter L, Piedade MTF. 2019. Trait divergence and habitat specialization in tropical floodplain forests trees. *PLoS One* **14**: 0212232.

Oliveira EA, Marimon-Junior BH, Marimon BS, Iriarte J, Morandi PS, Maezumi SY, Nogueira DS, Aragão L, Silva I, Feldpausch, T. 2020. Legacy of Amazonian Dark Earth soils on forest structure and species composition. *Global Ecology and Biogeography* **29**: 1458-1473.

Oliveira EA, Feldpausch TR, Marimon BS, Morandi PS, Phillips OL, Bird M, Murakami A, Arroyo L, Quesada CA. Marimon-Junior BH. 2022. Soil pyrogenic carbon in southern Amazonia: Interaction between soil, climate, and above-ground biomass. *Frontiers in Forests and Global Change* **5**: 880-963.

Oliveira RS, Costa FRC, van Baalen E, de Jonge A, Bittencourt PR, Almanza Y, de Barros FV, Cordoba EC, Fagundes MV, Garcia S et al. 2019. Embolism resistance drives the distribution of Amazonian rainforest trees pecies along hydrotopographic gradients. *New Phytologist* **221:** 1457–1465.

Oliveira RS, Eller CB, Barros FV, Hirota M, Brum M, Bittencourt P. 2021. Linking plant hydraulics and the fast–slow continuum to understand resilience to drought in tropical ecosystems. *New Phytologist*, **230**: 904-923.

Osazuwa-Peters O, Zanne AE. 2010. Wood density protocol. [WWW document] URL https://prometheusprotocols.net/structure/morphology/stem-morphology/wood-density-protocol/. [accessed 10 January 2024].

Oulehle F, Urban O, Tahovská K, Kolář T, Rybníček M, Büntgen U, Hruska J, Časlavsky J, Trnka, M. 2023. Calcium availability affects the intrinsic water-use efficiency of temperate forest trees. *Communications Earth & Environment* **4**: 199.

Paligi SS, Link RM, Isasa E, Bittencourt P, Cabral JS, Jansen S. Oliveira RS, Pereira L, Schuldt B. 2023. Assessing the agreement between the pneumatic and the flow-centrifuge method for estimating xylem safety in temperate diffuse-porous tree species. *Plant Biology* **25**: 1171-1185.

Peguero G, Coello F, Sardans J, Asensio D, Grau O, Llusià J, Ogaya R, Urbina I, Langenhove LV, Verrckt LT, et al. 2023. Nutrient-based species selection is a prevalent driver of community assembly and functional trait space in tropical forests. *Journal of Ecology* **111**: 1218-1230.

Pereira L, Bittencourt PRL, Oliveira RS, Junior MBM, Barros FV, Ribeiro RV, Mazzafera P. 2016. Plant pneumatics: stem air flow is related to embolism – new perspectives on methods in plant hydraulics. *New Phytologist* **211**: 357-370.

Phillips OL, Aragão LEOC, Lewis SL, Fisher JB, Lloyd J, Lopez-Gonzalez G, Malhi Y, Monteagudo A, Peacock J, Quesada CA et al. 2009. Drought sensitivity of the amazon rainforest. *Science* **323:** 1344–1347.

Pinheiro J, Bates D, DebRoy S, Sarkar D, R Core Team. 2024. Nlme: Linear and Nonlinear Mixed Effects Models. R package version 3.1-118. [WWW document]URL http://CRAN.R-project.org/package=nlme [accessed 1 August 2024].

Powers JS, Vargas GG, Brodribb TJ, Schwartz NB, Perez-Aviles D, Smith-Martin CM, Becknell JM, Aureli F, Blanco R, Calderon-Morales E et al. 2020. A catastrophic tropical drought kills hydraulically vulnerable tree species. *Global Change Biology* **26:** 3122–3133.

Quesada CA, Phillips OL, Schwarz M, Czimczik CI, Baker TR, Patino S, Fyllas NM, Hodnett MG, Herrera R, Almeida S et al. 2012. Basin-wide variations in Amazon forest structure and function are mediated by both soils and climate. *Biogeosciences* **9:** 2203–2246.

R Development Core Team. 2023. *R: a language and environment for statistical computing, v.4.3.2*. Vienna, Austria: R foundation for Statistical Computing. URL http://www.r-project.org.

Reich PB. 2014. The world-wide 'fast–slow' plant economics spectrum: a traits manifesto. *Journal of Ecology* **102:** 275–301.

Rowland L, da Costa AC, Galbraith DR, Oliveira RS, Binks OJ, Oliveira AA, Pullen AM, Doughty CE, Metcalfe DB, Vasconcelos SS et al. 2015. Death from drought in tropical forests is triggered by hydraulics not carbon starvation. *Nature* 528: 119

Rowland L, Ramírez-Valiente JA, Hartley IP, Mencuccini M. 2023. How woody plants adjust above-and below-ground traits in response to sustained drought. *New Phytologist* **239**: 1173-1189.

Sardans J, Peñuelas J. 2015. Potassium: a neglected nutrient in global change. *Global Ecology and Biogeography* **24:** 261-275.

Scholander PF, Bradstreet ED, Hemmingsen EA, Hammel HT. 1965**. Sap pressure in vascular plants: negative hydrostatic pressure can be measured in plants. *Science*, 148: 339-346.**

Scholz FG, Bucci SJ, Goldstein G, Meinzer FC, Franco AC, Miralles-Wilhelm F. 2007. Removal of nutrient limitations by long-term fertilization decreases nocturnal water loss in savanna trees. *Tree Physiology* 27: 551-559.

Schuldt B, Knutzen F, Delzon S, Jansen S, Muller-Haubold H, Burlett R, Clough € Y, Leuschner C. 2016. How adaptable is the hydraulic system of European beech in the face of climate change-related precipitation reduction? *New Phytologist* **210:** 443–458.

Silva CEM, Carvalho Gonçalves JF, Feldpausch TR. 2008. Water-use efficiency of tree species following calcium and phosphorus application on an abandoned pasture, central Amazonia, Brazil. *Environmental and Experimental Botany* **64**: 189-195.

Silva LCR, Corrêa RS, Wright JL, Bomfim B, Hendricks L, Gavin DG, Muniz AW, Martins GC, Motta AV, Barbosa JZ, et al. 2021. A new hypothesis for the origin of Amazonian Dark Earths." *Nature Communications* **12:** 127.

Shapiro SS, Wilk MB. 1965. An analysis of variance test for normality (complete samples). *Biometrika*, 52: 591-611.

Smith C, Baker JCA, Spracklen DV. 2023. Tropical deforestation causes large reductions in observed precipitation. *Nature*, **615**: 7951, 270-275.

Tardieu F, Simonneau T. 1998.Variability among species of stomatal control under fluctuating soil water status and evaporative demand: modelling isohydric and anisohydric behaviours. *Journal of Experimental Botany*, **49**: 419-432.

Tavares, JV, Oliveira RS, Mencuccini M, Signori-Müller C, Pereira L, Diniz FC, Gilpin M, Zevallos MM, Yapayccana CS, Acosta M, et al. 2023. Basin-wide variation in tree hydraulic safety margins predicts the carbon balance of Amazon forests. *Nature* **617**: 111-117.

Thomas R, Lello J, Medeiros R, Pollard A, Robinson P, Seward A *et al*. 2017. Data analysis with R Statistical Software: a guidebook for scientists. Eco-Explore, United Kindgom.

Toledo M, Peña-Claros M, Bongers F, Alarcón A, Balcázar J, Chuviña J, Leaño C, Licona JC, Poorter L. 2012. Distribution patterns of tropical woody species in response to climatic and edaphic gradients. *Journal of Ecology* **100**: 253-263.

Tränkner M, Tavakol E, Jákli B. 2018. Functioning of potassium and magnesium in photosynthesis, photosynthate translocation and photoprotection. *Physiologia Plantarum*, ***163***: 414-431.

Tyree MT, & Zimmermann M H. 2002. **Xylem Structure and the Ascent of Sap**. Heidelberg.

Wheeler EA, Baas P, Gasson P. 1989. IAWA list of microscopic features for hardwood identification. *IAWA Bulletin* **10**: 219- 332.

Watanabe T, Broadley MR, Jansen S, White PJ, Takada J, Satake K, Takamatsu T, Tuah SJ, Osaki M. 2007. Evolutionary control of leaf element composition in plants. *New Phytologist* **174**: 516-523.

White PJ, Broadley MR. 2003. Calcium in plants. *Annals of Botany* **92**: 487-511.

Wright SJ. 2019. Plant responses to nutrient addition experiments conducted in tropical forests. *Ecological Monographs* **89**: 013 -82.

Yin Y, Zhou YB, Li H, Zhang SZ, Fang Y, Zhang YJ, Zou X. 2022. Linking tree water use efficiency with calcium and precipitation. *Tree Physiology* **42**: 2419-2431.

CAPÍTULO 2

Wide variation in hydraulic safety margins across and within Southern Amazon forests.

Submitted to Journal of Ecology

ABSTRACT

1. Southern Amazon forests have experienced more accentuated changes in climate than other Amazon regions. To help conserve and manage these ecosystems, it is crucial to understand the sensitivity of these forests to these changes that are increasing the duration and intensity of drought events and increasing the evaporative demand of the atmosphere.
2. We sampled four forests at the southern edge of the Amazon and measured leaf water potential throughout the day (Ψ_{leaf}), the branch xylem water potential at which 50% of embolism occurs (Ψ_{50}), hydraulic safety margin (HSM_{50}), and wood density (WD). We also compared our results with measurements from the literature for ten additional forests distributed across the Amazon and subjected to different levels of climatic water deficit throughout the year. We weighed the species sampled within each forest by basal area to obtain community weighted mean values.
3. The resistance to hydraulic failure of forests at the southern edge of Amazon is high, with more negative Ψ_{50} compared to other Amazonian forests. However, while some southern edge forests and species operate with positive HSM_{50}, others had negative HSM_{50}, indicating a high risk of hydraulic failure. Along a climate gradient Ψ_{50_CWM} becomes more negative with increasing MCWD (climatic water deficit). In contrast, there was no significant relationship between HSM_{50_CWM} and MCWD.
4. Across species, we found a positive but weak coordination between Ψ_{50} and Ψ_{dry} (midday leaf water potential during driest period of the year). However, when partitioning the forests according to MCWD (dry, intermediate, and wet), this

coordination disappeared towards the dry and humid extremes and remained weak in the intermediate MCWD region.

5. *Synthesis*. Our results suggest that, although forests at the southern edge of the Amazon have selected species with high hydraulic resistance, they are not equally safe in terms of HSM. Furthermore, we did not observe a clear coordination between Ψ_{50} and Ψ_{dry} and between HSM_{50} and MCWD across forests distributed throughout the Amazon, which may be a consequence of species-specific responses to seasonal changes in water availability, possibly exerting a more determining influence on HSM than climatic conditions.

KEYWORDS: Amazon functional diversity, ecophysiology, hydraulic failure, hydraulic safety margins, plant hydraulics, plant–water relations, xylem embolism, xylem hydraulic traits

INTRODUCTION

Currently, due to climate change, some tropical forests have been facing longer drought events and more frequent changes in rainfall, with this scenario being intensively exacerbated by anthropogenic actions of environmental degradation (Philips et al., 2009; Marengo et al., 2011, 2018; Fu et al., 2013; IPCC 2019). One of the most endangered encompasses the Amazon-Cerrado transition, an area of high ecological importance, comprising a complex mosaic of different vegetation types (Ratter el al., 1973; Marimon et al., 2006, 2014; Marques et al., 2019) representing an ecological tension zone (Ratter et al., 1997; Fearnside, 2005; Silvério et al., 2015). It is the largest and most diverse forest-savanna transition on the planet. It also coincides with one of the largest agricultural frontiers in the tropics. It is estimated that nearly half of the original forest cover has already been affected, resulting in a negative carbon balance (Andersen et al., 2002; Coe et al., 2013; Gatti et al., 2021). In this complex context, studying the functioning of the remaining forests becomes a priority.

Water is one of the main factors limiting plant survival worldwide (Lambers et al., 2019), and ongoing climate change is expected to negatively impact the water balance of plants (Engelbrecht et al., 2007; McDowell, 2008; Hammond et al., 2022; Marengo et al., 2018). During extreme droughts, high evaporative demand and low soil moisture increase tension in the xylem, making water metastable and susceptible to cavitation, which can cause embolisms and lead to hydraulic failure (Tyree & Zimmermann, 2002). Xylem vulnerability to embolism is commonly assessed through vulnerability curves, which indicate the percentage loss of conductivity as a function of water potential, highlighting critical water potentials such as Ψ_{50} and Ψ_{88}, at which the plant loses 50% and 88% of hydraulic conductivity, respectively. These curves allow for the estimation of hydraulic safety margin (HSM), which is the difference between the minimum water

potential recorded in situ at the peak of the dry season and Ψ_{50} or Ψ_{88}, denoting how far the plant is operating from hydraulic failure (Delzon et al., 2014; Meinzer et al., 2009; Bhaskar et al., 2006). HSM is an indicator of plant survival, carbon balance, and is increasingly applied in models predicting ecosystem vulnerability to drier climates (Tavares et al., 2023; Oliveira et al., 2021; Powers et al., 2020; Eller et al., 2017; Christoffersen et al., 2016).

It has been observed that the transitional forests of the southern Amazon are hyperdynamic, with higher mortality and recruitment rates than other regions of the Amazon (Marimon et al., 2014), and that drought tolerance can be an important predictor of tree mortality (Tavares et al., 2023; Esquivel-Muelbert et al., 2020). Increased plant mortality related to drought has been reported in various forests around the world (Allen et al., 2010, 2015; Asner et al., 2016; Moore et al., 2016), and in many cases, drought-related mortality is associated with hydraulic failure in the plant water transport system (Rowland et al., 2015; Guillemot et al., 2022). Seasonal water deficits within the Amazon basin are more intense at its southern edge (Brando et al., 2014). It is expected that species in tropical areas with well-defined seasonality, with distinct dry and rainy periods, such as the Amazon-Cerrado transition, have evolved through natural selection to exhibit traits that allow them to thrive in this environment (Franco et al., 2014). However, recent studies have provided evidence that the forests at the southern edge of the Amazon may already be experiencing more extreme climatic conditions than those to which they are adapted (Tavares et al., 2023; Esquivel-Muelbert et al., 2020) and may already be acting as carbon sources rather than sinks (Gatti et al., 2021).

In light of the above, our goal is to advance the critically missing understanding of the hydraulic properties of forests at the southern edge of the Amazon. These forests are subject to climatic conditions characterized by high cumulative water deficits

(elevated MCWD), operating with highly negative Ψ_{dry} values (minimum leaf water potential during the driest period of the year; Soares-Jancoski et al., 2021; Tavares et al., 2023; Araújo et al., 2024), which favors the selection of species with more negative Ψ_{50} as a functional adaptation to water stress, since drought affiliation is an important characteristic for the region (Esquivel-Muelbert et al., 2017). Although climatic conditions at the southern edge of the Amazon are believed to be forcing plants to operate close to or beyond their hydraulic limit, to date, data on the hydraulic safety margin (HSM) are only available for a single site in this region (the VCR site in Tavares et al., 2023). It is crucial to assess whether the extremely negative HSM pattern observed at this site is representative of other forests at the southern edge of the Amazon. We also tested if the patterns of coordination between hydraulic metrics (Ψ_{dry}, Ψ_{50}, HSM_{50}) and MCWD, previously observed by Tavares et al. (2023), will still hold when considering additional forests from the southern Amazon. Specifically, we expect that forests in drier regions (more negative MCWD values) will exhibit more negative Ψ_{dry} and Ψ_{50} values and narrower HSM_{50}, while forests in wetter regions will not be as prone to hydraulic failure (high values of HSM). To address the first hypothesis, we performed a comparative study of four forests at the southern edge of the Amazon and measured leaf water potential throughout the day (Ψ_{leaf}), the water potential at which 50% and 88% of the hydraulic conductivity is lost (Ψ_{50} and Ψ_{88}, respectively), hydraulic safety margin (HSM_{50}), and wood density (WD) of dominant canopy and subcanopy trees. To address the second hypothesis, we include in our data set measurements made available by Tavares et al., (2023) for ten additional forests, extending the range of MCWD variation.

MATERIALS AND METHODS

Study Area

This study was conducted in four forests located close to the boundary between the Amazon and Cerrado (Brazilian savanna) biomes (Fig. 1), all located in the state of Mato Grosso, Brazil. We selected a semi-deciduous seasonal forest in the municipality of Nova Xavantina (VCR; 14º49'S; 52º06'W), and three evergreen seasonal forests located, one in the municipality of Querência (TAN; 13º07'S; 52º37'W), one in the municipality of Ribeirão Cascalheira (FLO; 12°56'S; 51°49'W), and one in the municipality of Gaúcha do Norte (GAU; 13°14'S; 53°04'W).

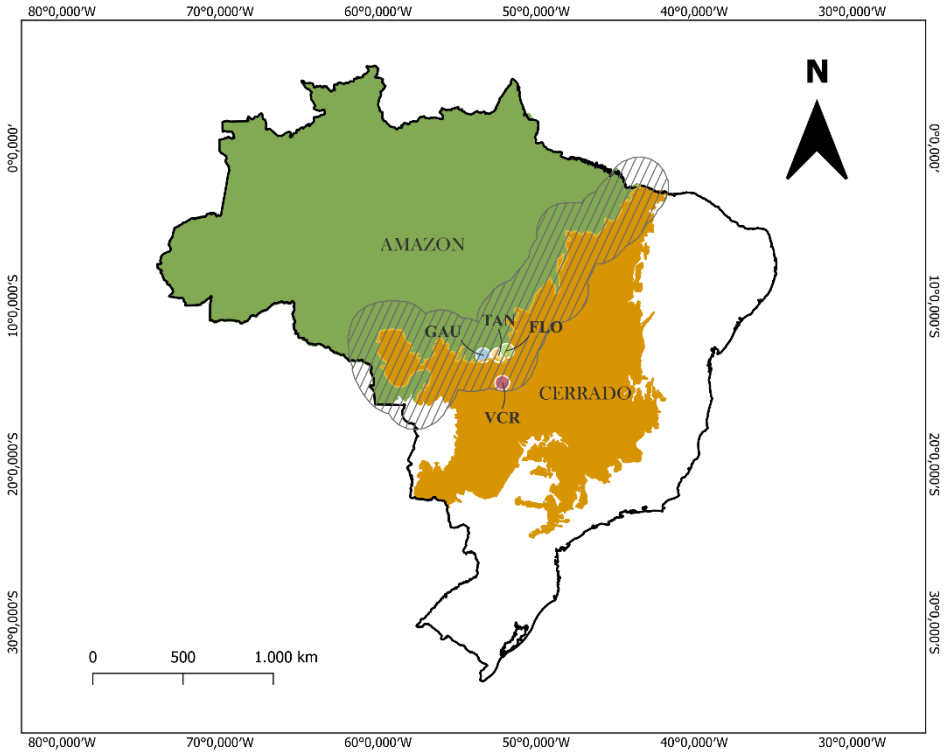

Fig. 1 Location of the four study sites on the southern edge of the Amazon, a region that encompasses the transition between the Amazon and Cerrado biomes. The dashed line indicates the broad transition zone according to Marques et al., 2020.

The Köppen classification for the climate of the region is Aw, that is, the study sites occur in a tropical region with a dry Southern hemisphere winter, with a dry period

typically from April to September and a rainy period from October to March (Alvares et al., 2013). Mean annual precipitation (MAP) ranges from 1516 mm in VCR, 1650 mm in FLO, 1700 mm in TAN, to 2061 mm in GAU. Mean annual temperature (MAT) ranges from 26.2°C in VCR, 25.6°C in TAN, 25.7°C in FLO, to 25.0°C in GAU. Maximum cumulative water deficit (MCWD) ranges from values of -606.3 mm in VCR, -591 mm in TAN, -577.4 mm in FLO, to -545.9 mm in GAU. We used 30 years (1981-2010) of monthly climate data from the CHELSA (climatologies at high resolution for the earth's land surface areas) database (KARGER et al.; 2020) to obtain MAP, MAT and MCWD (Aragão et al., 2007; Phillips et al., 2010). MCWD is a climate metric of drought severity, calculated as the maximum monthly cumulative water deficit (CWD) experienced over an average year, where the change in water deficit in any given month (n) is calculated as the difference between precipitation (P_n) and a fixed average value of 100 mm for monthly evapotranspiration (E_n) in Amazon forests (Aragão et al., 2007; Phillips et al., 2010).When CWD_n is negative (P_n is less than E_n) the forest enters into water deficit, which can accumulate over months according to the following rule:

$$CWD_n = CWD_n - 1 + P_n - E_n;\ \max(CWD_n) = 0; \qquad \text{(Eqn 1)}$$

$$CWD_nMCWD = \min(CWD_1, CWD_2, \ldots, CWD_{12})$$

Species selection

In each of these forests, permanent 1-hectare plots were established as part of the long-term monitoring projects PELD (Cerrado-Amazônia Transition: ecological and socio-environmental bases for conservation) and RAINFOR (Amazon network of forest inventories, http://www.forestplots.net). All trees with a diameter at breast height ≥ 10 cm were and continue to be identified, inventoried, and tagged. The criteria for species selection were based on the most dominant canopy and subcanopy tree species according

to the basal area. For determination of hydraulic traits, we sampled 10 species in VCR (61.2 % of total basal area), eight species in TAN (53.3% of total basal area), thirteen in FLO (55.0% of total basal area) and nine in GAU (67.9 % of total basal area). Some of the species sampled occurred on more than one site. Six of those occurred exclusively in VCR, three in FLO, seven in TAN and four in GAU (Table S1).

All measurements (*i.e.*, xylem hydraulic traits, wood density and leaf water potentials) were done from top-canopy branches (or branches at the maximum height reachable by the climber).

Hydraulic traits

Field measurements of leaf water potential (Ψ_{leaf})

We measured Ψ_{leaf} at VCR in August and, at GAU at the end of September, both in the dry season of 2021. We made the same measurements at FLO at the beginning of September 2022 and at TAN at the end of September 2024. We measured leaf water potentials with a 1505D-EXP pressure chamber (PMS Instruments Co., Albany, USA) (Scholander 1965). At VCR, we measured predawn (4 AM to 6 AM) and midday water potentials (12 PM to 2 PM). At TAN, FLO and GAU, we measured Ψ_{leaf} at several times throughout the day, starting at predawn (4 AM to 6 AM), and then at 9 AM to 10:30 AM, midday (12 PM to 2 PM) and 4 PM to 5 PM. We sampled five individuals of each species, collecting one branch per individual, and from each branch we selected three mature leaves with a healthy appearance and exposed to the sun for the leaf water potential measurements. The branches were collected, identified and placed inside a tightly closed black plastic bag, and quickly transported to the measurement point in the field. This

process was very fast, typically taking 5-10 minutes at most between branch collection and leaf water potential determination.

Embolism vulnerability measurements using the pneumatic method

We measured embolism resistance for trees of VCR, FLO and GAU in 2022 and TAN in 2024, at the rainy season/beginning of the dry season when the soil was fully hydrated. The predawn leaf water potential ranged from -0.1 to -1.0 MPa. Branches were collected in the field between 4 AM and sunrise, a time when the plants generally have a balanced water status with the soil. In the field, we collected two branches with lengths between 50 cm and 1 meter from 3 individuals of each species, placing them inside a moist black plastic bag and transporting them to the laboratory for measurements.

The vulnerability curves were constructed by simultaneously determining the amount of air extracted from the dehydrating branches and the xylem water potential using pneumatic method (Pereira et al., 2016, 2020; Bittencourt et al., 2018). For VCR, FLO and GAU, a manual apparatus was used while an automated version of the pneumatic method was used for TAN. The pneumatic method considers the volume of air discharged from the branches as a proxy for embolism formation. As commonly used when applying the manual pneumatic method, we considered an interval of 2.5 minutes to account for air discharge (Bittencourt et al., 2018, Tavares et al., 2023) and an interval of 15 seconds for the measurements with the automatic method. Between each measurement, the branches were exposed to the environment for 30 minutes to 1 hour to dehydrate, and thereafter were placed inside a black plastic bag, for 60 minutes, to equilibrate the leaf water potential (Ψ_{leaf}) with stem water potential (Ψ_{stem}). Ψ_{leaf} was measured using a 1505D-EXP pressure chamber (PMS Instruments Co., Albany, USA; Scholander 1965). We repeated the pneumatic air discharge and Ψ_{leaf} measurements until the branch was completely dehydrated or lost all its leaves.

We calculated Ψ_{50} and Ψ_{88} (xylem water potential associated with 50 and 88% embolism formation) by fitting a sigmoidal function to the data:

(Eqn 2)

$$PAD = \frac{100}{1 + exp\left(\frac{S}{25}(\Psi_x - \Psi_{50})\right)}$$

where PAD is the percent air discharged at Ψ_x, expressed as a percentage difference between the amount of air discharged when the branch was completely dehydrated and the amount of air discharged when the branch was fully hydrated. S is the slope of the curve, Ψ_x is the xylem water potential (MPa) and Ψ_{50} is the Ψ_x corresponding to a PAD of 50%.

Hydraulic safety margin (HSM_{50})

HSM_{50} was calculated as the difference between Ψ_{dry} and Ψ_{50}, where Ψ_{dry} is the Ψ_{leaf} measured at midday for the three individuals that we measured Ψ_{50}. We used Ψ_{50}, because it is more commonly used and Ψ_{50} estimated with the pneumatic method have been shown to agree well with those determined from other methods (Adams et al., 2017; Paligi et al., 2023).

Wood density

Wood density (WD_{branch}) was determined on the same branches that were collected for the vulnerability curves. In the laboratory, we cut fragments of approximately 2.5 centimeters in length, removed the bark, and immersed the samples in water for at least 12 hours. The fresh volume at saturation was calculated using the mass displacement

method, then the samples were dried at 60ºC for 72 hours, and the wood density calculated as the dry mass per volume at saturation ($g.cm^{-3}$) (Osazuwa-Peters & Zanne, 2010).

Data analysis

To understand how hydraulic and wood density vary across southern Amazon forests we compared hydraulic metrics (Ψ_{leaf}, Ψ_{dry}, Ψ_{50}, Ψ_{88}, and HSM_{50}) and branch wood density (WD_{branch}) across the four forests measured in this study. We used data from individuals of each species to construct mixed models with forest as a fixed effect and species as a random effect, and hydraulic metrics and WD_{branch} as response variables. For Ψ_{leaf}, we compared each time point separately. We applied mixed linear models to assess the relationships between Ψ_{dry} and Ψ_{50}, $\Psi_{predawn}$ and $\Psi_{dry,}$ $\Psi_{predawn}$ and Ψ_{50} and $\Psi_{predawn}$ and HSM_{50} across the four forests and had species as random factor, which was the most parsimonious model according to the Akaike information criterion.

For the second hypothesis, we evaluated whether hydraulic metrics differed for differing MCWD and whether there is a coordination between the hydraulic metrics and MCWD, as well as between Ψ_{50} and Ψ_{dry}. To do so, in addition to the data we collected from the southern Amazon edge, we include in our data set measurements made available by Tavares et al., (2023) for ten additional forests, extending the range of MCWD variation (Fig. S1). Tavares et al., (2023) also sampled VCR, however, here we used our own measurements made at VCR. We conducted analyses both with species averages and community-weighted means (CWMs). For CWM calculation, we weighed the species we sampled within each forest by basal area to make them comparable with the data extracted from Tavares et al., (2023). To assess whether communities in different MCWD regimes exhibited distinct hydraulic strategies, we divided the forests into three groups based on MCWD. The dry group included VCR, TAN, FLO, GAU, KEN 1, and KEN 2, with

MCWD values ranging from -472 to -606 mm. The intermediate group consisted of FEC, CAX, TAP, TAM, and MAN, with MCWD values between -184 and -288 mm. The wet group comprised ALP 1, ALP 2, and SUC, with MCWD values ranging from -23 to -15 mm. The group averages were compared using the Kruskal-Wallis test, followed by Dunn's post-hoc tests, as the data did not meet the assumptions of normality for parametric tests. To investigate the coordination between hydraulic metrics and MCWD, we performed linear regressions using CWM values for each hydraulic metric (Ψ_{50}, Ψ_{dry}, and HSM_{50}). We examined relationship between Ψ_{50} and Ψ_{dry}, both at the community (CWM) and species levels. At the community level, we used the community-weighted means calculated for each forest and applied SMA regressions. At the species level, we applied mixed linear models to assess the coordination of these traits across the entire dataset and within the dry, intermediate, and wet groups. In these models, Ψ_{50} was used as a fixed effect, Ψ_{dry} as the response variable, and species identity as a random effect, which was the most parsimonious model according to the Akaike information criterion. This approach allowed us to account for species-specific variation while examining the general trend.

For all analyses, a significance level of 0.05 was used. We performed all analyses using R software version 4.3.1 (R Core Team 2023). For linear mixed models, we used the lmerTest function (Kuznetsova et al., 2017) in the lme4 package (Crawley, 2013; Pinheiro et al., 2024). We followed Zuur et al. (2009) and Thomas et al. (2017) to assess the significance of model terms and validate model assumptions. We used the R package 'emmeans' (Lenth, 2019) to conduct post-hoc comparisons between the forests using Tukey's tests. We assessed model performance using marginal (R^2_m) and conditional (R^2_c) pseudo-R^2 calculated using the "r.squaredGLMM" function from the "MuMIn" package (Barton, 2024). SMA regressions were performed using the smart package

(Warton et al., 2012). To compare group means we used the plyr, dunn.test and FSA packages (Dunn, 1964; Wickham, 2011).

RESULTS

Vulnerability to drought of four forests on the southern edge of the Amazon

Diurnal course of leaf water potential (Ψ_{leaf})

Ψ_{leaf} values at VCR were significantly more negative than at TAN, FLO and GAU (Fig. 2), at predawn (VCR= -2.5 ± 1.32 MPa; TAN= -1.57 ± 1.25 MPa; FLO = -0.84 ± 0.71 MPa; GAU= -0.74 ± 0.53 MPa, mean ± SD, $P < 0.05$, Fig. 2) and midday (VCR= -3.64 ± 1.33 MPa; TAN= -2.48 ± 1.04 MPa; FLO= -2.19 ± 0.85 MPa; GAU= -1.7 ± 0.95 MPa, $P < 0.05$). Ψ_{leaf} did not differ between FLO, GAU and TAN ($P > 0.05$, Fig 2, Tables S2 and S3) at any time.

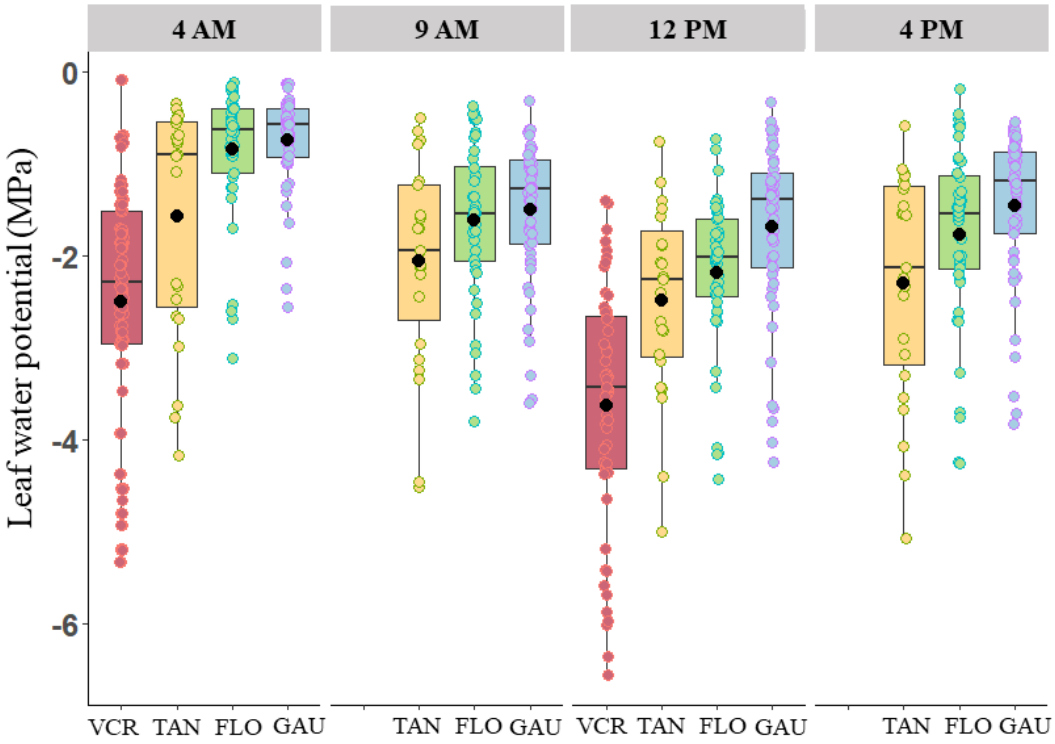

Fig. 2 Leaf water potential measured at the peak of the dry season in four forests at the southern Amazon edge. Measurements were taken at 4 AM (predawn) and 12 PM (midday) in all four forests (TAN, VCR, FLO, and GAU), and additionally at 9 AM and 4 PM for TAN, FLO, and GAU. Sampling of 5 individuals per species. The boxplots show the 25th percentile, median, and 75th percentile. The vertical bars represent the interquartile range, and data points beyond these bars are considered outliers. In each forest, the color dots represent individual trees, and the black dots are the mean value across species.

Hydraulic metrics

TAN exhibited significantly more negative Ψ_{50} (Fig. 3a) and Ψ_{88} (Tables S2 and S3) compared to the other three forests (Fig. 3a) however it did not differ significantly from the others in Ψ_{dry} (Fig. 3b, Tables S2 and S3). VCR exhibited the lowest HSM_{50}, with a species mean of -0.09 MPa, while the other three forests showed higher HSM_{50} values, ranging from 1.05 MPa in FLO to 1.8 MPa in TAN (Fig. 3c). Branch wood density at VCR was lower than at FLO and GAU (Tables S2 and S3).

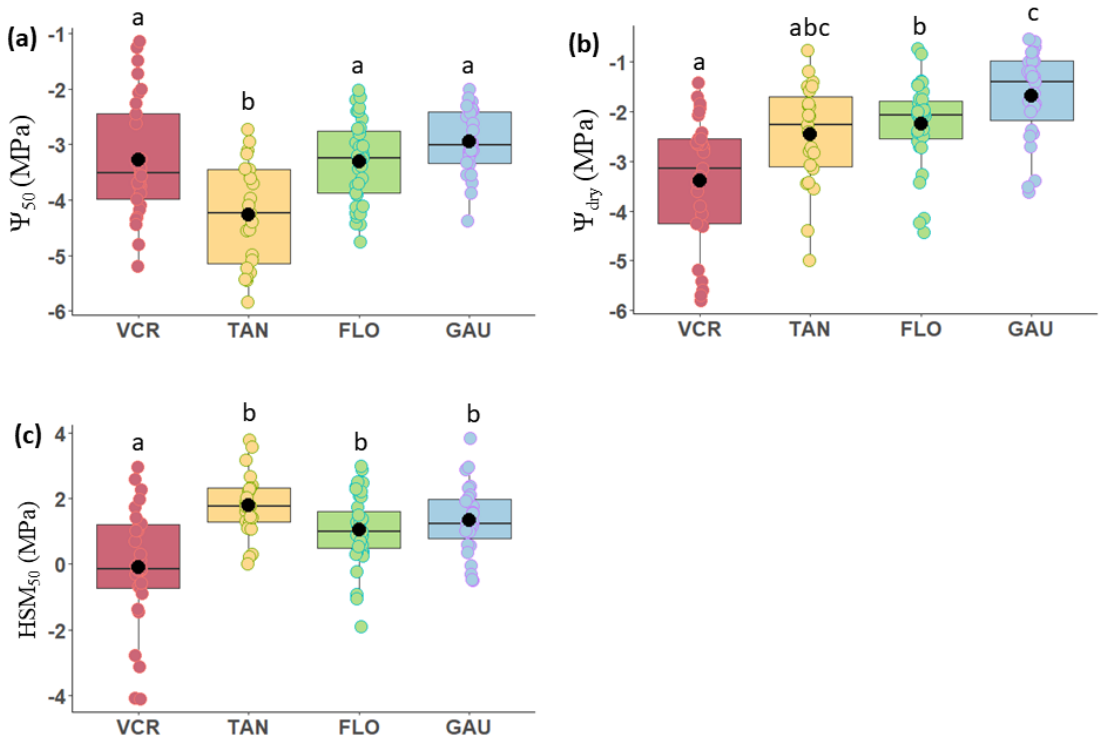

Fig. 3 Hydraulic traits for four forests at the southern Amazon edge. Values of (a) branch xylem water potential at which 50% of embolism occurs (Ψ_{50}), (b) leaf water potential measured at midday in the field during the dry season (Ψ_{dry}), (c) hydraulic safety margin (HSM_{50}). Sampling of 3 individuals per species. The boxplots show the 25th percentile, median, and 75th percentile. The vertical bars represent the interquartile range, and data points beyond these bars are considered outliers. Different letters indicate statistically significant differences between the forests ($P < 0.05$). In each forest, the color dots represent individual trees, and the black dots are the mean values across species.

We detected a significant relationship between $\Psi_{predawn}$ and HSM_{50} ($P < 0.001$; $R_m^2 = 0.35$ and $R_c^2 = 0.67$, Fig. 4a) and between $\Psi_{predawn}$ and Ψ_{dry} ($P < 0.001$; $R_m^2 = 0.61$ and $R_c^2 = 0.86$, Fig. 4b). $\Psi_{predawn}$ and Ψ_{dry} did not correlate significantly with Ψ_{50} (Fig. S2, Table S4).

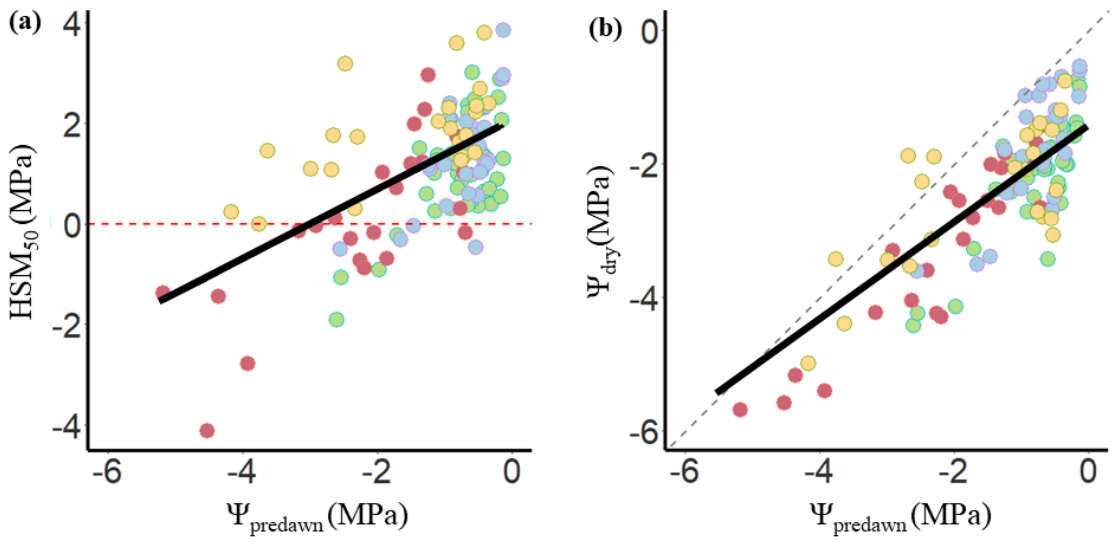

Fig. 4 Relationship between (a) water potential measured at 4 AM ($\Psi_{predawn}$) and hydraulic safety margin (HSM_{50}), (b) $\Psi_{predawn}$ and leaf water potential measured at midday in the field during the dry season (Ψ_{dry}) for four forests at the southern Amazon edge. The colors dots represent measurements made at TAN (yellow), VCR (red), FLO (green), and GAU (blue) for individual trees. The 1:1 relationship in "b" is indicated by a broken line.

Hydraulic trait variation for Amazon forests along a MCWD gradient

The three MCWD groups (dry, intermediate and wet) showed significant differences in relation to Ψ_{50} and Ψ_{dry} ($P < 0.001$, Fig 5a, b and c, Table S5). In the wet group, the mean values were Ψ_{dry} = -0.76 MPa and Ψ_{50} = -1.62 MPa, for the intermediate group Ψ_{dry} = -1.85 MPa and Ψ_{50} = -2.09 MPa, while for the dry group it was Ψ_{dry} = -2.49 MPa and Ψ_{50} = -3.1 MPa. Regarding HSM_{50}, the intermediate group differed from the wet and dry groups ($P < 0.001$), while we did not detect significant differences between the dry and wet groups ($P = 0.983$).

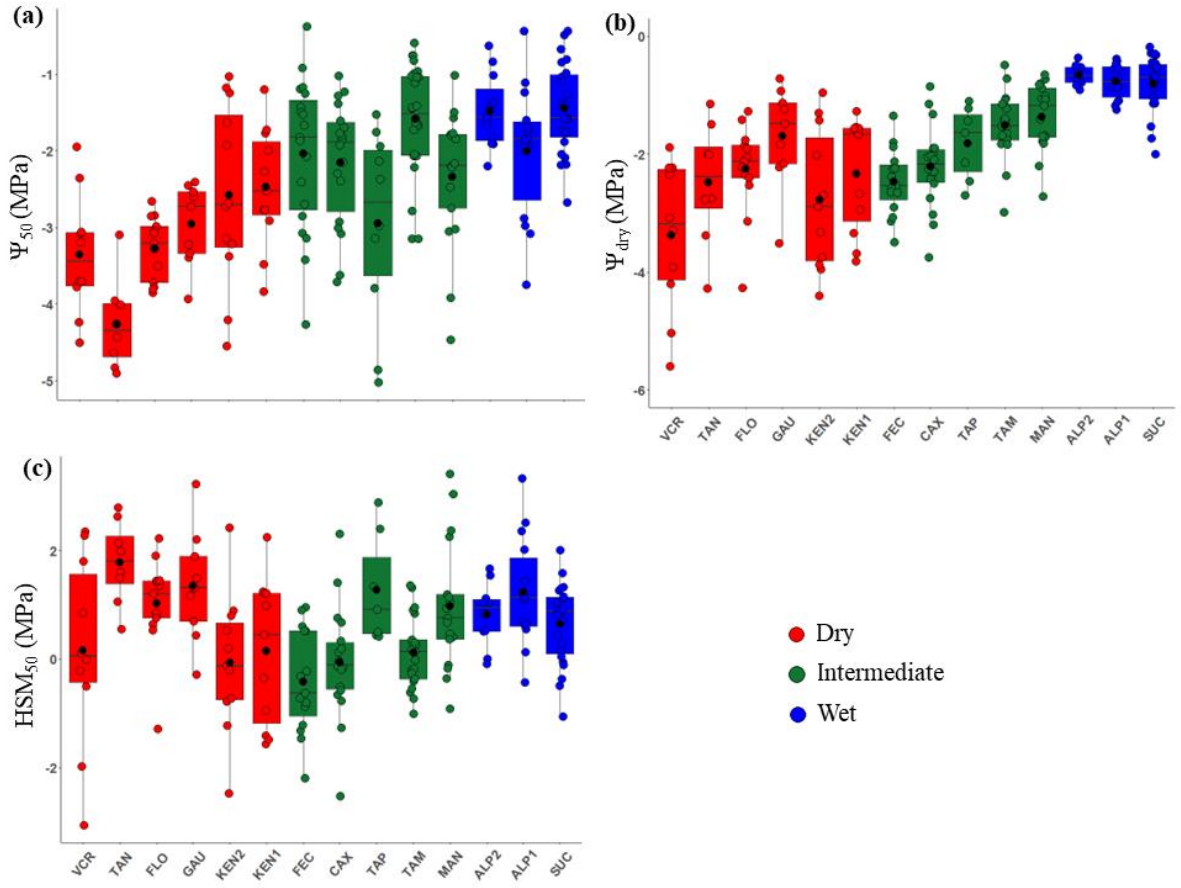

Fig. 5 Hydraulic trait variation across fourteen Amazon forest sites covering a large variation in water availability, calculated as the maximum monthly cumulative water deficit (MCWD; see Material and Methods for MCWD calculations). (a) branch xylem water potential at which 50% of embolism occurs (Ψ_{50}), (b) leaf water potential measured at midday in the field during the dry season (Ψ_{dry}), and (c) hydraulic safety margin (HSM_{50}). The boxplots show the 25th percentile, median, and 75th percentile. Each red, green or blue dot represents species average, and the black dots are the means across species for each site. The vertical bars represent the interquartile range, and data points beyond these bars are considered outliers. The sites are ordered according to increasing water availability.

Both community weighted mean values of Ψ_{50_CWM} (Fig.6a, Table S6) and Ψ_{dry_CWM} (Fig.6b) became more negative as MCWD became more severe ($P < 0.05$), with

a tighter relation between MCWD and Ψ_{50_CWM} (r^2_{adj} = 0.66) in relation to Ψ_{dry_CWM} (r^2_{adj} = 0.41). HSM_{50_CWM} was not significantly related to the MCWD, but we noticed that the HSM_{50_CWM} of the more humid forests (in regions with less negative values of MCWD) had positive values of HSM (mean of 0.58 MPa) with the variation in HSM_{50_CWM} increasing for the forests of intermediate and dry regions (Fig. 6c). Two forests in the intermediate region and one forest in the dry region had negative values of HSM_{50_CWM}.

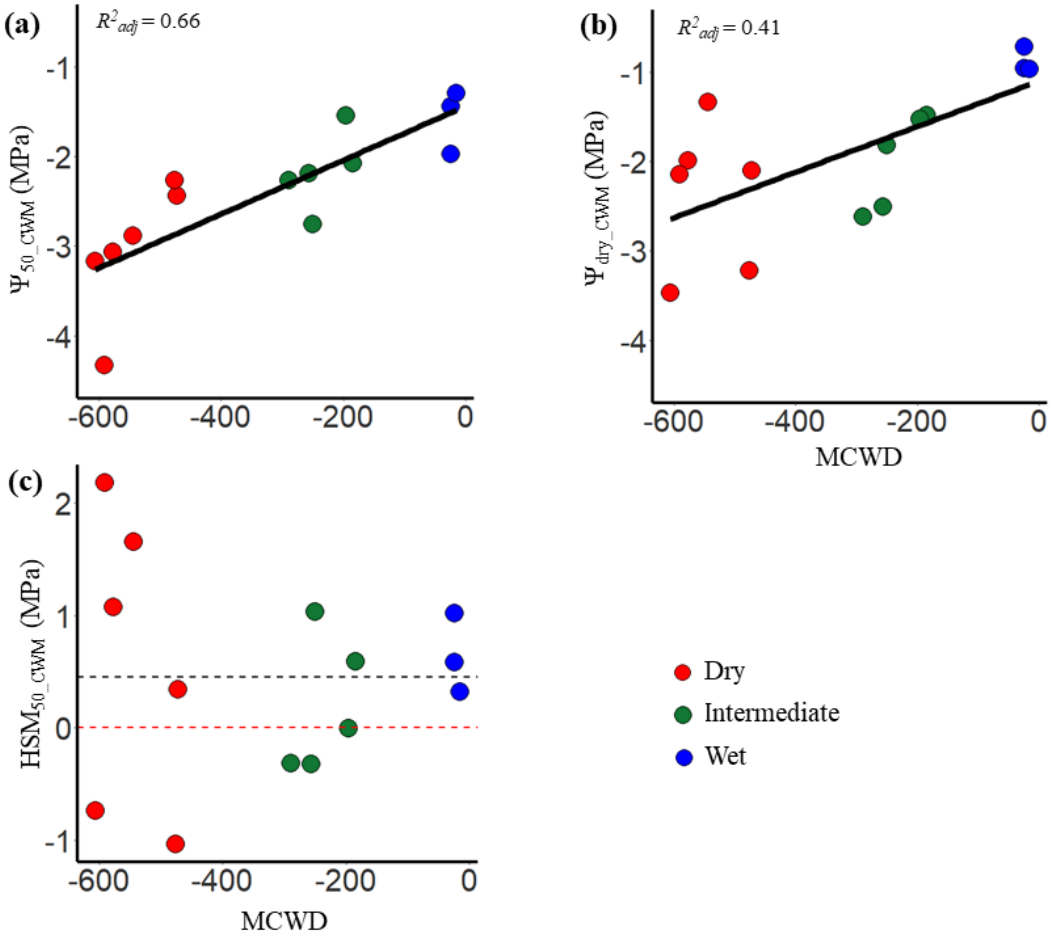

Fig. 6 Relationships between community weighted hydraulic metrics weighed by basal area (CWM) and the maximum monthly cumulative water deficit (MCWD) for fourteen forests distributed across the Amazon region. MCWD and (a) branch xylem water potential at which 50% of embolism occurs (Ψ_{50_CWM}), (b) leaf water potential measured at midday in the field during the dry season (Ψ_{dry_CWM}), and (c) hydraulic safety margin

(HSM_{50_CWM}). The colors represent the partitioning of MCWD into dry region (red), intermediate region (green), and wet region (blue). Solid black lines were drawn for the relationships that were significant ($P < 0.05$). The dashed black line indicates the average value for the 14 forests, and the dashed red line indicates HSM_{50_CWM} equal to zero. Straight line equation for figure 5a: Ψ_{50_CWM} = -1.4 + 0.0030 MCWD, R^2_{adj}= 0.66 (P = 0.0002),5b: Ψ_{dry_CWM} = -1.1 + 0.0025 MCWD, R^2_{adj}= 0.41 (P = 0.008).

Coordination between hydraulic traits for Amazon forests along a MCWD gradient

We observed coordination between Ψ_{dry} and Ψ_{50} in the model using the full dataset of species from each site (Fig. 7a, $P < 0.001$, R^2_m= 0.12 and R^2_c=0.54, Table S7). The relationship was not significant when considering the community-weighted means (Fig. 7b, P = 0.08). When analyzing this relationship by partitioning the forests according to MCWD (Fig. 8a = dry, 8b = intermediate, and 8c = wet), the coordination between these hydraulic metrics remained significant only for the intermediate region but with low explanatory power (Fig. 7b, P = 0.009, R^2_m = 0.09 and R^2_c=0.62).

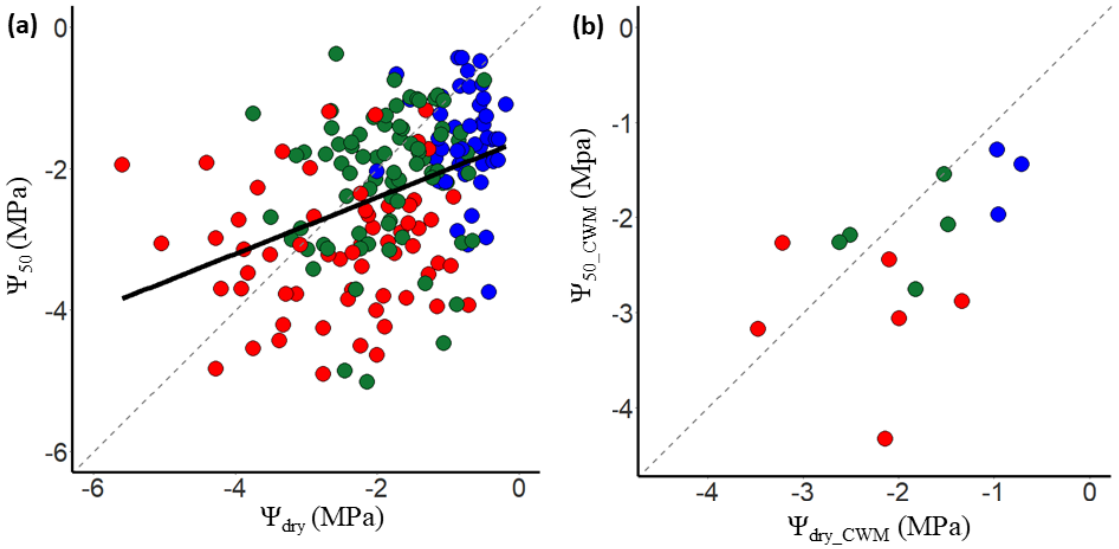

Fig. 7 Relationships between the branch xylem water potential at which 50% of embolism occurs (Ψ_{50}) and (a) leaf water potential measured at noon during the dry season (Ψ_{dry}) for all species considering their respective means, and (b) data from the weighted averages (CWM) for Ψ_{50_CWM} and Ψ_{dry_CWM} of fourteen forests incorporating a moisture gradient in the Amazon. The colors represent the partitioning of MCWD into dry (red), intermediate (green) and wet (blue) regions. A solid black line was drawn for the relationship that was significant ($P < 0.05$). A dashed line is used to represent the 1:1 line.

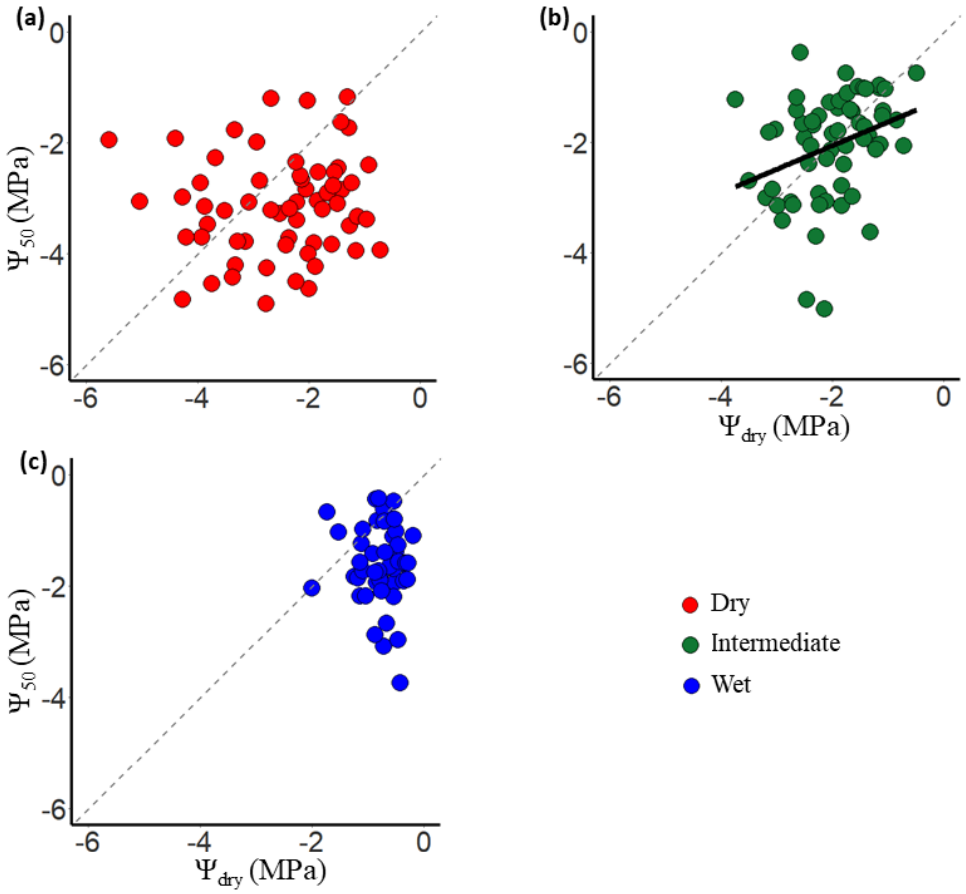

Fig. 8 Relationships between the branch xylem water potential at which 50% of embolism occurs (Ψ_{50}) and leaf water potential measured at midday during the dry season (Ψ_{dry}), using data from twelve forests incorporating a wide range of MCWD. Forests were

grouped according to MCWD into (8a) dry region (red), (8b) intermediate region (green), and (8c) wet region (blue). A solid black line was drawn for the relationship that was significant ($P < 0.05$) and a dashed line is used to represent the 1:1 line. Straight line equation for figure 8b: $\Psi_{50} = -1.2 + 0.43\ \Psi_{dry}$, $R^2_{adj} = 0.086$

DISCUSSION

In this study, we sought a better understanding of tree vulnerability to drought and hydraulic safety margins in forests on the southern edge of the Amazon. We determined that these forests are more resistant to hydraulic failure, reflected in more negative Ψ_{50} (the branch xylem water potential at which 50% of embolism occurs) than what was measured in other forests in the Amazon region. However, we noted variation in the hydraulic safety margin (HSM), with some forests operating with negative HSM_{50} which suggests risk of drought-induced hydraulic failure while others maintained positive HSM_{50} values. Moreover, on a local scale, there was a large variability in HSM_{50} across species.

On a broader scale, by integrating our data from forests on the southern edge with forests from wetter regions of the Amazon and using the community-weighted means calculated for each forest, we observed that both Ψ_{dry_CWM} (leaf water potential measured at midday in the field during the dry season) and Ψ_{50_CWM} became more negative with increasing maximum cumulative water deficit (MCWD). On the other hand, unlike what was found by Tavares et al. (2023), HSM_{50_CWM} did not show any relationship with MCWD. Ψ_{dry} and Ψ_{50} were positively correlated across species, however, when partitioning the species sampled in the forests into groups according to MCWD, this coordination was significant for the intermediate MCWD group, albeit of low explanatory power, while no coupling was observed at the extremes (dry and wet).

Hydraulic trait and safety margin variability in Southern Amazonian forests

Our results indicate that not all tropical forests are equally vulnerable to hydraulic failure, especially those at the southern edge of the Amazon, contrary to what was suggested by Choat et al. (2012). While VCR operates with an extremely low HSM_{50} (HSM_{50} = -0.09 MPa), FLO, TAN, and GAU exhibited considerably higher HSM_{50} values (HSM_{50} > 1 MPa). This variation in HSM_{50} was also observed in the leaf water potential measured throughout the day. Even at predawn, we recorded extremely negative water potential values in the VCR, while other forests, such as GAU, maintained higher values.

The HSM_{50} values reported by Tavares et al. (2023) for VCR are slightly more negative than those we obtained, likely due to differences in species sampling. Our analysis included four additional species compared to Tavares et al. (2023). The average for the shared set of species was similar (Table S8), even though measurements were taken in different years. Although the lower wood density observed in VCR may contribute to greater capacitance and, consequently, to water storage (Choat et al., 2005; Meinzer et al., 2003; Scholz et al., 2007) and could mitigate changes in Ψ_{leaf}, VCR remained the forest with the most negative Ψ_{dry} and HSM_{50} values. Data collected at VCR in 2016 by Soares-Jancoski et al., (2022) showed that variations in Ψ_{leaf} were primarily explained by species, most of which were classified as anisohydric.

VCR is the forest with the driest climatic conditions among those studied. It is on a rocky outcrop located at a depth of 90 cm beneath the surface, which limits soil water availability and maybe the reason for the extremely negative $\Psi_{predawn}$ and Ψ_{dry} values observed for this forest (Soares-Jancoski et al., 2022; Oliveira et al., 2019) and significantly more negative than at TAN, FLO and GAU. In contrast, TAN, which has the highest HSM among the four forests on the southern edge of the Amazon, likely

occurs over deeper soils, as indicated by studies conducted near our research site (Silverio et al., 2024; Balch et al., 2008).

In addition to previous findings showing that tree species in VCR exhibit some of the highest thermotolerance recorded for tropical trees (Tiwari et al., 2020), our results indicate that these species, along with those from other evaluated forests, also operate with high hydraulic resistance. However, in the case of VCR, this high embolism resistance was insufficient to ensure a safe HSM, which may explain the reports of high tree mortality in this forest (Esquivel-Muelbert et al., 2020; Prestes et al., 2024). This finding aligns with previous studies that link HSM to tree mortality (Peters et al., 2020) and to reductions in plant biomass in the Amazon (Tavares et al., 2023). Forests that already operate with high drought resistance, such as VCR, may be close to their adaptive limits. Conditions that amplify extreme conditions, such as shallow soil depth for example, could subject trees to conditions beyond those to which they are adapted. Phenotypic plasticity to xylem vulnerability to embolism may be limited in Amazon trees. On a long-term forest drought experiment, hydraulic traits of Amazon trees did not adjust following 15 years of experimentally imposed soil moisture deficit (Bittencourt et al., 2020). However, drought responses vary among species, which can lead to high floristic turnover under extreme events and favoring the survival of drought-adapted species. This process may result in compositional changes over time towards a drought-affiliated tree flora, as might already be occurring in VCR after El Niño events (Prestes et al., 2024). Furthermore, while the other forests still operate with a safe HSM, the critical state of VCR under more extreme environmental conditions highlights the need for further studies in the region. This is particularly urgent as this area is already experiencing the most severe temperatures and droughts.

The average Ψ_{50} value of forests on the southern edge of the Amazon is more negative (-3.42 MPa) compared to Ψ_{50} values reported for other Amazonian forests (Tavares et al., 2023; Barros et al., 2019). For instance, Barros et al., (2019) reported less negative average Ψ_{50} values for central Amazon forest with low seasonality (Ψ_{50}= -2.34 MPa) and high seasonality (Ψ_{50}= -2.90 MPa), as well as for the global average (-1.6 MPa, Choat et al., 2012). Among the four forests analyzed on the southern Amazonian edge, TAN was the only one that differed in relation to Ψ_{50}, showing the lowest values. However, it did not differ in Ψ_{dry} to the other three forests, and we did not detect any correlation between Ψ_{dry} and Ψ_{50} and between $\Psi_{predawn}$ and Ψ_{50} across the four forests (Fig. S2).

On the other hand, $\Psi_{predawn}$ and Ψ_{dry} were tightly correlated (Fig. 4b) suggesting functional convergence on water transport regulation across species and constrained variation in Ψ_{leaf}. The slope value was 0.78 MPa MPa^{-1} and the intercept value was -1.4 MPa which are similar to the values reported by Martínez-Vilalta et al. (2014) using a global database of leaf water potentials. Slope values close to 1 are consistent with partial anisohydric behavior, i.e., close coordination between stomatal and hydraulic responses to drought (Martínez-Vilalta et al., 2014), although species-level differences and their vertical distribution in the canopy should not be ignored and explain part of the variation in the $\Psi_{predawn}$ and Ψ_{dry} relation (Table S4) (Penha et al., 2024). The large variation in $\Psi_{predawn}$ across species suggests wide differences in rooting extension and depth, although other factors such as small-scale variation in edaphic conditions, the strength of root competition for soil water and transpiration rates under drought can also be important to drive the observed variation in $\Psi_{predawn}$ (Martínez-Vilalta and Garcia-Forner, 2017; Brum et al., 2019).

Variation in the hydraulic properties of tropical forests

On a broader scale, we observed a significant coordination between Ψ_{50_CWM} and Ψ_{dry_CWM} with MCWD (Fig. 5a and 5b). When grouping the Amazon forests according to the partitioning of MCWD into dry region (MCWD < -400 mm), intermediate region (MCWD between -184 to -288 mm), and wet region (MCWD between -23 to -15 mm), Ψ_{dry_CWM} of the forests in the dry group were the most negative and, consequently, Ψ_{50_CWM} values, reflecting how the species composition of these communities is driven to greater resistance to hydraulic failure under limited water availability (Ciemer et al., 2019). Embolism resistance is advantageous in water-limited environments exposed to strong atmospheric evaporative demand, acting as a mechanism to prevent significant hydraulic impairment or mortality during severe water stress episodes (Sanchez-Martinez et al., 2020).

However, unlike the findings by Tavares et al., 2023, we did not find an association between MCWD and HSM_{50_CWM}. This discrepancy in results is due to our increased forest sampling across the southern Amazon, which has revealed greater diversity in risk of hydraulic failure among forests at the southern edge of the Amazon. The similar pattern of HSM_{50_CWM} for the extreme groups (dry group = 0.68 MPa, wet group = 0.85 MPa), however, results from distinct strategies leading to higher HSM_{50_CWM} in environments with contrasting water availability compared to the intermediate group, which exhibited the lowest HSM_{50_CWM} (0.26 MPa). This difference becomes more evident when analyzing the coupling separately for the three groups defined by MCWD. In the dry and wet extremes, the coupling does not persist. Contrasting environments on either end of the water availability spectrum might need more extreme hydraulic strategies, resulting in plant community distributions driven by water (Blackman et al., 2014; Cosme et al., 2017).

In the dry group, there is a high variability in hydraulic traits among species, with $\Psi_{50} > \Psi_{dry}$ for many of them, which may be due to the selective pressure being so high that plants require a broader set of strategies or because several of them are at the limits of their distributions in seasonally dry environments (Peters et al., 2021; Schwinning & Kelly 2013; Grime 2006). In contrast, in the wet group, $\Psi_{50} \leq \Psi_{dry}$ for most species, which suggests weaker selective pressure on hydraulic traits related to drought tolerance, and that other traits may be more relevant for dealing with their environmental conditions (Reich et al., 2014; Sánchez-Martinez et al., 2020). Finally, most species in the intermediate group may be at the center of their distribution, which favors hydraulic coupling. These differences and the forces driving this variation offer an interesting avenue for future research.

Our results highlight the importance of considering variation in hydraulic metrics across multiple scales, from local spatial scales to broader ones, and among forests, considering both community-weighted means and species averages. Further work on Southern Amazon forests is needed to assess species-level water-use -and conservation strategies, which, in fact, are associated to patterns of root distribution and the temporal dynamics of leaf phenology and play a crucial role on plant water balance and as such on how plants cope with periods of water limitation (Goldstein et al., 2008; Fu et al., 2012; Brum et al., 2019). Although with different proportions, evergreen, deciduous, and semi-deciduous trees co-occur in all four forests. Small-scale variation in soil conditions may also play a role in explaining the large species-level differences in HSM_{50} within each forest.

SUPPORTING INFORMATION

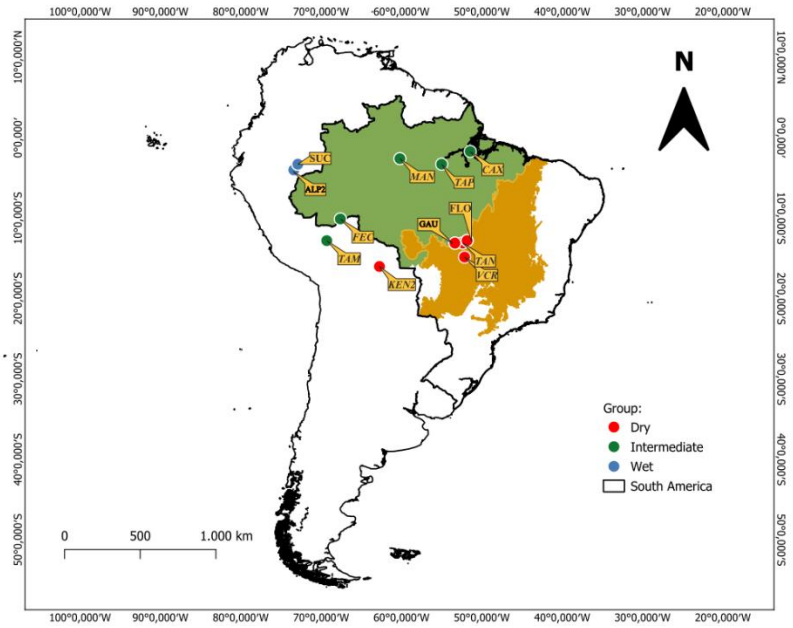

Fig. S1 Location of the sites sampled in this study and in the study by Tavares et al., (2023). The sites were distributed along a gradient of variation of maximum monthly cumulative water deficit (MCWD; see Material and Methods for MCWD calculations).

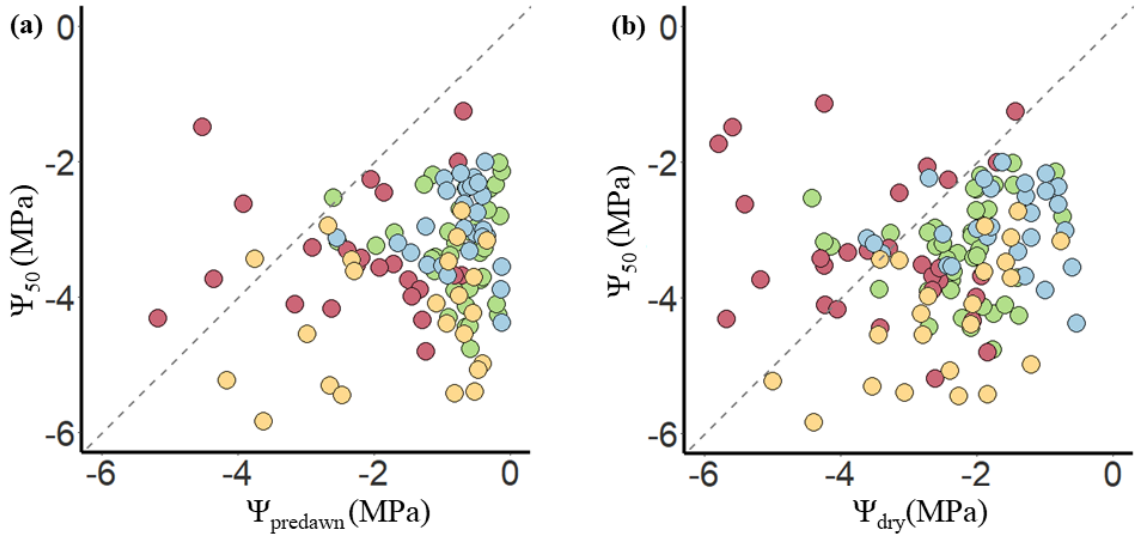

Fig. S2 Relationship between (a) leaf water potential measured at 4 AM ($\Psi_{predawn}$) and branch xylem water potential at which 50% of embolism occurs (Ψ_{50}), (b) leaf water

potential measured at midday (Ψ_{dry}) and Ψ_{50} for four forests on the southern Amazon edge. VCR = red, TAN = yellow, FLO= green, and GAU = blue. Data for the three individuals of each species within each forest that we measured $\Psi_{predawn}$, Ψ_{dry}, and Ψ_{50}. A dashed line is used to represent the 1:1 line.

Table S1: List of species and their respective botanical family for each forest and their relative dominance (DoR). DoR is the percentage of the basal area of the species in relation to the basal area of all species in the community.

Species	**DoR %**			
	VCR	**TAN**	**FLO**	**GAU**
Amaioua guianensis Aubl. (Rubiaceae)	5.3	-	6.2	2.9
Apuleia leiocarpa (Vogel) J.F.Macbr. (Fabaceae)	2.8	-	-	-
Aspidosperma discolor A.DC. (Apocynaceae)	-	-	13.0	-
Aspidosperma excelsum Benth (Apocynaceae)	-	18.3	-	-
Brosimum rubescens Taub. (Moraceae)	5.3	-	-	-
Chaetocarpus echinocarpus (Baill.) Ducke (Peraceae)	8.7	-	1.2	4.7
Cheiloclinium cognatum (Miers) A.C.Sm. (Celastraceae)	6.2	2.4	2.4	-
Dacryodes microcarpa Cuatrec (Burseraceae)	-	3.6	-	23.3
Ephedranthus parviflorus S.Moore (Annonaceae)	8.3	-	-	-
Hymenaea courbaril L. (Fabaceae)	16.0	-	3.3	-
Matayba arborescens (Aubl.) Radlk. (Sapindaceae)	-	-	-	5.7
Miconia pyrifolia Naudin (Melastomataceae)	-	-	3.7	-
Micropholis venulosa (Mart. & Eicher) Pierre (Sapotaceae)	-	-	3.8	-
Moquilea minutiflora (Sagot) Fritsch (Chrysobalanaceae)	-	-	6.1	-
Mouriri apiranga Spruce ex Triana (Melastomataceae)	1.2	-	-	-
Myrciaria floribunda (H. West ex Will.) O. Berg	-	-	-	0.36
Ocotea dispersa (Nees & Mart.) Mez (Lauraceae)	1.4	-	-	-
Ocotea guianensis Aubl. (Lauraceae)	-	1.2	-	-
Ocotea velloziana (Meisn.) Mez	-	-	-	10.5
Protium altissimum (Aubl.) Marchand (Burseraceae)	9.2	-	-	-
Protium pilosissimum Engl. (Burseraceae)	-	-	-	4.1
Pseudolmedia macrophylla Trécul (Moraceae)	-	1.5	-	-
Sacoglottis guianensis Benth. (Humiriaceae)	-	3.2	-	6.9
Sloanea sinemariensis Aubl (Elaeocarpaceae)	-	-	6.7	-
Terminalia tetraphylla (Aubl.) Gere & Boatwr. (Combretaceae)	0.5	-	-	-
Trattinnickia glaziovii Swart (Burseraceae)	-	8.8	-	-
Vochysia vismiifolia Spruce ex Warm (Vochysiaceae)	-	-	-	6.5
Xylopia amazonica R.E.Fr (Annonaceae)	-	3.1	3.4	4.0
Xylopia sericea A.St.-Hil. (Annonaceae)	0.7	-	-	-

Table S2. Means and standard deviations of leaf water potential (Ψ_{leaf}) measured at different times throughout the day (4 AM, 9 AM, 12 PM, 16 PM), hydraulic metrics (Ψ_{50}, P_{88}, Ψ_{dry}, HSM_{50}), and woody density (WD_{branch}) for four forests on the southern edge of the Amazon, as well as the P-value of the mixed model testing for differences among forests for each metric. The symbol "–" indicates that no data are available for that forest at the corresponding time. Ψ_{50} = branch xylem water potential at which 50% of embolism occurs. Ψ_{dry} = The average midday water potential for the three individuals that we measured Ψ_{50}. HSM_{50} = hydraulic safety margin.

Traits	***Mean ± standard deviation***				
	VCR	**TAN**	**FLO**	**GAU**	***P*-value***
Ψl_{eaf} (4 AM)	-2.5 ± 1.32	-1.57 ± 1.25	-0.84 ± 0.71	-0.74 ± 0.53	**<0.0001**
Ψl_{eaf} (9 AM)	-	-2.06 ± 1.12	-1.62 ± 0.85	-1.5 ± 0.78	0.459
Ψl_{eaf} (12 PM)	-3.64 ± 1.33	-2.48 ± 1.04	-2.19 ± 0.85	-1.7 ± 0.95	**<0.0001**
Ψl_{eaf} (4 PM)	-	-2.3 ± 2.13	-1.77 ± 0.98	-1.46 ± 0.82	0.072
Ψ_{50}	-3.27 ± 1.08	-4.27 ± 0.94	-3.3 ± 0.73	-2.95 ± 0.59	**0.0004**
Ψ_{88}	-4.31 ± 1.45	-7.23 ± 1.62	-5.11 ± 1.16	-5.06 ± 1.3	**<0.0001**
Ψ_{dry}	-3.38 ± 1.29	-2.47 ± 1.05	-2.25 ± 0.81	-1.69 ± 0.89	**<0.0001**
HSM_{50}	-0.09 ± 1.82	1.8 ± 0.97	-1.06 ± 1.05	1.35 ± 1.06	**<0.0001**
WD_{branch}	0.56 ± 0.08	-	0.62 ± 0.08	0.64 ± 0.12	**0.0027**

***Bold *P*-values** indicate significant differences among forests for that metric ($P < 0.05$).

Table S3: *P*-values for the pairwise comparisons of leaf water potential (Ψ_{leaf}) measured at different times throughout the day (4 AM, 9 AM, 12 PM, 4 PM), hydraulic metrics (Ψ_{50}, P_{88}, Ψ_{dry}, HSM_{50}) and wood density (WD_{branch}) between forests on the southern edge of the Amazon. Differences between forests were tested by means of adjusted multiple comparisons using the Tukey test.

	Traits								
Plots	**Ψ_{leaf} (4 AM)**	**Ψ_{leaf} (9 AM)**	**Ψ_{leaf} (12 PM)**	**Ψ_{leaf} (4 PM)**	**Ψ_{50}**	**Ψ_{88}**	**Ψ_{dry}**	**HSM_{50}**	**WD_{branch}**
FLO – GAU	0.999	0.998	0.574	0.563	0.575	0.987	**0.0009**	0.236	0.682
FLO – TAN	0.185	0.597	0.687	0.440	**0.005**	**0.0001**	0.744	0.697	
FLO – VCR	**<0.0001**		**<0.0001**		0.923	**0.055**	**<0.0001**	**<0.0001**	**0.019**
GAU – TAN	0.131	0.473	0.133	0.084	**0.0005**	**0.0001**	0.054	1	
GAU – VCR	**<0.0001**		**<0.0001**		0.933	0.187	**<0.0001**	**<0.0001**	**0.005**
TAN – VCR	**0.001**		**0.009**		**0.002**	**<0.0001**	0.365	**0.001**	

***Bold *P*-values** indicate significant differences ($P < 0.05$) between forests for that metric. Ψ_{50} = branch xylem water potential at which 50% of embolism occurs. Ψ_{dry} = The average midday water potential for the three individuals that we measured Ψ_{50}. HSM_{50} = hydraulic safety margin.

Table S4: Results of the linear mixed models (LMM) examining the relationships between hydraulic traits for trees from four forests on the southern Amazon edge. The presented parameters include the intercept, the estimated coefficients (including standard errors), the *P*-value for model significance, and the marginal (R^2_m) and conditional (R^2_c) coefficients of determination. (1|Species) indicates species is being treated as a random effect, with each species having a unique intercept drawn from a common distribution.

Model	Results		
$HSM_{50} \sim \Psi_{predawn} + (1\|Species)$	Parameters	Value	Standard Error
	Intercept	2.04	0.19
	$\Psi_{Predawn}$	0.69	0.10
	Species		
	P value = <**0.0001**		
	$R^2_m = 0.352$		
	$R^2_c = 0.679$		
$\Psi_{dry} \sim \Psi_{predawn} + (1\|Species)$	Parameters	Value	Standard Error
	Intercept	- 1.40	0.12
	$\Psi_{predawn}$	0.78	0.06
	Species		
	P value = <**0.0001**		
	$R^2_m = 0.61$		
	$R^2_c = 0.86$		
$\Psi_{50} \sim \Psi_{predawn} + (1\|Species)$	Parameters	Value	Standard Error
	Intercept	-3.21	0.15
	$\Psi_{predawn}$	0.03	0.09
	Species		
	P value = 0.6814		
	$R^2_m = 0.002$		
	$R^2_c = 0.261$		
$\Psi_{50} \sim \Psi_{dry} + (1\|Species)$	Parameters	Value	Standard Error
	Intercept	-3.09	0.26
	Ψ_{dry}	0.15	0.10
	Species		
	P value = 0.105		
	$R^2_m = 0.03$		
	$R^2_c = 0.40$		

Bold *P*-values indicate statistically significant differences ($P < 0.05$) among forests for that metric. $\Psi_{predawn}$ = leaf water potential measured at 4 AM. Ψ_{50} = branch xylem water

potential at which 50% of embolism occurs. Ψ_{dry} = leaf water potential measured at midday. HSM_{50} = hydraulic safety margin. Data for the three individuals of each species within each forest that we measured $\Psi_{predawn}$, Ψ_{dry}, and Ψ_{50}.

Table S5: Results of the Kruskal-Wallis test for differences and post-hoc multiple comparison tests between the three forest groups split by MCWD (dry, intermediate, and wet) for the metrics Ψ_{50}, Ψ_{dry}, and HSM_{50}. In the first column, the *P*-values of the Kruskal-Wallis test are shown. The Z test value and the adjusted p-value (*P.adj*) for multiple comparison correction for the pairwise comparisons between the groups are shown for each variable in the next columns.

Traits	**Kruskal Wallis**	**Comparison**					
		Dry – Intermediate		**Dry – Wet**		**Intermediate - Wet**	
		Z	*P.adj*	*Z*	*P.adj*	*Z*	*P.adj*
Ψ_{50}	*P* = **<0.0001**	-5.75	**<0.0001**	-7.28	**<0.0001**	-2.51	**<0.0001**
Ψ_{dry}	*P* = **<0.0001**	-2.75	**<0.0001**	-9.17	**<0.0001**	-7.07	**<0.0001**
HSM_{50}	*P* = **0.0009**	2.93	**0.009**	-0.55	0.983	-3.29	**0.002**

***Bold** ***P.adj*-values** indicate statistically significant differences (*P*< 0.05) between MCWD forest groups for that metric. Ψ_{50} = branch xylem water potential at which 50% of embolism occurs. Ψ_{dry} = leaf water potential measured at midday during the dry period. HSM_{50} = hydraulic safety margin.

Table S6: Results of linear regression analyses between MCWD and the hydraulic traits (Ψ_{50_CWM}, Ψ_{dry_CWM}, and HSM_{50_CWM}). The table presents the estimated coefficients (Estimate), standard errors, t-values, significance values (*P*-value), and the adjusted R^2. R^2 represents the proportion of variance explained by the model.

Traits	Estimate	Standard error	t-value	*P*-value*	adjusted R^2
Ψ_{50_CWM}	0.003	0.0005	5.08	**0.0002**	0.66
Ψ_{dry_CWM}	0.002	0.0008	3.17	**0.008**	0.41
HSM_{50_CWM}	-0.0003	0.0011	-0.29	0.779	-0.07

*__Bold__ *P*-values indicate statistically significant ($P < 0.05$) relationships. Ψ_{50} = branch xylem water potential at which 50% of embolism occurs. Ψ_{dry} = corresponds to Ψ_{leaf} values measured at midday during the dry period. HSM_{50} = hydraulic safety margin and MCWD = Maximum Cumulative Water Deficit.

Table S7: Results of the mixed linear model (LMM) adjusted for the relationship between Ψ_{dry} and Ψ_{50} considering different conditions across the entire dataset and the groups partitioned by MCWD (all groups, dry, intermediate, and wet. The presented parameters include the intercept, the estimated coefficients for Ψ_{dry} (including standard errors), the *P*-value* for model significance, and the marginal (R^2m) and conditional (R^2c) coefficients of determination. (1|Species) indicates that species is being treated as a random effect, with each species having a unique intercept drawn from a common distribution

Model	All groups			Dry		
$\Psi_{50} \sim \Psi dry+(1\|Species)$	Parameters	Value	Standard Error	Parameters	Value	Standard Error
	Intercept	-1.71	0.14	Intercept	-2.92	0.29
	Ψ_{dry}	0.30	0.07	Ψ_{dry}	0.08	0.10
	Species			Species		
	P value <**0.0001**			*P* value = 0.449		
	$R^2_m = 0.12$			$R^2_m = 0.01$		
	$R^2_c = 0.54$			$R^2_c = 0.15$		
	Intermediate			**Wet**		
	Parameters	Value	Standard Error	Parameters	Value	Standard Error
	Intercept	-1.24	0.33	Intercept	-2.01	0.317
	Ψ_{dry}	0.41	0.15	Ψ_{dry}	-0.22	0.209
	Species			Species		
	P value = **0.009**			*P* value = 0.365		
	$R^2_m = 0.09$			$R^2_m = 0.01$		
	$R^2_c = 0.62$			$R^2_c = 0.29$		

*__Bold values__ indicate significant *P*-values ($P < 0.05$). Ψ_{50} = branch xylem water potential at which 50% of embolism occurs. Ψ_{dry} = corresponds to Ψ_{leaf} values measured at midday during the dry period. HSM_{50} = hydraulic safety margin and MCWD = Maximum Cumulative Water Deficit.

Table S8: Hydraulic metrics (mean ± standard deviation) for the VCR with the same set of species as Tavares et al. (2023). Ψ_{50} = branch xylem water potential at which 50% of embolism occurs. Ψ_{dry} = corresponds to Ψ_{leaf} values measured at midday during the dry period. HSM_{50} = hydraulic safety margin.

Hydraulic metrics (MPa)	2022 (present study)	2017 (Tavares et al., 2023)
Ψ_{50}	-2.99 ± 0.73	-2.90 ± 1.03
Ψ_{dry}	-3.96 ± 1.14	-4.00 ± 0.76
HSM_{50}	-0.91 ± 1.53	-1.10 ± 0.89

REFERENCES

Adams, H.D., Zeppel, M.J., Anderegg, W.R., Hartmann, H., Landhäusser, S.M., Tissue, D.T., Hudson, P.J., Franz, T.E., Allen, C.D., Anderegg, L.D., Barron-Gafford, G.A., Beerling, D.J., Breshears, D.D., Brodribb, T.J., Bugmann, H., Cobb, R.C., Collins, A.D., Dickman, L.T., Duan, H., Ewers, B.E., … McDowell, N.G. (2017). A multi-species synthesis of physiological mechanisms in drought-induced tree mortality. *Nature Ecology & Evolution*, **1**, 1285-1291.

Allen, C.D., Breshears, D.D., & McDowell, N.G. (2015). On underestimation of global vulnerability to tree mortality and forest die-off from hotter drought in the Anthropocene. *Ecosphere*, **6**, 1–55.

Allen, C.D., Macalady, A.K., Chenchouni, H., Bachelet, D., McDowell, N., Vennetier, M., Kitzberger, T., Rigling, A., Breshears, D.D., Hogg, E.H.T, Gonzalez, P., Fensham, R., Zhang, Z., Castro, J., Demidova, N., Lim, J.H., Allard, G., Running, A.S., & Cobb, N. (2010). A global overview of drought and heat-induced tree mortality reveals emerging climate change risks for forests. *Forest Ecology and Management*, **259**, 660-684.

Alvares, C.A., Stape, J.L., Sentelhas, P.C., Gonçalves, J.D.M. & Sparovek, G., (2013). Köppen's climate classification map for Brazil. *Meteorologische Zeitschrift*, **22**, 711-728.

Andersen, L. E. (2002). The dynamics of deforestation and economic growth in the Brazilian Amazon. Cambridge University Press.

Aragão, L. E. O., Malhi, Y., Roman-Cuesta, R. M., Saatchi, S., Anderson, L. O., & Shimabukuro, Y. E. (2007). Spatial patterns and fire response of recent Amazonian droughts. *Geophysical Research Letters*, **34**.

Araújo, I., Marimon, B.S.,Marimon-Junior, B.H., Oliveira, C. H., Silva, J.W., Beú, R.G., Silva, I.V., Simioni, P.F., Tavares, J.V., Phillips, O. L., Gloor, M.U., & Galbraith, D. R. (2024). Taller trees exhibit greater hydraulic vulnerability in southern Amazonian forests. *Environmental and Experimental Botany*, **226**, 105905.

Asner, G.P., Brodrick, P.G., Anderson, C.B., Vaughn, N., Knapp, D.E., & Martin, R.E. (2016). Progressive forest canopy water loss during the 2012–2015 California drought. *Proceedings of the National Academy of Sciences*, **113**, E249-E255.

Balch, J. K., Nepstad, D.C., Brando, P.M., Curran, L.M., Portela, O., de Carvalho Jr, O., & Lefebvre, P. (2008). Negative fire feedback in a transitional forest of southeastern Amazonia. *Global Change Biology*, **14**, 2276-2287.

Barros, F.d.V., Bittencourt, P.R.L., Brum, M., Restrepo-Coupe, N., Pereira, L., Teodoro, G.S., Saleska, S.R., Borma, L.S., Christoffersen, B.O., Penha, D., Alves, L.F., Lima, A.J.N., Carneiro, V.M.C., Gentine, P., Lee, J.-E., Aragão, L.E.O.C., Ivanov, V., Leal, L.S.M., Araujo, A.C. & Oliveira, R.S. (2019), Hydraulic traits explain differential responses of Amazonian forests to the 2015 El Niño-induced drought. *New Phytologist*, **223,** 1253-1266.

Bhaskar, R., & Ackerly, D.D. (2006). Ecological relevance of minimum seasonal water potentials. *Physiologia Plantarum*, **127**, 353–359.

Bittencourt, P. R., Oliveira, R. S., Costa, A. C., Giles, A. L., Coughlin, I., Costa, P. B., Bartholomew, D.C., Ferreira, L.V., Vasconcelos, S.S., Barros, F.V., Junior, J.A.S., Oliveira, A.A., Mencuccini, M., Meir, P., & Rowland, L. (2020). Amazonia trees have limited capacity to acclimate plant hydraulic properties in response to long-term drought. *Global Change Biology*, ***26***, 3569-3584.

Bittencourt, P.R.L., Pereira, L., Oliveira, R.S. (2018). Pneumatic Method to Measure Plant Xylem Embolism. Bio-protocol, 8: 20.

Blackman, C.J., Gleason, S.M., Chang, Y., Cook, A.M., Laws, C., & Westoby, M. (2014). Leafhydraulic vulnerability to drought is linked to site water availability across a broadrange of species and climates. *Annals of Botany*, **114**, 435–440.

Brando, P.M., Balch, J.K., Nepstad, D.C., Morton, D.C., Putz, F. E., Coe, M. T., ... & Soares-Filho, B. S. (2014). Abrupt increases in Amazonian tree mortality due to drought–fire interactions. *Proceedings of the National Academy of Sciences*, **111**, 6347-6352.

Brum, M., Vadeboncoeur, M.A., Ivanov, V, Asbjornsen, H., Saleska, S., Alves, L.F., Penha, D., Dias, J.D., Aragão, L.E.O.C., Barros, F. Bittencourt, P., Pereira, L., Oliveira, R.S. (2018). Hydrological niche segregation defines forest structure and drought tolerance strategies in a seasonal Amazon forest. Journal of Ecology, **107**, 318-333.

Choat, B., Ball, M.C., Luly, J.G. & Holtum, J.A. (2005). Hydraulic architecture of deciduous and evergreen dry rainforest tree species from north-eastern Australia. *Trees*, **19**, 305-311.

Choat, B., Jansen, S., Brodribb, T.J., Cochard, H., Delzon, S., Bhaskar, R., Bucci, S.J., Feild, T.S., Gleason, S.M., Hacke, U.G. & Jacobsen, A.L., (2012). Global convergence in the vulnerability of forests to drought. *Nature*, **491**, 752-755.

Christoffersen, B. O., Gloor, M., Fauset, S., Fyllas, N. M., Galbraith, D. R., Baker, T. R., Kuijt, B., Rouwland, L., Fisher, R.A., Binks, O. J., Sevanto, S., Xu, C., Jansen, S., Choat, B., Mencuccini, McDowell, N.G., & Meir, P. (2016). Linking hydraulic traits to tropical forest function in a size-structured and trait-driven model (TFS v. 1-Hydro). *Geoscientific Model Development*, **9**, 4227-4255.

Ciemer, C., Boers, N., Hirota, M., Kurths, J., Müller-Hansen, F., Oliveira, R.S., & Winkelmann, R. (2019). Higher resilience to climatic disturbances in tropical vegetation exposed to more variable rainfall. *Nature Geoscience*, **12**, 174-179.

Coe, M. T., Marthews, T. R., Costa, M. H., Galbraith, D. R., Greenglass, N. L., Imbuzeiro, H. M., Levine, N.M., Malhi, Y., Moorcroft, P.R., Muza, N.M., Powell, T.L., Saleska, S.R., Solorzano, L.A., & Wang, J. (2013). Deforestation and climate feedbacks threaten the ecological integrity of south–southeastern Amazonia. *Philosophical Transactions of the Royal Society B: Biological Sciences*, **368**, 20120155.

Cosme, L. H.M, Schietti, J., Costa, F.R.C., & Oliveira, R.S. (2017) The importance of hydraulic architecture to the distribution patterns of trees in a central Amazonian forest. *New Phytologist*, **215**, 113-125.

Crawley MJ. (2013). The R book. Wiley Publishing.

Delzon, S., & Cochard, H. (2014) Recent advances in tree hydraulics highlight the ecological significance of the hydraulic safety margin. *New Phytologist*, **203**, 355–358.

Dunn, O. J. (1964). Multiple comparisons using rank sums. *Technometrics*, **6,** 241-252.

Eller, C.B.C., Barros., F.V., Bittencourt, P.R.L, Rowland, L., Mencuccini, M., & Oliveira, R. S. (2018). Xylem hydraulic safety and construction costs determine tropical tree growth. *Plant, Cell & Environment*, **41**, 548-562.

Engelbrecht, B.M., Comita, L.S., Condit, R., Kursar, T.A., Tyree, M.T., Turner, B.L., & Hubbell, S.P. (2007). Drought sensitivity shapes species distribution patterns in tropical forests. *Nature*, **447**, 80-82.

Esquivel-Muelbert, A., Baker, T.R., Dexter, K.G., Lewis, S.L., Ter Steege, H., Lopez-Gonzalez, G., Mendoza, A.M., Brienen, R., Feldpausch, T.R., Pitman, N., Alonso, A., Heijden, V.D.G., Peña-Claros, M., Ahuite, M., Alexiaides, M., Dávila, E.Á., Murakami, A.A., Arroyo, L., Aulestia, M., Balslev, H., ... & Phillips, O. L. (2017). Seasonal drought limits tree species across the Neotropics. *Ecography*, **40**, 618-629.

Esquivel-Muelbert, A., Phillips, O.L., Brienen, R.J., Fauset, S., Sullivan, M.J., Baker, T. R., Chao, K.J., Feldpausch, T.R., Gloor, E., Higuchi, N., Houwing-Duistermaat, J., Lloyd, J., Liu, H., Malhi, Y., Marimons, B. S., Mamimon-Junior, B., Monteagudo-Mendoza, A., Poorter, L., Silveira, M., ... & Galbraith, D. (2020). Tree mode of death and mortality risk factors across Amazon forests. *Nature Communications*, **11**, 5515.

Fearnside, P.M. (2005) Deforestation in Brazilian Amazonia: History, Rates and Consequences. *Conservation Biology*, **19**, 680-688.

Franco, A.C., Rossatto, D. R., Silva, L.C.R., & da Silva Ferreira, C. (2014) Cerrado vegetation and global change: the role of functional types, resource availability and disturbance in regulating plant community responses to rising CO2 levels and climate warming. *Theoretical and Experimental Plant Physiology*, **26**, 19-38.

Fu, P.L., Jiang, Y.J., Wang, A.Y., Brodribb, T.J., Zhang, J.L., Zhu, S.D. & Cao, K.F. (2012). Stem hydraulic traits and leaf water-stress tolerance are co-ordinated with the leaf

phenology of angiosperm trees in an Asian tropical dry karst forest. *Annals of Botany*, **110**, 189-199.

Fu, R., Yin, L., Li, W., Arias, P.A., Dickinson, R.E., Huang, L., Chakraborty, S., Fernandes, K., Liebmann, B., Fisher, R. & Myneni, R.B. (2013). Increased dry-season length over southern Amazonia in recent decades and its implication for future climate projection. *Proceedings of the National Academy of Sciences*, **110**, 18110-18115.

Gatti, L.V., Basso, L.S., Miller, J.B., Gloor, M., Gatti Domingues, L., Cassol, H.L., ... & Neves, R. A. (2021). Amazonia as a carbon source linked to deforestation and climate change. *Nature*, **595**, 388-393.

Gloor, M., J. Barichivich, G. Ziv, R. Brienen, J. Schöngart, P. Peylin, B. B. Ladvocat Cintra, T. Feldpausch, O. Phillips, & J. Baker (2015). Recent Amazon climate as background for possible ongoing and future changes of Amazon humid forests. *Global Biogeochemical Cycles*, **29**, 1384-1399.

Goldstein, G., Meinzer, F. C., Bucci, S.J., Scholz, F. G., Franco, A. C., Hoffmann, W. A. (2008). Water economy of Neotropical savanna trees: six paradigms revisited, Tree Physiology, **28**, 395–404.

Guillemot, J., Martin-StPaul, N.K., Bulascoschi, L., Poorter, L., Morin, X., Pinho, B.X., le Maire, G., Bittencourt, P. R. L., Oliveira, R. S., Bongers, F., Brouwer, R., Pereira, L., Gonzalez Melo, G.A., Boonman, C.C.F., Brown, K.A., Cerabolini, B.E.L., Niinemets, Ü., Onoda, Y., Schneider, J. V., … Brancalion, P. H. S. (2022). Small and slow is safe: On the drought tolerance of tropical tree species. *Global Change Biology*, **28**, 2622-2638.

Hammond, W.M., Williams, A.P., Abatzoglou, J.T., Adams, H.D., Klein, T., López, R., Sáenz-Romero, C., Hartmann, H., Breshears, D.D.., & Allen, C.D. (2022). Global field observations of tree die-off reveal hotter-drought fingerprint for Earth's forests. *Nature Communications*, **131**, 1761.

IPCC, Climate change and land: An IPCC special report on climate change, desertification, land degradation, sustainable land management, food security, and greenhouse gas fluxes in terrestrial ecosystems (Intergovernmental Panel on Climate Change, 2019).

Karger, D.N., Schmatz, D., Detttling, D., Zimmermann, N.E. (2020): High resolution monthly precipitation and temperature timeseries for the period 2006-2100. Scientific Data. https://doi.org/10.1038/s41597-020-00587-yenth, 2020.

Kuznetsova A, Brockhoff PB, Christensen, RHB. (2017). lmerTest Package: Tests in linear mixed effects models. *Journal of Statistical Software*, **82**, 1–26.

Lambers, H.; Oliveira, R.S. Plant Physiological Ecology. Springer Nature Switzerlan, 2019.

Lenth, RV., 2020. emmeans: Estimated Marginal Means, aka Least-Squares means R package version 1.4.7. https://CRAN.R-project.or.

Marengo, J.A., Tomasella, J., Alves, L.M., Soares, W.R., & Rodriguez, D.A. (2011). The drought of 2010 in the context of historical droughts in the Amazon region. *Geophysical Research Letters*, **38**, L12703.

Marengo, J.A., Souza Jr, C.M., Thonicke, K., Burton, C., Halladay, K., Betts, R.A., Alves, L.M., & Soares, W.R. (2018). Changes in climate and land use over the Amazon region: current and future variability and trends. Frontiers in Earth Science, **6**, 228.

Marimon, B.S., Marimon-Junior, B.H., Feldpausch, T.R., Oliveira-Santos, C., Mews, H.A., Lopez-Gonzalez, G., Lloyd, J., Franczak, D.D., de Oliveira, E.A., Maracahipes, L. & Miguel, A. (2014). Disequilibrium and hyperdynamic tree turnover at the forest–cerrado transition zone in southern Amazonia. *Plant Ecology & Diversity*, **7**, 281-292.

Marimon, B.S., Oliveira-Santos, C., Marimon-Junior, B.H., Elias, F., de Oliveira, E.A., Morandi, P.S., S Prestes, N.C.C.D., Mariano, L.H., Pereira, O.R., Feldpausch, T.R. and Phillips, O.L., (2020). Drought generates large, long-term changes in tree and liana regeneration in a monodominant Amazon forest. *Plant Ecology*, **221**,733-747.

Markesteijn, L., Poorter, L., Bongers, F., Paz, H. and Sack, L. (2011). Hydraulics and life history of tropical dry forest tree species: coordination of species' drought and shade tolerance. *New Phytologist*, 191, 480-495.

Marques, E.Q., Marimon-Junior, B.H., Marimon, B.S., Matricardi, E.A., Mews, H.A., & Colli, G. R. (2020). Redefining the Cerrado–Amazonia transition: implications for conservation. *Biodiversity and Conservation*, **29**, 1501-1517.

Martínez-Vilalta, J., & Garcia-Forner, N. (2017). Water potential regulation, stomatal behaviour and hydraulic transport under drought: deconstructing the iso/anisohydric concept. *Plant, Cell & environment*, **40**, 962-976.

Martínez-Vilalta, J., Poyatos, R., Aguadé, D., Retana, J., & Mencuccini, M. (2014). A new look at water transport regulation in plants. *New Phytologist*, **204**, 105-115.

Mattos, C. R., Mazzochini, G.G., Rius, B.F., Penha, D., Giacomin, L.L., Flores, B.M., Silva, M.C., Xavier, R.O., Nehemy, M.F., Petroni, A. R., Silva, J.S.G.M., Schlickmann., M.B., Rocha, M., Rodrigues, G., Costa, S. S., Barros, F.V., Tavares, J.T., Furtado, M.N., Verona, L.S., ... & Hirota, M. (2023). Rainfall and topographic position determine tree embolism resistance in Amazônia and Cerrado sites. *Environmental Research Letters*, **18**, 114009.

McDowell, N., Pockman, W.T., Allen, C.D., Breshears, D.D., Cobb, N., Kolb, T., Plaut, J., Sperry, J., West, A., Williams, D.G. and Yepez, E.A. (2008). Mechanisms of plant survival and mortality during drought: why do some plants survive while others succumb to drought? *New Phytologist*, **178**, 719-739.

Meinzer, F. C., James, S. A., Goldstein, G., and Woodruff, D. (2003). Whole-tree water transport scales with sapwood capacitance in tropical forest canopy trees. *Plant, Cell & Environment*, **26**: 1147-1155.

Meinzer, F.C., Johnson, D.M., Lachenbruch, B., McCulloh, K.A., & Woodruff, D.R. (2009). Xylem hydraulic safety margins in woody plants: coordination of stomatal control of xylem tension with hydraulic capacitance. *Functional Ecology*, **23**, 922–930.

Moore, G.W., Edgar, C.B., Vogel, J.G., Washington-Allen, R.A., March, R.G., & Zehnder, R. (2016). Tree mortality from an exceptional drought spanning mesic to semiarid ecoregions. *Ecological Applications*, **26**, 602-611.

Oliveira, R.S., Costa, F.R.C., van Baalen, E., de Jonge, A., Bittencourt, P.R., Almanza, Y., Barros, F.d.V., Cordoba, E.C., Fagundes, M.V., Garcia, S., Guimaraes, Z., Hertel, M., Schietti, J., Rodrigues-Souza, J. & Poorter, L. (2019), Embolism resistance drives the distribution of Amazonian rainforest tree species along hydrotopographic gradients. *New Phytologist*, **221**,1457–1465.

Oliveira, R. S., Eller, C. B., Barros, F.V., Hirota, M., Brum, M., & Bittencourt P. (2021). Linking plant hydraulics and the fast–slow continuum to understand resilience to drought in tropical ecosystems. *New Phytologist*, **230**, 904-923.

Osazuwa-Peters O, Zanne AE. 2010. Wood density protocol. [WWW document] URL https://prometheusprotocols.net/structure/morphology/stem-morphology/wood-density-protocol/. [accessed 10 January 2024].

Paligi, S.S., Link, R.M., Isasa, E., Bittencourt, P., Cabral, J.S., Jansen, S., Oliveira, R.S., Pereira, L., & Schuldt, B. (2023). Assessing the agreement between the pneumatic and the flow-centrifuge method for estimating xylem safety in temperate diffuse-porous tree species. *Plant Biology*, **25**, 1171-1185.

Pereira, L., Bittencourt, P.R.L., Oliveira, R.S., Junior, M.B.M., Barros, F.V., Ribeiro, R.V., & Mazzafera, P. (2016). Plant pneumatics: stem air flow is related to embolism – new perspectives on methods in plant hydraulics. *New Phytologist*, **211**, 357-370.

Pereira, L., Bittencourt, P. R., Pacheco, V. S., Miranda, M. T., Zhang, Y., Oliveira, R. S., Groenendijk, P., Machado, E.C., Tyree, M.T., Jansen, S., Rowland, L., & Ribeiro, R. V. (2020). The Pneumatron: an automated pneumatic apparatus for estimating xylem vulnerability to embolism at high temporal resolution. *Plant, Cell & Environment*, **43,** 131-142.

Phillips, O.L., Aragão, L.E., Lewis, S.L., Fisher, J.B., Lloyd, J., López-González, G., Maolhi, Y., Monteagudo, A., Peacock, J., Quesada, A.A., Heijden, G.V.D., Almeida, S., Amaral, I., Arroyo, L., Aymard, G., Baker, T.R., Nánki, O., Blanc, L., Bona, D., ... & Torres-Lezama, A. (2009). Drought sensitivity of the Amazon rainforest. *Science*, **323**, 1344-1347.

Pinheiro, J., Bates, D., DebRoy, S., Sarkar, D., R Core Team. (2024). Nlme: Linear and Nonlinear Mixed Effects Models. R package version 3.1-118. [WWW document]URL http://CRAN.R-project.org/package=nlme [accessed 1 August 2024].

Powers, J.S., Vargas, G.G., Brodribb, T.J., Schwartz, N.B., Pérez-Aviles, D., Smith-Martin, C.M., Becknell, J.M., Aureli, F., Blanco, R., Calderón-Morales, E., Calvo-Alvarado, J.C., Calvo-Obando, A.J., Chavarría, M.M., Carvajal-Vanegas, D., Jiménez-Rodríguez, C.D., Chacon, E.m., Schaffner, C.M., Werden, L.K., Xu, X., & Medvigy, D. (2020). A catastrophic tropical drought kills hydraulically vulnerable tree species. *Global Change Biology*, **26**, 3122–3133.

Prestes, N. C., Marimon, B. S., Morandi, P. S., Reis, S. M., Junior, B. H. M., Cruz, W. J., Oliveira, E. A., Mariano, L.H., Elias, F., Santos, D.M., Esquiviel-Muelbert, A., & Phillips, O. L. (2024). Impact of the extreme 2015-16 El Niño climate event on forest and savanna tree species of the Amazonia-Cerrado transition. *Flora, 319*, 152597.

R Development Core Team. 2023. R: a language and environment for statistical computing, v.4.3.2. Vienna, Austria: R foundation for Statistical Computing. URL http://www.r-project.org.

Reich PB. (2014). The world-wide 'fast–slow' plant economics spectrum: a traitsmanifesto. Journal of Ecology, **102**, 275–301.

Reis, S. M., Marimon, B. S., Marimon Junior, B. H., Morandi, P. S., Oliveira, E. A. D., Elias, F., Neves, E.C., Oliveira, B., Nogueira, D.S., Umetsu,R.K., Feldpausch, T.R., & Phillips, O. L. (2018). Climate and fragmentation affect forest structure at the southern border of Amazonia. *Plant Ecology & Diversity*, **11**, 13-25.

Rowland, L. Costa, A.C.L., Galbraith, D.R., Oliveira, R.S., Binks, O.J., Oliveira, A.A.R., Pullen, A.M., Doughty, C. E., Metcalfe, D. B., Vasconcelos, S. S., Ferreira, L. V., Malhi, Y., Grace, J., Mencuccini, M., & Meir, P. (2015). Death from drought in tropical forests is triggered by hydraulics not carbon starvation. *Nature*, **528**, 119-122.

Sanchez-Martinez, P., Martínez-Vilalta, J., Dexter, K.G., Segovia, R.A., & Mencuccini, M. (2020). Adaptation and coordinated evolution of plant hydraulic traits. *Ecology Letters*, **23**, 1599-1610.

Scholander, P.F., Bradstreet, E.D., Hemmingsen, E.A., & Hammel, H.T. (1965). Sap pressure in vascular plants: negative hydrostatic pressure can be measured in plants. *Science*, **148**, 339-346.

Scholz, F. G., Bucci, S. J., Goldstein, G., Meinzer, F. C., Franco, A. C., and Miralles-Wilhelm, F. (2007). Biophysical properties and functional significance of stem water storage tissues in Neotropical savanna trees. *Plant, Cell & Environment*, **30**: 236-248.

Silveiro, A. C., Silvério, D. V., Macedo, M. N., Coe, M. T., Maracahipes, L., Uribe, M., Maracahipes-Santos, L., Oliveira, P.T.S., Rattis, L., & Brando, P. M. (2024). Droughts amplify soil moisture losses in burned forests of southeastern Amazonia. *Journal of Geophysical Research*: *Biogeosciences*, **129**, 10, e2024JG008011.

Smith-Martin, C.M., Muscarella, R., Hammond, W.M., Jansen, S., Brodribb, T. J., Choat, B., Johnson, D.M., Vargas-G, G., & Uriarte, M. (2023). Hydraulic variability of tropical forests is largely independent of water availability. *Ecology Letters*, **26**, 1829-1839.

Soares Jancoski, H., Marimon, B.S., Scalon, M.C., Barros, F.V., Marimon-Junior, B. H., Carvalho, E., Oliveira, R.S., & Menor, I. O. (2022). Distinct leaf water potential regulation of tree species and vegetation types across the Cerrado–Amazonia transition. *Biotropica*, **54**, 431-443.

Tavares, J.V., Oliveira, R.S., Mencuccini, M., Signori-Müller, C., Pereira, L., Diniz, F.C., Gilpin, M., Zevallos, M.J.M., Yupayccana, C.A.S., Acosta, M., Mullisaca, F.M.P., Barros, F.V., Bittencourt, P., Jancoski, H., Scalon, M.C., Marimon, B.S., Menor, I.M., Marimon-Junior, B.H., Fancourt, M., & Galbraith, D.R. (2023) Basin-wide variation in

tree hydraulic safety margins predicts the carbon balance of Amazon forests. *Nature*, **617**, 111-117.

Tiwari, R., Gloor, E., Cruz, W.J.A., Marimon, B.S., Marimon-Junior, B.H., Reis, S.M., Aráujo, I.S., Krause, H.G., Slot, M., Winter, K., Ashley, D., Beú, R.G., Borges, C.S., Cunha, M., Fauset, S., Ferreira, L.D.S., Gonçalves, M.D.A., Lopes, T., Marques, E.Q., ... & Galbraith, D. (2021). Photosynthetic quantum efficiency in south-eastern Amazonian trees may be already affected by climate change. *Plant, Cell & Environment*, **44**, 2428-2439.

Tyree, M.T., & Zimmermann, M. H. (2002). Xylem Structure and the Ascent of Sap. Heidelberg.

Vargas G, G., Brodribb, T.J., Dupuy, J.M., González-M, R., Hulshof, C.M., Medvigy, D., Allerton, T.A., Pizano, C., Salgado-Negret, B., Schwartz, N.B. & Van Bloem, S.J., (2021). Beyond leaf habit: generalities in plant function across 97 tropical dry forest tree species. *New Phytologist*, **232**, 148-161.

Warton, D. I., Duursma, R. A., Falster, D. S., & Taskinen, S. (2012). smatr 3-an R package for estimation and inference about allometric lines. *Methods in Ecology & Evolution*, ***3,*** **257-259**.

Wolfe, B.T., Sperry, J.S. & Kursar, T.A., (2016). Does leaf shedding protect stems from cavitation during seasonal droughts? A test of the hydraulic fuse hypothesis. *New Phytologist*, **212**, 1007-1018.

CONCLUSÃO

A borda sul da Amazônia, uma região naturalmente dinâmica por estar na interface entre dois grandes biomas, Amazônia e Cerrado, também é considerada uma zona de tensão ecológica. O intenso uso antrópico do solo amplifica os efeitos das mudanças climáticas, tornando essa região cada vez mais propensa a condições climáticas extremas. Este estudo contribuiu para a compreensão da vulnerabilidade à seca das florestas dessa região. Nossos resultados mostraram que as árvores da borda sul da Amazônia apresentam alta resistência à embolia, com valores de Ψ_{50} (potencial hídrico do xilema associado a formação de 50% de embolia) mais negativos do que em outras regiões da Amazônia. No entanto, a margem de segurança hidráulica (HSM_{50}) variou entre as florestas, sugerindo que, enquanto algumas comunidades ainda operam dentro de limites seguros, outras já excedem seu limite hidráulico. Por meio de um experimento natural, evidenciamos a influência da disponibilidade de nutrientes do solo nas estratégias hidráulicas das árvores, demonstrando que florestas sobre solos mais ricos em nutrientes (ADE) apresentam menor HSM_{50} do que aquelas em solos pobres (NDE), especialmente ao comparar as espécies que foram encontradas nos dois ambientes.

Esses achados têm implicações importantes para a conservação e manejo das florestas da borda sul da Amazônia. As condições climáticas extremas já afetam a dinâmica dessas florestas, e a variabilidade observada na HSM_{50} indica que algumas comunidades podem estar mais suscetíveis a eventos de seca prolongada. Este estudo reforça a complexidade das respostas das florestas amazônicas à seca e destaca a necessidade de uma abordagem integrada para avaliar sua resiliência frente às mudanças climáticas. A variabilidade nas estratégias hidráulicas das espécies e que se reflete na comunidade vegetal, tanto em função da fertilidade do solo quanto do regime hídrico, sugere que não existe um padrão geral de vulnerabilidade à seca dessas florestas. Assim, considerar a heterogeneidade ambiental e de respostas das plantas será essencial para avaliar riscos ecológicos e propor estratégias de conservação das florestas da Amazonia que sejam mais eficazes e que as tornem mais resilientes aos impactos do aquecimento climático em curso no planeta.